LA-UR-03-6415

Approved for public release;
distribution is unlimited.

Title:	SMALL-SCALE EXPERIMENTS: EFFECTS OF CHEMICAL REACTIONS ON DEBRIS-BED HEAD LOSS
Author(s):	R. C. Johns and B. C. Letellier Los Alamos National Laboratory K. J. Howe and A. K. Ghosh University of New Mexico
Submitted to:	US Nuclear Regulatory Commission

Form 836 (8/00)

LA-UR-03-6415

SMALL-SCALE EXPERIMENTS: EFFECTS OF CHEMICAL REACTIONS ON DEBRIS-BED HEAD LOSS

A Subtask of GSI-191

November 2003

Principal Investigator: B. C. Letellier

Prepared by
R. C. Johns, B. C. Letellier, K. J. Howe,* and A. K. Ghosh*

Los Alamos National Laboratory
Los Alamos, NM 87545

Subcontractors:
*University of New Mexico
Department of Civil Engineering
Albuquerque, NM 87110

T. Y. Chang, NRC Project Manager

Prepared for
Division of Engineering Technology
Office of Nuclear Regulatory Research
US Nuclear Regulatory Commission
Washington, DC 20555-0001
NRC Job Code Y6041

FOREWORD

by

The United States Nuclear Regulatory Commission

In response to a concern raised by the Advisory Committee on Reactor Safeguards (ACRS) in February 2003, the Nuclear Regulatory Commission Office of Nuclear Regulatory Research sponsored a limited-scope study at the University of New Mexico under the direction of Los Alamos National Laboratory. This study was performed to assess the potential for chemically induced corrosion products to impede the performance of Emergency-Core-Cooling-System (ECCS) recirculation after a loss-of-coolant accident (LOCA) at pressurized-water-reactor (PWR) plants. Evidence cited by the ACRS to support this concern included the gelatinous debris found in the post-LOCA sump pool at the Three Mile Island plant after the 1979 accident.

A number of small-scale tests were performed to determine whether post-LOCA debris generation and sump-screen head loss in a PWR containment can be affected by chemical interactions between the ECCS/containment-spray water (which contains boric acid and sodium hydroxide at elevated temperatures) and exposed materials such as metal surfaces, inorganic zinc-based paint chips, and fiberglass insulation debris. These tests confirmed that temperature-dependent corrosion of zinc metal can occur and that precipitation of dissolved metals in the form of gelatinous material can cause additional pressure drops across fibrous debris beds. However, because of the limited scope of this study, no integrated tests to demonstrate the complete progression of these chemical interactions were conducted. Only separate-effects tests were performed for each of the potential stages of the progression, i.e., quiescent-immersion corrosion/leaching tests, and artificially induced saturation/precipitation combined with transport/head-loss flow tests.

It should be noted that no precipitation products resulted from the quiescent zinc immersion tests. Instead, an alternative corrosion product in the form of crystalline surface growth was observed on the samples. Furthermore, precipitation was artificially induced in the head-loss flow tests by the addition of metallic salts to the fluid. Since no integrated tests were performed, the complete progression from metal corrosion to the ultimate formation of precipitation products was not demonstrated.

The principal findings of this study are that it is possible for precipitated gelatinous material, if formed, to transport to PWR sump screens and that such materials can increase head loss across a fibrous debris bed. The findings lend credibility to the concern raised by the ACRS, but are not sufficient to provide a basis for plant-specific quantitative assessment of the issue. Integrated testing to evaluate the overall effect is being explored as a follow-on activity.

LA-UR-03-6415

SMALL-SCALE EXPERIMENTS: EFFECTS OF CHEMICAL REACTIONS ON DEBRIS-BED HEAD LOSS

by

R. C. Johns, B. C. Letellier, K. J. Howe, and A. K. Ghosh

ABSTRACT

Small-scale head-loss flow tests and quiescent-immersion corrosion tests were performed to determine whether post-loss-of-coolant-accident debris generation and sump-screen head loss in a pressurized-water-reactor containment system can be affected by chemical interactions between the emergency-core-cooling-system water, which contains boric acid and sodium hydroxide at elevated temperatures, and (1) exposed metal surfaces, (2) inorganic zinc-based paint chips, and (3) fiberglass insulation debris. The principal findings of this study are that: (1) temperature-dependent corrosion of zinc metal can occur at typical temperatures and pH; (2) precipitation of dissolved iron, aluminum, and zinc in excess of their low solubility limits produces transportable gelatinous material that can cause additional pressure drops across a fibrous debris bed; (3) dissolved zinc can be leached from zinc-based coatings debris; and (4) silica can be leached from typical fiberglass insulation debris and may be an important constituent of the chemical system. However, the implied progression from metal corrosion to the ultimate precipitation of a flocculent material was not demonstrated conclusively. One alternative corrosion product observed in the zinc immersion tests was a crystalline surface growth, suggesting redeposition of zinc compounds initiated in a saturated solution. Electron microscopy, energy dispersive spectrometry, and x-ray diffraction methods were employed to determine the composition of the surface corrosion product.

CONTENTS

CONTENTS (cont)

FIGURES

FIGURES (cont)

TABLES

LA-UR-03-6415

SMALL-SCALE EXPERIMENTS: EFFECTS OF CHEMICAL REACTIONS ON DEBRIS-BED HEAD LOSS

by

R. C. Johns, B. C. Letellier, K. J. Howe, and A. K. Ghosh

EXECUTIVE SUMMARY

The U. S. Nuclear Regulatory Commission (NRC) Office of Nuclear Regulatory Research has developed a comprehensive research program to support resolution of Generic Safety Issue (GSI)-191, which addresses the potential for debris accumulation on pressurized water reactor (PWR) sump screens with the consequent loss of emergency-core-cooling-system (ECCS) pump net-positive-suction-head (NPSH) margin. Among the GSI-191 research program tasks is the experimental investigation of chemical effects that may exacerbate sump-screen clogging. The data presented in this report focus on the corrosion of metal surfaces and the potential for subsequent precipitation as a hydrated gelatinous material that can induce additional head loss across a fibrous debris bed. Particular emphasis was placed on zinc corrosion because of the large surface areas known to be present in PWR containments, though similar results were also obtained for aluminum and iron. Cursory tests were also performed on the leaching of zinc from inorganic primer debris and the leaching of silicates from fiberglass insulation debris.

The purpose of this limited-scope experimental study was to assess the potential for chemically induced corrosion products and chemical degradation effects to impede the performance of ECCS recirculation after a loss-of-coolant accident (LOCA). This concern was raised by the Advisory Committee on Reactor Safeguards (ACRS) in February 2003. The study included a literature search and a review of previous experimental investigations to establish the chemical and thermal environments that might exist in the ECCS spray and sump water following a LOCA.

Small-scale head-loss flow tests and quiescent-immersion corrosion tests were performed to determine whether debris generation and sump-screen head loss can be affected by chemical interactions between the ECCS recirculation water, which contains chemical additives, and (1) exposed metal surfaces, (2) inorganic zinc-based paint chips, and (3) fiberglass insulation debris. These tests were conducted in the Department of Civil Engineering of the University of New Mexico under the direction of Los Alamos National Laboratory. The principal conclusions of this study are that it is possible for gelatinous material, if formed, to transport to PWR sump screens and that such materials can increase head loss across a fibrous debris bed. These results lend credibility to the concerns raised by the ACRS. Specific technical findings include: (1) temperature-dependent corrosion of metal can occur at temperatures and pH typical of chemical conditions in the post-LOCA accident environment; (2) precipitation of dissolved metals in excess of their relatively low solubility limits produces transportable gelatinous material that can cause additional pressure drops across a fibrous debris bed; (3) dissolved zinc can be leached

from zinc-based coating debris typical of that generated in the zone of influence near a high-pressure pipe break; and (4) silica can be leached from typical fiberglass insulation debris and may be an important constituent of the chemical system.

Although the necessary chemical conditions and plausible physical mechanisms exist under typical accident conditions, the natural progression from corrosion to the ultimate precipitation of a flocculent material was not conclusively demonstrated by an integrated test. Alternative reaction paths may occur preferentially. For example, secondary metallic corrosion products were observed in high-temperature immersion tests as a crystalline surface growth; although solubility limits were exceeded in these tests, no visible precipitant was formed. Final determination of combined reaction mechanisms and cumulative head-loss effects in a realistic accident environment could best be determined in an integrated flowing system using typical structural metals.

Head-loss flow tests were conducted in a small-scale (10 liter), vertical, closed-loop circulation, hydraulic-test system built for measuring the head loss across a fiber-laden screen in a chemical environment typical of that found in the ECCS recirculation sump. Calibration tests were first performed to confirm that head losses induced by a debris bed in the small test system were consistent with previous experiments and with standard correlations documented in NUREG\CR-6224. Subsequent tests examined the additional head loss incurred by the precipitation of dissolved metals within the closed circulation loop. These tests were performed in chemical conditions that included 3.3×10^{-2} M boric acid, sodium hydroxide, and 2.0×10^{-4} M lithium in deionized water over a range of temperatures approaching 45ºC and pH levels of 7.0 and 9.0. Precipitation was artificially induced by adding metal nitrate salts to the water in concentrations above their solubility limit. The first tests incorporated the simultaneous precipitation of aluminum, iron, and zinc metals. Head losses across a pre-established fiber mat were observed almost immediately after precipitation was induced. Later tests examined each metal precipitant individually with similar results. Detailed chemical analyses were not performed to determine the composition of the precipitants, but equilibrium chemistry models of the closed system suggest that the products formed in these tests were either metal hydroxides or metal silicates.

More than 20 experiments were conducted with various concentrations of metallic salts. Trends in these tests were consistent and repeatable over a range of temperatures despite the difficulty of controlling the uniformity of the initial fiber debris bed. Larger quantities of metal precipitant lead to higher head losses. Although a predictive correlation was not derived, equivalent head losses can be induced by a much smaller quantity of dissolved metal than the amount of particulate material that would be needed to produce the same effect. Physical examination of the beds after the tests revealed the presence of a gelatinous coating on the entire surface of the bed. This continuous hydrated layer appears to cause more resistance to water flow than mixed beds containing fibers and discrete particles. Examination of desiccated beds by scanning electron microscopy (SEM) showed residual material adhered to individual fibers rather than captured in the interstitial spaces between fibers as is more typical for hard particulates.

Corrosion tests were conducted by immersing zinc materials in 1-liter, quiescent, aqueous solutions at several temperatures for periods of several days and measuring both the change in sample weight after the immersion period and the concentration of zinc in solution. Tests were

performed with zinc granules, zinc coupons, and crumbled inorganic zinc primer. Most tests were performed with solutions representative of the water in the containment pool during a LOCA, although some tests were completed as a control group using only deionized water. Experimental variables included pH, temperature, and the duration of immersion.

Repeatable corrosion rates of 0.055 $g/m^2/hr$ were obtained for zinc coupons and granules in solutions of pH 7.0 at 22ºC. Good comparisons with literature-reported values confirm the experimental procedure and lend credibility to the faster corrosion rates reported for higher temperatures (6 $g/m^2/hr$ near 100ºC). Leaching of zinc from crumbled inorganic coatings was also observed, suggesting that damaged coatings may represent another important reservoir for the dissolution of metal, but leaching rates were not established.

Immersion tests performed at 40ºC and 80ºC were less successful in producing quantitative corrosion rates. A number of the tests resulted in sample-weight increases, indicating the formation of a corrosion product with a higher molecular weight than the original substrate. This product was observed in the form of a black coating on the zinc granules and coupons that could be scraped off easily to reveal pure metal. Several methods were employed to identify the chemical and physical characteristics of this corrosion product. Examination with a visible-light microscope emphasized the change in sample appearance where zinc granules exhibited a shiny, light gray appearance before immersion and either a dull gray or dull black appearance after immersion. SEM imaging revealed the formation of a crystalline platelet structure that was not characteristic of the original zinc substrate. The observed growth of this material is more consistent with a process of external deposition than with a process of internal penetration and fracture, which suggests that zinc is first dissolved from the surface and then recrystallized in a new chemical compound using the metal as a nucleation site. Elemental composition analysis by energy dispersive spectrometry (EDS) and zinc content by mass balance both suggested that the corrosion product contained about 60 percent zinc. EDS analysis also indicated significant amounts of silicon and oxygen. Chemical composition by X-ray diffraction suggested the presence of zinc oxide but could not conclusively identify other zinc compounds.

High-temperature corrosion tests attempted in this study were clearly confounded by exceeding the solubility limits of zinc in solution. Because the immersion beakers were quiescent, it is possible that only the local concentration near the sample surface exceeded saturation when crystallization was initiated rather than the bulk concentration. This is not a condition that would be expected in a system with flowing water like the containment pool. Corrosion rates under well-oxygenated spray conditions were not examined in this study.

On the recommendation of a chemical test peer review panel, the last series of immersion tests was examined for the presence of silica. Silica was determined to be present during all of the corrosion tests and was found in trace amounts in both the deionized water stock and in the chemicals used to adjust pH. However, it was also observed that: (1) silica can leach from fiberglass insulation under the same corrosion conditions; (2) it will be present in containment dust; (3) it may be introduced as debris from ablated concrete; and (4) it may dominate pool chemistry when calcium silicate insulations are damaged. Therefore, the presence of silica in these tests is not inconsistent with pool conditions that might be expected during a LOCA. Silica can reduce the solubility of metals, participate in many coprecipitation reactions, and ultimately

reach its own saturation limits with subsequent preferential precipitation within a fiberglass debris bed.

ACKNOWLEDGMENTS

The NRC Office of Nuclear Regulatory Research sponsored the work reported here. Dr. T. Y. Chang, the technical monitor for this task, provided technical direction and actively participated in reviewing the report, providing valuable comments. The authors would also like to acknowledge Professor Peter Griffith of the Massachusetts Institute of Technology, Dr. Edward Lahoda of the Westinghouse Electric Company, and Professor Adrian Hanson of the New Mexico State University for their timely technical review of the report.

The authors would like to acknowledge Nancy Butner and James F. Lime for their contributions in integrating and reviewing this document and Lisa Rothrock of IM-1, Los Alamos National Laboratory, and Tamara Hallman, The Plus Group, for their editing support.

ACRONYMS

ACRS	Advisory Committee for Reactor Safety
ANS	American Nuclear Society
ANSI	American National Standards Institute
BOC	Beginning of Cycle
BSE	Backscattered Electrons
BWR	Boiling-Water Reactor
CAT	Chemical-Additive Tank
DEGB	Double-Ended Guillotine Break
DI	Deionized Water
ECCS	Emergency Core-Cooling System
EDS	Energy-Dispersive Spectrometer/Spectrometry
EOC	End of Cycle
EPA	Environmental Protection Agency
ESEM	Environmental Scanning Electron Microscope
FSAR	Final Safety Analysis Report
GSI	Generic Safety Issue
HFP	Hot Full Power
HPSI	High-Pressure Safety Injection
ICONE	International Conference on Nuclear Engineering
LANL	Los Alamos National Laboratory
LLOCA	Large Loss-of-Coolant Accident; also called Large-Break LOCA
LOCA	Loss-of-Coolant Accident
LOFW	Loss of Feedwater Flow
LOSP	Loss of Off-Site Power
LPSI	Low-Pressure Safety Injection
MDI	Materials Data Incorporated
M	Molarity, the number of moles of solute per liter of solution
Mgal.	Million Gallons
MOC	Middle of Cycle
N	Normality, the number of gram-equivalent weight of a compound per liter of solution
NPSH	Net Positive Suction Head
NPSHR	Net Positive Suction Head Required
NRC	Nuclear Regulatory Commission

ACRONYMS (cont)

NUREG	Nuclear Regulatory Commission Publications; formerly referred to as Guides
NUREG/CR	NUREG published by another agency or company, under contract with the Nuclear Regulatory Commission (Contractor Report)
PORV	Pilot-Operated Relief Valve
PP	Polypropylene
PVC	Polyvinyl Chloride
PWR	Pressurized-Water Reactor
RCP	Reactor Coolant Pump
RCS	Reactor Coolant System
SAR	Safety Analysis Report
SAT	Spray-Additive Tank
SE	Secondary Electron
SEM	Scanning Electron Microscope/Microscopy
SI	Safety Injection
SKI	Swedish Nuclear Power Inspectorate
SLOCA	Small (Break) Loss-of-Coolant Accident
SS	Stainless Steel
STUK	Finnish Centre for Radiation and Nuclear Safety
TMI	Three Mile Island
TSP	Trisodium Phosphate
UECI	United Engineers and Constructors, Inc.
UNM	University of New Mexico (at Albuquerque)
US	United States
US EPA	United States Environmental Protection Agency
WDS	Wavelength-Dispersive Spectrometer
Z	Atomic Number
ZP	Zero Potential
ZPC	Zero Point of Charge

1.0 INTRODUCTION

In the event of a loss-of-coolant accident (LOCA) within the containment of a pressurized-water reactor (PWR), piping thermal insulation will be damaged and dislodged by break jet impingement. A fraction of this damaged insulation and other materials, such as paint chips and concrete dust, will be transported to the containment floor by the steam/water flows that are induced by the break and containment sprays. Some of this debris eventually may be transported to and accumulated on the sump screens of the emergency core-cooling system (ECCS) pumps. Debris accumulation increases the differential pressure across the sump screen and, in some cases, could degrade ECCS performance to the point of failure.

The United States Nuclear Regulatory Commission (NRC) Office of Nuclear Regulatory Research has developed a comprehensive research program to support the technical assessment of Generic Safety Issue (GSI)-191, which addresses the potential for debris accumulation on PWR sump screens with consequent loss of ECCS-pump net positive suction head (NPSH). Studies performed by Los Alamos National Laboratory (LANL), including the report "Parametric Evaluations for PWR Recirculation Sump Performance" (Vol. 1 of NUREG/CR-6762 [14]), established that ECCS sump screen blockage is a credible concern for LOCA-generated debris and resident dust loadings that may be transported to the screen. However, no previous work related to GSI-191 has addressed the potential for chemical interactions between the cooling water and exposed materials within containment that could (1) generate new forms of debris with unique screen-blockage characteristics or (2) affect the head-loss behavior of previously investigated debris types. Materials of primary concern that will be exposed to either spray-water impingement or sump-pool immersion include containment coatings; structural metals such as iron, zinc, and aluminum; and insulation debris. All previous GSI-191 transport and head-loss studies were performed with chemically neutral water.

This concern of chemical effects was first raised by the Advisory Committee on Reactor Safeguards (ACRS) in February 2003 for the following reasons: (1) the PWR ECCS recirculation water following a LOCA would be chemically active because of reactor coolant system (RCS) additives, such as boric acid and lithium hydroxide, as well as spray additives, such as sodium hydroxide, at pH conditions ranging between 7 and 10; (2) the amount of debris generated by chemical reactions could be significant; and (3) chemically generated debris may exhibit significantly different interactions with an existing debris bed. Water quality in the containment vessel following a LOCA is also influenced by the elevated temperatures resulting from the initial blowdown of the RCS and from continued decay heat generation.

Among the evidence cited to support these concerns were post-Three-Mile-Island (TMI) analyses of gelatinous debris suspensions in the sump [7] that pose different head-loss challenges to a sump screen than those from more commonly studied debris types. Although historical evidence of debris characteristics related to chemical reactions is an important motivation for commissioning this study, it was not the intent of the investigation to recreate conditions present in the TMI accident environment. GSI-191 research is concerned with debris loadings and head-loss impacts that would precede loss-of-recirculation flow so that plant-specific vulnerabilities can be identified and mitigated to prevent severe reactor accidents from developing. TMI suffered significant fuel damage and subsequent release of radionuclides to containment.

Radiolytic decomposition of cable jackets and disassociation of atmospheric nitrogen can release chlorides and nitric acid, respectively, to the containment pool. Neither of these effects were considered in this study because they are not specifically relevant to pre-fuel-damage events. River water was also injected at TMI, which might have contributed to the color, turbidity, and consistency of the residue found in the sump at the time of recovery. Only the normal PWR additives to deionized water were considered here.

Following a LOCA, a good portion of materials in containment are exposed to alkaline emergency-cooling and containment spray solutions and some may corrode. The phenomenon of corrosion and its potential consequences as a debris source on the long-term cooling of the reactor and containment building have received little attention. Metal corrosion may represent two possible concerns. First, surface deposits of frangible corrosion products may detach in small transportable flakes and particles that can eventually reach the sump screen and collect on an existing fibrous debris mat. Second, the continued dissolution of metal into the recirculation pool may eventually reach saturation, with subsequent precipitation of a flocculent product. Both mechanisms represent new debris sources that have not been studied previously under the GSI-191 research program.

The known corrosion of zinc and aluminum suggests that other exposed metals such as iron might also be vulnerable, and because zinc is present in some inorganic coating materials, it raises the question of whether zinc can be leached out of the coating matrix. In regard to the potential degradation of coatings material, this study focuses on paint-chip debris that would be generated in the damage zone of a high-pressure-break jet. Qualified applications of coatings systems are robust with respect to the LOCA chemical environment, and thus, were not considered at this time. Nonqualified, alkyd-based paint that is typical of coatings applied to electrical and mechanical equipment remains a candidate for future investigation because no relevant chemical degradation data are available for this material. Alkyd paints could not be incorporated into the test matrix of this limited-scope study.

The objective of this report is to present observations on scoping tests that were carried out to assess experimentally the degree of influence and the mechanisms by which water chemistry and temperature may influence the head-loss characteristics of an ECCS sump screen following a LOCA in a PWR nuclear power plant. The scope of work for this test program spans a limited number of experiments in three basic categories: (1) head-loss tests performed with fibrous debris beds and chemically induced precipitants, (2) tests performed on zinc metal and paint-chip samples immersed in borated water to determine corrosion rates, and (3) head-loss tests performed with fibrous debris in borated water to monitor for long-term chemical changes in a familiar debris type. Because the array of possible chemical effects is so large, only a limited number of concentration, pH, temperature, and sample types could be investigated. The purpose of this limited-scope experimental study was to generate data that establish whether chemical reactions and chemical conditions could play important roles in debris generation and sump-screen head-loss phenomena. The intent was to establish a minimum level of credible evidence for any identified chemical reaction mechanisms that could increase the concern for ECCS recirculation failure rather than to develop a comprehensive understanding of any single chemical effect or the data necessary to quantitatively assess its potential impacts on sump blockage.

In Section 2, this report provides a review of previous experiments and the literature search performed under this program. Section 3 examines the potential for corrosion and chemical interactions to occur between the ECCS water and exposed materials. The rationale for the selected chemical test conditions is presented in this section as well. Section 4 presents the small-scale head-loss experiments that were performed to determine the effect of artificially induced precipitants on head loss, and Section 5 presents results from the corrosion tests that were performed to determine the potential for dissolution of metal and corrosion product formation. Finally, Section 6 presents conclusions, limitations of the test program, and suggestions for future research.

On September 15, 2003, a peer review panel meeting was convened in Albuquerque, New Mexico, at the University of New Mexico, where the chemical test experiments were conducted. The purpose of this meeting was to review the LANL draft report on the effects of chemical reactions on debris-bed head loss. The peer review panel members included:

Professor Peter Griffith, Massachusetts Institute of Technology;
Dr. Edward J. Lahoda, P.E., Westinghouse Electric Company; and
Professor Adrian Hanson, New Mexico State University.

Their review comments, suggestions, and contributions were well received and very much appreciated. Comments and recommendations received from the peer review panel members are included in this report as Appendix A, and were incorporated into the report to the extent possible within the available time and programmatic constraints.

2.0 BACKGROUND

In 1992, an event occurred at the Barseback boiling-water reactor (BWR) in Sweden that raised a concern for a potential loss in ECCSs for all nuclear power plants [1]. A reactor vessel safety valve accidentally opened, discharging high-pressure steam into the reactor containment drywell. Reactor scram systems and ECCSs initiated automatically; however, steam from the open safety valve impinged on thermally insulated piping and equipment, thereby dislodging approximately 440 lb of metal-jacketed mineral wool. An estimated 220 lb of the material was washed into the suppression pool and plugged some of the suppression pool strainers. The plugging caused pressure to decrease significantly across the strainers and caused cavitation in one of the ECCS pumps. This concern of BWR suction strainer clogging was resolved in 1996 by NRC Bulletin 96-03 [19] and the Boiling Water Reactor Owners Group (BWROG) Utility Resolution Guidance (URG) [20]. The NRC established GSI-191 in September 1996 to conduct further research into the PWR sump screen clogging issue.

The PWR plant designs rely on the ECCS to mitigate a variety of accidents, including postulated breaks in the coolant lines. A pipe break in the nuclear plant's primary system leads to a rapid depressurization of the primary reactor system. Piping thermal insulation (e.g., fiberglass insulation) and other materials near the break will be dislodged by the dynamic propagation of the pressure wave followed by the ensuing steam/water-jet impingement. A fraction of this fragmented and dislodged insulation and other materials (e.g., chips of paint, paint particulates, and concrete dust) will be transported to the ECCS sump by the break-induced steam/water flows and the containment sprays. This scenario is depicted in Fig. 2-1. Some of the debris would then be transported to the ECCS pump sump screens (see Fig. 2-2) that are designed to screen out debris, thus preventing the debris from entering the reactor core. The accumulation of debris on these sump screens would induce pressure drops greater than the NPSH and lead to ECCS pump cavitation, which is a major safety issue for nuclear power plants and thus for the NRC.

A comprehensive study of LOCAs was conducted by LANL, using a simulation of a Westinghouse four-loop plant [2]. Of the initiating events and resulting accident scenarios, we have selected the Large LOCA as the basis for chemical effects studies, as the highest debris generation occurs with this incident and the containment spray system is on for the maximum duration, allowing for more surfaces to be involved in potential reactions. A detailed description of the sequence of events during a large LOCA is given in Appendix B. A discussion of the chemical environment as a function of the accident sequence is given in section 3.2.5.

The strainer experience at Barseback in 1992 [1] showed that a relatively small amount of insulation materials can cause rapid clogging of the debris screens that are part of the systems for core spray and containment spray. As a result, a large number of investigations were initiated to understand the head-loss characteristics of the sump screen. The cooling water contains boric acid, lithium, and, after initiation of the containment spray, sodium hydroxide. A high pH is essential to prevent fibers and small particles from coagulating and depositing on the sump screen, which would subsequently cause differential pressure buildup over the sump screen [5]. Dissolved concrete, pyrolytic products, and acidic products could be important after 24 hours, as the formation and dissolution of these products requires time to become appreciable.

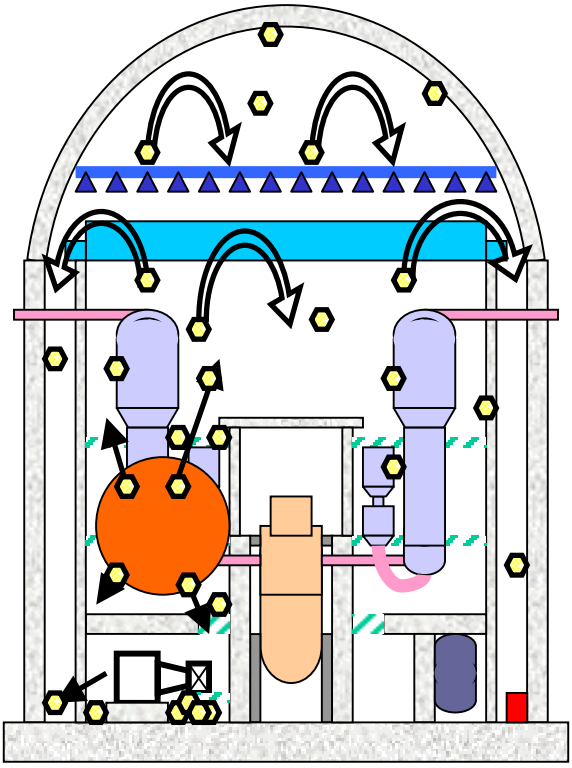

Fig. 2-1. Illustration of a LLOCA event occurring in a PWR plant.

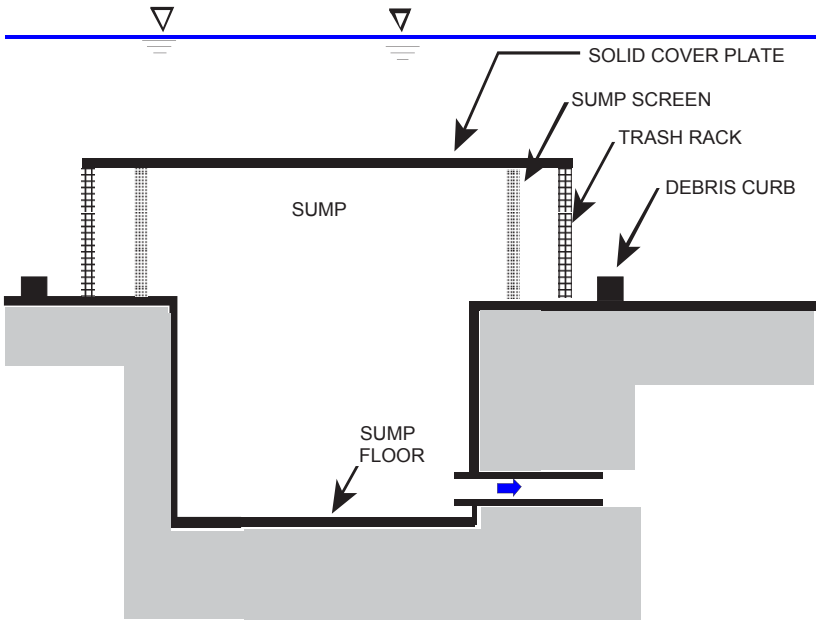

Fig. 2-2. Illustration of an ECCS sump pit and debris screens.

In a nuclear power plant, zinc and aluminum are used as anodic coatings and isolation materials. Sources of zinc can be paints and galvanized surfaces in steel liners, cable trays, conduits, walkways, gratings, insulation covers, and various supports. Aluminum is found in fans, blades, hubs, and valves; estimates of typical quantities of the metals can be found in [3,4], as well as in the individual plant SAR documents. At high temperatures, oxidation of these metals can occur, which can produce large amounts of gaseous and solid corrosion products [3, 13]. The gaseous product is primarily hydrogen. The solubility of zinc and aluminum and the stability of the corrosion products can be estimated from chemical and thermodynamic calculations.

Piippo et al. [3], reported that the corrosion of zinc appears to be relatively fast in neutral or mildly alkaline aerated water, while high pH and de-aeration both tend to reduce the corrosion rates. The use of borated alkaline water induces rapid corrosion at high temperature. Zn corrosion did not always slow down when the temperature decreased. Aeration and pH elevation decrease the corrosion rate of aluminum.

Corrosion during a severe accident may be enhanced also due to the release of chloride, which is contained in the cable insulation material during normal operation [3]. Both metals corroded more rapidly in the presence of chlorides in acidic and alkaline conditions than in the absence of chlorides in a neutral environment.

Loyola and Womelsduff [13] studied the relative importance of parameters (temperature, pH, and boric acid concentration) in the corrosion of zinc from galvanized steel. Temperature was the strongest effect followed by pH. Boric acid was found to be a weak parameter. Corrosion was highest for high temperature high pH (167 °C, pH 10)

A number of tests for corrosion of various metals under simulated spray and immersion conditions were conducted at ORNL [16, 17, 18]. While much of the tests focused on structural integrity of the specimens undergoing corrosion, corrosion rates were found to be higher in spray conditions than immersion conditions for both aluminum and zinc[16]. These rates appear to be between 6 and 7 times greater than for the ANS 56.1 correlation. One of the runs using aluminum test coupons produced large amounts of flocculent aluminum hydroxide [17] and another run with both copper and aluminum specimens in the presence of thiosulfate plugged the small diameter spray nozzle [18]. Runs with copper samples alone in the presence of thiosulfate produced a gelatinous material [18]. Modern spray additive systems do not include thiosulfate.

Niyogi et al. [4] have made extensive efforts to study, through literature survey, the solubility of the corrosion products from aluminum and zinc to determine the potential for massive precipitation in the containment sump.

Kallstrom et al. [5] studied the risk of coagulation of particles/fibers with subsequent clogging of the strainers. They performed the following measurements and observations during their experiments to analyze the risks:

- electrophoretic mobility—the speed of movement of charged particles when a voltage field is created between electrodes;

- coagulation tendency—using coagulation kinetics;
- calculation of zeta (ζ)-potential—quantify surface charge; and
- appearance and size of particles/fibers.

They noticed that some of the materials (iron oxide hydroxide, fiberglass, and "minileit") showed a tendency toward coagulation at pH less than 4. Scanning electron microscope (SEM) investigation of the filtered materials did not indicate a clear tendency toward coagulation at isoelectric points (pH at 0 charge). The conclusions of their study were that

- mineral wool can be a greater problem for strainer filtration than fiberglass;
- small suspended particles are more dangerous than larger ones; and
- corrosion products and biological slime can cause a high pressure drop.

If the accident results "only" in a flow of water and steam, the probable pH will end up in the range of 7 to 9. However, if the accident combines with fire or some other source of significantly higher temperature that involves the breakdown of organic material, a decrease in pH can be expected. These investigators used a pH range of 2 to 10.

Fiberglass insulation materials are normally impregnated with phenol resin to prolong their useful life. Resin glue can decay over time and cause fiberglass to age and alter and can behave differently. The coating is likely to be removed in the initial stages by the hot water and to contribute to the water chemistry at a LOCA. Thus, aged fibers, which can have different strengths, fragment sizes, wetabilities, and flotation properties will behave differently. Past studies have demonstrated that smaller fragments cause higher head loss; thus, long-term head-loss studies are important.

Vicena et al. [6] have carried out experimental studies on the risk of sump plugging in a 900-MWe PWR. The objective of their test program was to verify and quantify the kinetics and disintegration of thermal insulation under the mechanical effects of falling water and the chemical and thermal effects of working fluids on insulation samples.

Based on experimental studies, NUREG-0897 [15] concluded that debris generation by LOCA jets is a complex function that is significantly influenced by a variety of factors, including break diameter, break location, break stagnation pressure and temperature, type of insulation, mode of encapsulation, and orientation of the target with respect to the break jet.

Nitrogen gas bubbles can affect the time required for clogging by causing a more rapid transport of loose and suspended material to the sump screen. The solubility of nitrogen in water can also influence debris (it is minimal at the final containment temperature of 75°C).

3.0 CONTEXT FOR THE EXPERIMENT

3.1 Potential For Corrosion Products to Affect Sump Screen Performance

Previous studies on sump screen performance have focused on debris generated by damage from the force of high-pressure, high-temperature water impinging on materials inside the containment structure. Therefore, debris has consisted of pieces or shards of the original building materials. However, chemical reactions between the building materials and the containment cooling water might generate new materials that have a different effect on sump screen performance than the source materials.

There are at least two sources of corrosion. First, hot high-pressure water impinges on pipe supports, brackets, cable trays, or other metallic materials in the containment structure. This spray can cause an erosion of the metals, thus resulting in small particles of metal suspended in the pool water. The small particles of metal have a large surface area exposed to water, which can subsequently corrode.

A second source of corrosion is the cooling water spray inside the containment. This spray will wet the metal materials, and the resulting moisture can accelerate the corrosion of these metals. The corrosion of these metals will cause an accumulation of metal ions in the pool water; however, aluminum, iron, and zinc are very insoluble, and the solubility is controlled by compounds other than the base metals (for instance, the solubility of aluminum is controlled by amorphous aluminum hydroxide, not metallic aluminum). Hypothetically, the accumulation of metal ions in the pool water can continue until the pool water is supersaturated with respect to specific compounds. Water can exist in a supersaturated state for long periods of time when maintained in clean, quiescent conditions.

However, during a LOCA, the pool water will be turbulent because of pumping, water running across floors, or water being sprayed within containment. In addition, the presence of dirt, debris, and rough surface will provide nucleation sites for precipitate formation. Under these conditions, the pool water may not become supersaturated largely but will precipitate soon after saturation limits are reached. In this case, the metal ions may precipitate and form products that originally did not exist in the containment structure. Likely precipitation products include oxides and hydroxides of aluminum, iron, and zinc. These corrosion products may have different properties that cause significantly more head loss than other debris.

After the TMI incident, a gelatinous material was noted on the walls and floors of the containment sump [7]. This material did not appear to correspond to any building materials used inside the containment structure, and the source for this material was unknown at the time. However, it is known that aluminum and iron oxides and hydroxides precipitate as amorphous materials that could easily appear as gelatinous coatings on walls and floors.

Experience from other industries can be used to predict the impact of metal corrosion products on the ECCS sump screen. Aluminum and iron salts are used as coagulants in the water-treatment industry. Aluminum and iron salts (typically added as salts of sulfate or chloride), when added to water, rapidly form amorphous aluminum hydroxide and iron hydroxide

precipitates. The precipitates interact with particles (dirt, sediment, and microorganisms) in natural surface waters, causing the particles to aggregate (or flocculate) into larger masses that settle more easily than do small individual particles. Coagulation with metal salts also improves filtration efficiency (by improving the capture of particles). Coagulation is an integral part of granular media filtration and is used at water-treatment facilities throughout the industrialized world. The use of aluminum and iron salts to improve filtration efficiency in water treatment suggests that any formation of aluminum or iron precipitates during a LOCA may have a detrimental effect on the head loss across the ECCS sump screen.

3.2 Chemical Environment of a Representative US PWR

3.2.1 Chemical Sources

The chemical environment in the sump during a LOCA is a combination of contributions from three classes of sources: design-basis sources (e.g., chemicals placed in the coolant by design); environmental sources (e.g., dust and latent fiber); and accident-progression sources—sources created from events during the accident (e.g., the production of chloride by radiolysis and the pyrolytic combustion of PVC cable insulation).

For the purposes of these tests, we chose conservative best-estimate values for the parameters. For example, we are using middle-of-cycle (MOC) values for lithium and boron concentrations in the RCS loop.

3.2.1.1 Design-Basis Sources

Chemicals considered for interaction in sump screen performance include those in regular RCS water chemistry: accumulator water chemistry, RWST water chemistry, chemical-additive tank (CAT) or spray-additive tank (SAT) chemistry, and any other engineered chemical source.

Nominal values from our volunteer plant are listed in Table 3-1. Additional chemicals are sodium hydroxide from the CAT or SAT, which is added to the containment spray to achieve a pH range of 8.5 to 10. Some plants other than our volunteer plant use trisodium phosphate (TSP) around the containment for iodine sequestration.

TABLE 3-1
CHEMICAL COMPOSITION OF COOLING-SYSTEM WATER

Chemical	RCS BOC*	RCS MOC	RCS EOC†	Accumulator	RWST
Boron	1300 ppm	500 ppm	10 ppm	~2000 ppm	2500 ppm
Lithium	2.5–4.3 ppm	1.3–1.7 ppm	0.3–0.4 ppm	~10 ppb	~10 ppb
Cations	~10 ppb				
Anions	~5 ppb				

*BOC = beginning of cycle.
†EOC = end of cycle.

The initial chemistry at the LOCA site is assumed to be that of the RCS coolant. This is quickly dominated by RWST chemistry because the RWST volume is approximately 5 to 14 times larger than the RCS volume.

3.2.2 Design-Basis Contribution to Sump Chemistry for Experimentation

Table 3-1 contains the nominal values used to represent the water chemistry sources. TSP was not selected for addition into the chemical basis because some plants do not employ it; however, it should be a mitigating factor. We assume that those facilities that employ TSP will demonstrate its effectiveness and its timely presence in the sump coolant for this application and receive appropriate credit within the context of this issue.

3.2.3 Environmental Sources

Environmental sources of chemicals include all of the materials and equipment inside containment that have exposed surfaces. Of most concern are items of large surface area, where small reactions may become significant due to the sheer bulk that is present in containment. Materials of interest are listed in Table 3-2, along with quantities in containment, their susceptibility to chemical interaction, and any barriers to interaction with spray or pool.

We have chosen to ignore most contributions from the environmental class because of preliminary investigations and uncertain composition of materials, such as dust and latent fiber. The notable exceptions are zinc and aluminum from various sources, which are all inventoried because of a known spray-metal reaction that produces hydrogen gas. Because of the known reaction, large surface areas, and low solubility of the byproducts, zinc and aluminum were considered to be prime sources for investigation. Allowable inventories for three PWR plants that were surveyed range from 233,000 to 550,000 ft^2 of zinc and 3000 to 20,000 ft^2 of aluminum ([4], [21], and [22]).

TABLE 3-2
MATERIALS PRESENT IN A PWR CONTAINMENT

Material	Quantity Available	Susceptibility	Barriers
Steel	large	medium	coatings
Qualified coatings	large	low	none
Unqualified coatings	medium	medium	none
NUKON™	large	low	SS* jacket
CalSil	large	low	none
Stainless RMI†	large	low	none
Latent Fiber	medium	unknown	none
Latent particulate/dust	medium	unknown	none
Zinc	100,000s ft^2	medium	none
Concrete	large	medium	coatings
Aluminum	1000s ft^2	medium	none

*SS = stainless steel.
†RMI = reflective metallic insulation.

3.2.4. Accident-Progression Sources

Hydrochloric acid (HCl) and nitric acid (HNO_3) are common chemicals produced during an accident. Hydrochloric acid is produced by radiolysis and the pyrolytic combustion of cable insulation. Nitric acid is radiolytically produced in combination with water vapor and nitrogen in the air. Other chemicals would include all of the radiological byproducts of the core, which would be dominated by the production of tritium from the water.

In a design-basis LOCA, most of these chemicals will either not be produced in quantity or will remain contained inside the fuel rods. Under design-basis conditions, the vessel remains intact; hence, there is no large radiation flux to containment. Additionally, the size of the LOCA will affect temperatures inside containment, thus influencing the total amount of pyrolytic-based chemicals produced.

The most probable chemical to be introduced into the sump chemistry is hydrochloric acid, which occurs from pyrolytic decomposition of cable insulation. Chloride increases corrosion and is a known complexing agent.

3.2.5 Chemical Evolution over the Accident Sequence

At the start of the LOCA, the sump is presumed dry and all parameters are that of RCS coolant at hot-full-power (HFP) conditions. The boron and lithium conditions will depend on cycle timing. For the purposes of this study, mid-cycle conditions were assumed.

Shortly after initiation of the break, the reactor is tripped and the safety injection systems are actuated. Once fully aligned, the safety injection systems draw from the RWST, which is a source of borated water. Until injection of the accumulators, at between 10 to 20 s, the effluent that will eventually reach the sump screens is primarily RCS coolant—perhaps slightly elevated in boron—plus insulation and other debris generated in close vicinity to the break. Plants with TSP baskets will have small amounts of TSP dissolved in the coolant.

The blow-down phase in a large-to-medium LOCA should be complete in less than a minute and shortly thereafter will have consumed the entire accumulator volume. At this point, the effluent that will eventually reach the sump screens is still primarily RCS coolant, although perhaps with slightly elevated boron levels due to mixing of the accumulator volume (approximately equal to the vessel volume). Again, the insulation, eroded concrete, and other debris in the vicinity of the break may be fractionally transported toward the sump. Plants with TSP baskets will have increasing amounts dissolved in the coolant.

During the next phase, the low-head safety injection becomes effective and refloods the core with borated water, in conjunction with the remaining volume of the accumulator. Containment sprays also become active during this period, thus raising the pH of the effluent. The concentration of TSP should peak during this time because most of the TSP should be dissolved; however, the RWST is not yet empty. Most of the mechanical damage from the break should have occurred. The chemistry at the sump screen should be marked by rising boron and pH

levels and slowly decreasing levels of lithium due to dilution, plus early corrosion products, impurity materials, and debris.

During this last phase, all coolant tanks have been emptied and containment operates in recirculation mode. All design-basis chemicals are present in their maximum quantities. The sprays will cease rather early in this phase, thus reducing the potential surface area for contributions to pool chemistry. The only surfaces involved after this point are those in the break vicinity and lower containment vicinity and the path between the two. It is anticipated that most reactions with importance to the sump screen would occur at this time because adequate corrosion to reach solubility limits may have occurred.

Table 3-3 summarizes these parameters for the various phases as a function of time. The data are taken from a simulation of the Ringhals facility.

TABLE 3-3
CHEMICAL ENVIRONMENT AS A FUNCTION OF TIME IN A LOCA

Time	Temperature (°C)	pH	Boron (ppm)	Lithium (ppb)	TSP (m)
0 s	40	7.7	800	1400	0
10 s	124	7.0	800	1400	2.3E-4
23 s	128	7.2	800	1400	4.2E-4
940 s	118	8.4	1400	630	7.7E-3
24 h	68	7.9	2070	115	5.4E-3
48 h	63	7.8	2070	115	5.4E-3

3.3 Potential for Corrosion and Rates of Corrosion

Corrosion rates previously documented in the literature provide a means of prioritizing the materials chosen for testing in this study and provide a basis for comparing the accuracy of results that are presented in the following sections. The corrosion of metal building materials used in containment structures has been previously studied. Niyogi et al. [4] presented an equation for zinc corrosion that predicts a corrosion rate of 0.12 g/(m^2·h) at 80°C to 2.1 x 10^{-3} g/(m^2·h) at 22°C. Based on these rates and the surface area of zinc in a containment, that report predicted that as much as one ton of zinc may corrode in 30 days during a LOCA. Corrosion at this rate would produce a potential zinc concentration in solution of 8.8 × 10^{-3} M. Piippo et al. [3] measured corrosion rates experimentally and found zinc corrosion rates ranging from about 0.05 to 11.27 g/(m^2·h) under a variety of experimental conditions typical of accident scenarios in BWRs.

Niyogi et al. also investigated corrosion rates for aluminum from several sources and found rates ranging from 0.1 to 0.8 g/(m^2·h) at 22°C and from 3.2 to 14.4 g/(m^2·h) at 80°C. Based on these rates and the surface area of aluminum in containment, that report predicted that as much as 918

pounds of aluminum could corrode in 30 days during a LOCA. Corrosion at this rate would produce a potential aluminum concentration in solution of 9.2×10^{-3} M for the facility studied.

3.4 Solubility of Aluminum, Zinc, and Iron

Water chemistry modeling involves determining the concentration of all species that may be present in the solution after the introduction of reactants. The concentration of each species is determined by using equilibrium constants for chemical reactions. For instance, a chemical reaction between two soluble species of aluminum can be written as

$$Al^{+3} + H_2O \rightleftarrows AlOH^{+2} + H^{+} \quad . \tag{3-1}$$

The equilibrium constant for this reaction is expressed as

$$K_{EQ} = \frac{\left[AlOH^{+2}\right]\left[H^{+}\right]}{\left[Al^{+3}\right]\left[H_2O\right]} \quad . \tag{3-2}$$

In addition to equilibrium constant expressions, water chemistry modeling involves the conservation of mass of each species present. If the two aluminum species in Eq. (3-1) were the only ones that formed when aluminum was added to water (which, as will be seen shortly, is not the case), an expression for the total amount of aluminum could be written as

$$Al_T = \left[Al^{+3}\right] + \left[AlOH^{+2}\right] \quad . \tag{3-3}$$

In the aqueous chemical environment of a PWR cooling system, aluminum, iron, and zinc combine with other constituents to form a large number of chemical species. Some of these reaction products are soluble, whereas others are insoluble. Possible soluble and insoluble compounds are listed in Table 3-4. At equilibrium, all soluble species may be present in various concentrations, whereas typically, a single insoluble species may be present. The insoluble species present will be the compound with the lowest solubility at the reaction conditions. Carbonates are present because the system was modeled as being open to the atmosphere, which would be the case during a LOCA. Carbonate enters the system due to the dissolution of atmospheric carbon dioxide.

To determine the equilibrium concentration of each of species in Table 3-4, total mass expressions for each element and equilibrium constant expressions for the formation of each species are written, where the number of mathematical expressions is equal to the number of chemical species. Because 38 chemical species are identified in Table 3-4, modeling of this system involves the simultaneous solution of 38 equations with 38 unknowns. In this project, Visual Minteq Version 2.15a was used for chemical equilibrium modeling. Visual Minteq is a graphical interface to MINTEQA2, a chemical speciation equilibrium model for aqueous systems developed by the US Environmental Protection Agency (EPA) [8]. The species list in Table 3-4 was developed from the chemical species database provided with Visual Minteq.

The list of species in Table 3-4 demonstrates several aspects with respect to aluminum, iron, and zinc corrosion products. First, none of the species in Table 3-4 contains lithium. Lithium reacts with borate to form one compound ($LiH_2BO_{3\ (aq)}$), but modeling showed that less than 2% of the lithium combined with borate, and the remainder was present as a free lithium ion (Li^+). Thus, the presence of lithium has no effect on the distribution of aluminum, iron, and zinc species. Second, borate also has very little impact on the aluminum, iron, and zinc chemistry. No aluminum species and only two iron species containing boron have been identified. In addition, the iron borates are present in negligible quantities (less than 10^{-16} M); therefore, borate has no effect on the distribution of aluminum and iron. The situation is somewhat different with zinc because of the presence of one insoluble zinc compound in addition to two soluble species. With a sufficiently high borate concentration, $Zn(BO_2)_2$ can precipitate and control the solubility of zinc.

Boron does not exist in isolation in a solution, but combines with hydroxide to form borate. Borate is a weak acid; the first acid dissociation constant is $pK_a = 9.24$. As a result, boric acid (H_3BO_3) is the predominant boron-containing species at pH values below 9.24 and borate ($H_2BO_3^-$) is the predominant species at higher pH values. The distribution of borate species as a function of pH is shown in Fig. 3-1.

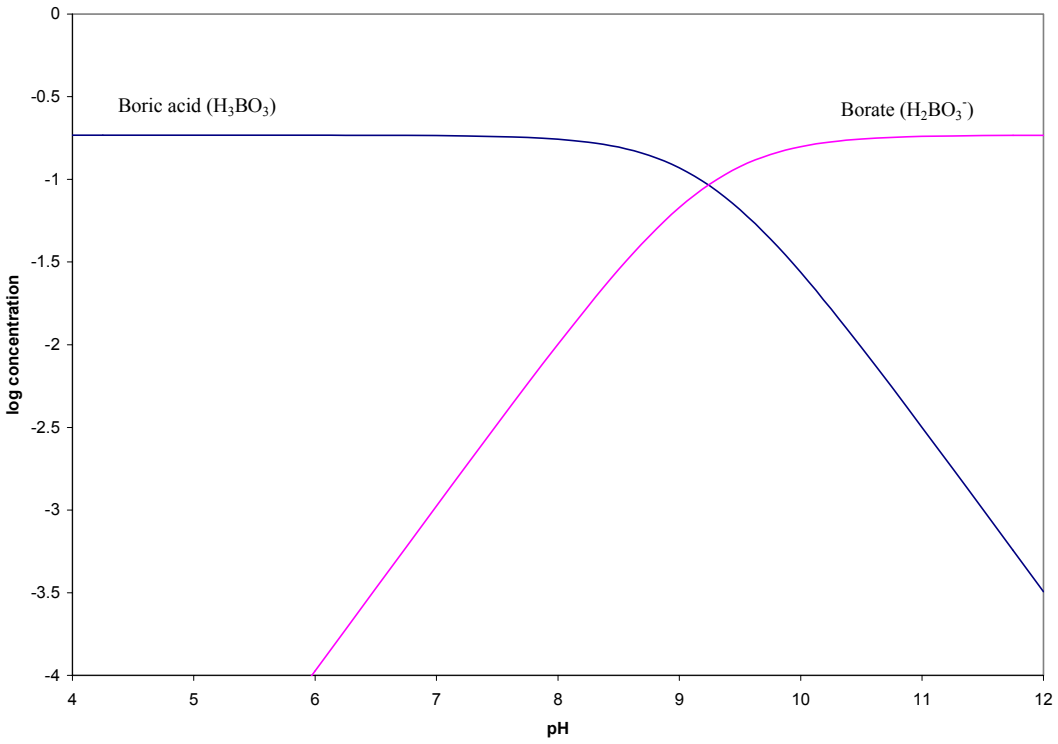

Fig. 3-1. Distribution of borate species as a function of pH.

The solubility of aluminum, iron, and zinc depend on pH, temperature, and ionic strength, as well as the presence of other chemical species. Metal solubility at the conditions in these experiments is shown in Fig. 3-2 as predicted by Visual Minteq. The pH values of minimum solubility for aluminum, iron, and zinc are 6.5, 8.5, and 9.0 respectively. For each metal, solubility increases as the pH deviates from this value. Over the pH range of 7 to 9, aluminum and iron are more soluble at 80°C than at room temperature (22°C), but zinc is less soluble under high-temperature conditions.

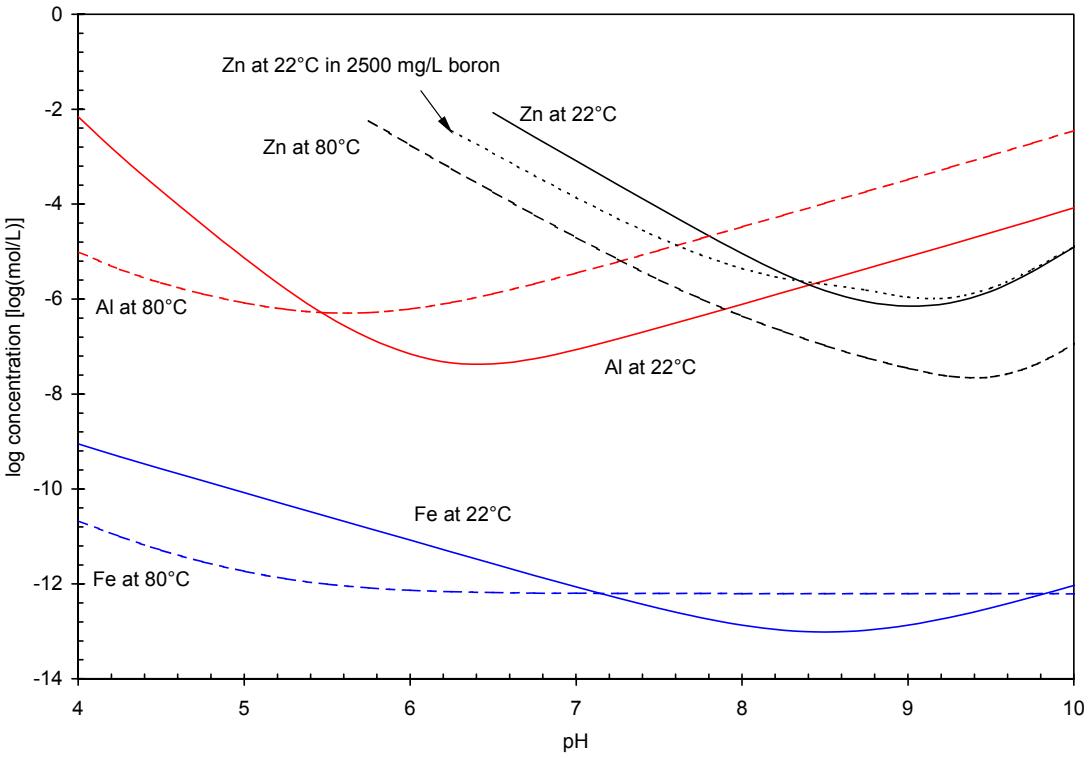

Fig. 3-2. Solubility of aluminum, iron, and zinc at conditions of experiment.

The most significant information from Fig. 3-2 is that all three metals have very low solubility at the conditions of these tests. At a pH of 9 and 22°C, the maximum metal concentrations in solution are 7.8×10^{-6} M for aluminum, 1.4×10^{-13} M for iron, and 7.1×10^{-7} M for zinc. Low solubility leads to greater opportunity for precipitation.

Table 3-5 gives the precipitation reactions and solubility constants for aluminum, iron, and zinc compounds. The predicted precipitates formed under the test conditions are $Al(OH)_3$ and Fe_2O_3 for aluminum and iron. For zinc, the solubilities of $Zn_5(CO_3)_2(OH)_6$ and $Zn(BO_2)_2$ are similar, and either product may form. With a borate concentration of 0.033 M, $Zn_5(CO_3)_2(OH)_6$ is the predicted precipitate over the entire pH range; however, with a borate concentration of 0.23 M, $Zn(BO_2)_2$ may precipitate at pH values below 8.5.

TABLE 3-4
ALUMINUM, IRON, AND ZINC SPECIES FORMED IN PWR COOLING WATER

Aluminum	Iron	Zinc
Soluble species		
Al^{+3}	Fe^{+3}	Zn^{+2}
$AlOH^{+2}$	$FeOH^{+2}$	$ZnOH^{+}$
$Al(OH)_2^{+}$	$Fe(OH)_2^{+}$	$Zn(OH)_{2\ (aq)}$
$Al(OH)_{3\ (aq)}$	$Fe(OH)_{3\ (aq)}$	$Zn(OH)_3^{-}$
$Al(OH)_4^{-}$	$Fe(OH)_4^{-}$	$Zn(OH)_4^{-2}$
$Al_2(OH)_2^{+4}$	$Fe_2(OH)_2^{+4}$	$ZnHCO_3^{+}$
$Al_3(OH)_4^{+5}$	$Fe_3(OH)_4^{+5}$	$ZnCO_{3\ (aq)}$
$Al_2(OH)_2CO_3^{+2}$	$FeH_2BO_3^{+2}$	$Zn(CO_3)_2^{-2}$
	$Fe(H_2BO_3)_2^{+}$	$ZnH_2BO_3^{+}$
		$Zn(H_2BO_3)_{2\ (aq)}$
Insoluble species		
$Al(OH)_3$	$Fe(OH)_3$	ZnO
$AlOOH$	$FeOOH$	$Zn(OH)_2$
Al_2O_3	Fe_2O_3	$ZnCO_3$
		$Zn_5(CO_3)_2(OH)_6$
		$Zn(BO_2)_2$

TABLE 3-5
PRECIPITATION REACTIONS AND SOLUBILITY CONSTANTS
FOR ALUMINUM, IRON, AND ZINC

Chemical Reaction	Log (Ksp)
$Al(OH)_3 + 3H^+ \rightleftarrows Al^{+3} + 3H_2O$	11.0
$AlOOH + 3H^+ \rightleftarrows Al^{+3} + 2H_2O$	8.8
$Al_2O_3 + 6H^+ \rightleftarrows Al^{+3} + 3H_2O$	20.1
$Fe(OH)_3 + 3H^+ \rightleftarrows Fe^{+3} + 3H_2O$	3.3
$FeOOH + 3H^+ \rightleftarrows Fe^{+3} + 2H_2O$	0.6
$Fe_2O_3 + 6H^+ \rightleftarrows Fe^{+3} + 3H_2O$	-1.19
$ZnO + 2H^+ \rightleftarrows Zn^{+2} + H_2O$	11.35
$Zn(OH)_2 + 2H^+ \rightleftarrows Zn^{+2} + 2H_2O$	11.68
$ZnCO_3 \rightleftarrows Zn^{+2} + CO_3^{-2}$	-10.8
$Zn_5(CO_3)_2(OH)_6 + 6H^+ \rightleftarrows 5Zn^{+2} + 2CO_3^{-2} + 6H_2O$	9.12
$Zn(BO_2)_2 + 2H_2O + 2H^+ \rightleftarrows Zn^{+2} + 2H_3BO_3$	8.29

4.0 HEAD-LOSS TESTS

4.1 Test Objectives

This phase of the test program has the following objectives:

1. to assess experimentally the degree of influence that water pH and temperature have on the head-loss characteristics of a fibrous bed during a LOCA in a PWR power plant;

2. to determine the additional head loss due to the precipitation of iron, zinc, and aluminum on a fibrous bed; and

3. to determine the head-loss characteristics of a fibrous bed under a prolonged-time-period test in a chemical environment.

4.2 Experimental Protocol

The current experiments evaluate the head loss caused by fibrous debris after being exposed to varying temperature and pH environments. The tests were performed in a small-scale hydraulic test loop, as shown in Fig. 4-1. A schematic of the test loop is shown in Fig. 4-2. The tests performed can be classified into three categories.

1. Tests were performed to validate the results obtained with the small-scale hydraulic test system with the test results obtained from an earlier large-scale hydraulic test system. Comparisons are made to the parametric equation developed for BWRs given in NUREG/CR-6224 [9].

2. Tests were performed in different chemical environments to understand the influence of water chemistry and temperature on head-loss characteristics.

3. Long-term head-loss tests were performed to determine if the fibrous bed head loss increases with time.

4.3 Experimental Test Loop

A closed-loop, vertical hydraulic test system, with a total fluid volume of 10.4 L, was built exclusively for measuring the head loss across a debris-laden screen in a chemical environment. This test facility, which was scaled down from an earlier test system that had a total volume of 110 gal. (416 L), was also used to perform head-loss tests. The large system was used to evaluate head loss produced by various debris that was generated during a LOCA, including NUKON™, CalSil, and RMI insulation. A detailed description, schematics, and photographs of the large-scale hydraulic test system are presented in Ref. 10. The large-scale system could not be used for the chemical effects testing because the large volume of that system would have required substantial quantities of chemicals to produce the required concentrations of boric acid, lithium, and metal ions, and the disposal of large volumes of chemically contaminated waters would have been problematic. To rectify this problem, the small-scale test system was built to mimic the

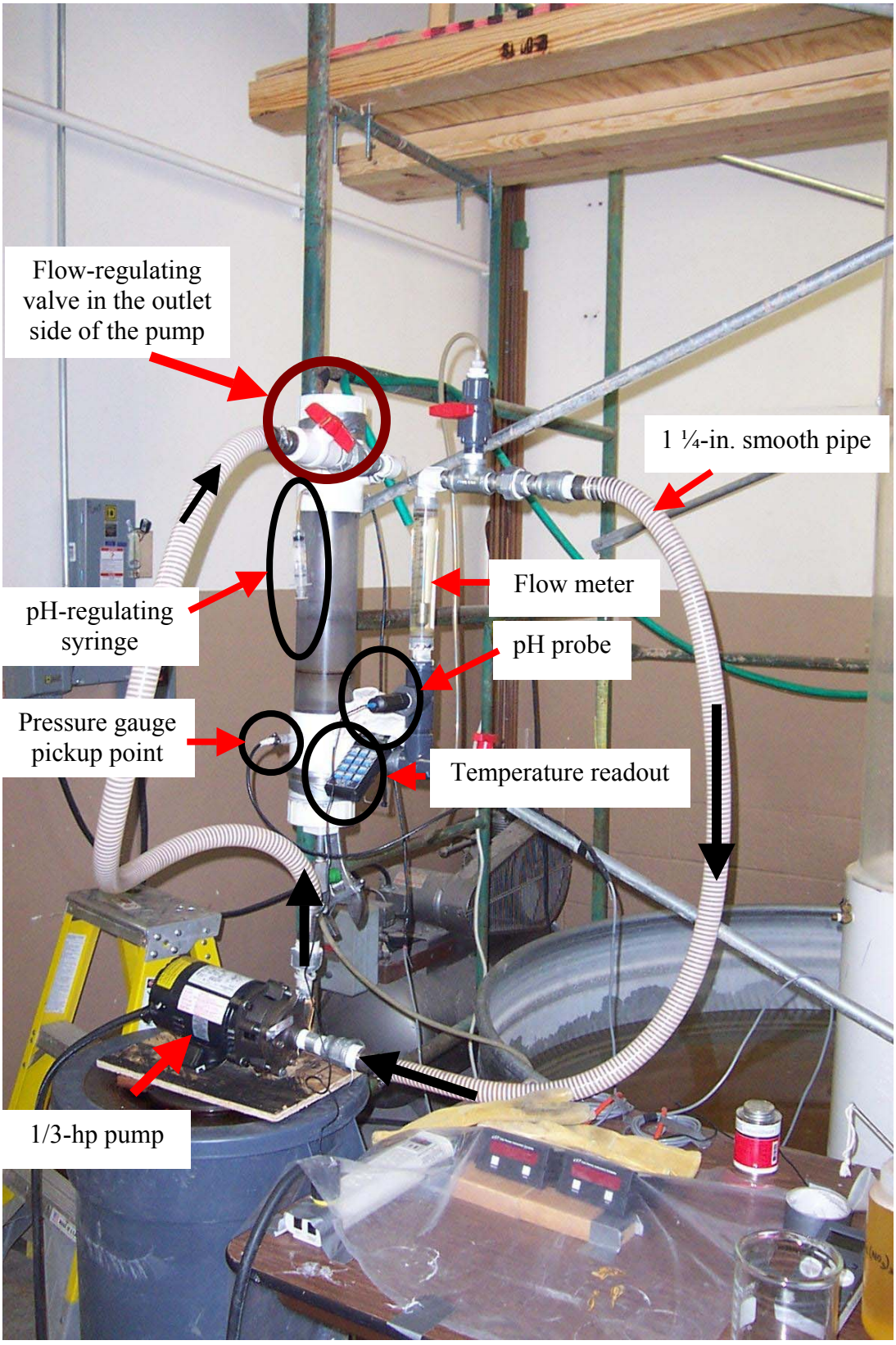

Fig. 4-1. Small-scale test loop for chemical head-loss tests.

hydraulics of the large system but with a smaller volume of water. As shown in Figs. 4-1 and 4-2, the primary test section of the experimental apparatus is a vertically oriented, 4-in.-diam clear PVC test section. A horizontal debris-bed test screen (1/8-in. rectangular mesh), shown in Fig. 4-3, is mounted approximately at mid-height within this pipe. The test screen is supported in the test section by a steel reinforcement screen, also shown in Fig. 4-3. The test screen mesh size is prototypic of the mesh size of actual screens used in some PWRs. (Please note that Fig. 4-3 is a photograph of the test screen and reinforcement screen used in the large-scale head-loss facility. The same types of test screen and reinforcement screen are used for the small-scale facility.)

The return line was equipped with an acrylic in-line flow meter that provided flow measurements between 2 and 20 gal./min, which corresponds to a test-section flow velocity between 0.05 ft/s and 0.5 ft/s, with an accuracy of ±5% and a repeatability of ±1%. The correlation between bulk flow, measured with one of these devices, and approach velocity at the debris screen was developed based on the principles of continuity and the geometry of the hydraulic loop. A thermocouple is located 6 in. below the test-screen level to measure the temperature of the flowing water in the test section. An online pH probe located below the flow meter provided continuous display of the pH level of the water in the test system. For controlling the pH level of the water, acid or base can be injected through a syringe, as shown in Fig. 4-1.

Instrument Calibration

Digital pressure gauges were used to measure head loss. The pressure gauges were calibrated in the test system by changing the water level progressively (increasing and decreasing) by a known quantity and measuring the differential readings between the top and bottom gauges. Actual water-level height was simultaneously measured with a ruler scale having 1/8-in. accuracy.

Closed-Loop Flow Control

Flow control within the closed hydraulic loop was controlled by adjusting the flow-regulating valve located downstream of the recirculation pump. To begin an experiment, the section is initially filled with deionized (DI) water. Once the loop is full of water, the hydraulic loop is operated in a recirculation mode. Water flow through the loop is maintained by operating a 1/3-hp recirculation pump located as shown in Fig. 4-1.

4.4 Test Procedure

Debris Preparation

Methods for debris preparation were developed in earlier experimental programs. Shredded NUKON™ fiber samples were generated by passing moderately sized (4-in. × 4-in. × 1-in.-thick) pieces of fiber blanket through a common leaf shredder. The shredded fibers were then cut into smaller lengths using scissors. The resulting fiber fragments were boiled for 20 min before use.

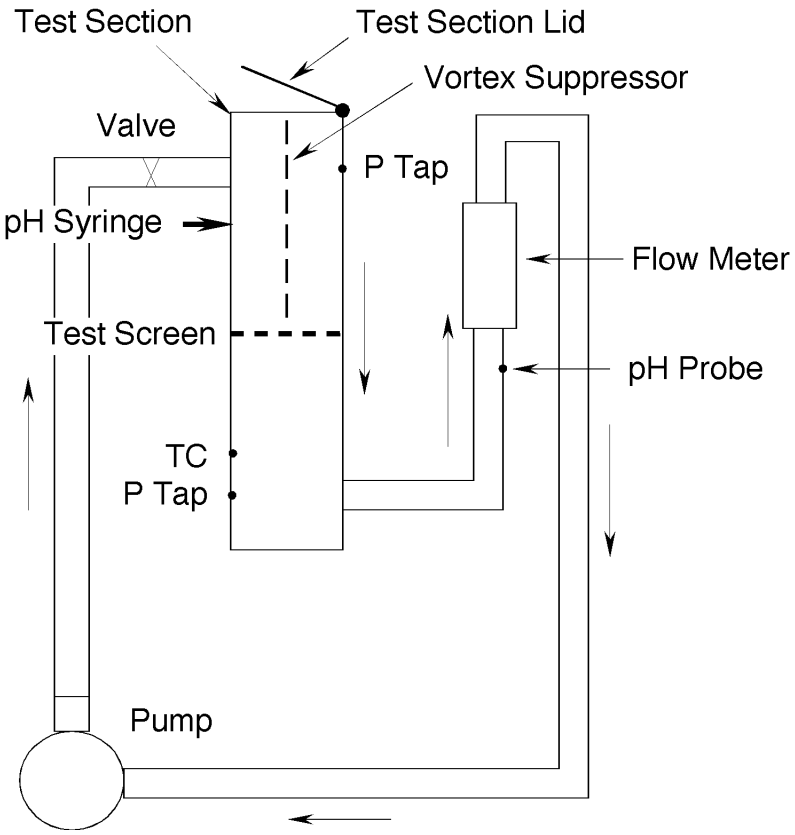

Fig. 4-2. Schematic of small-scale test loop.

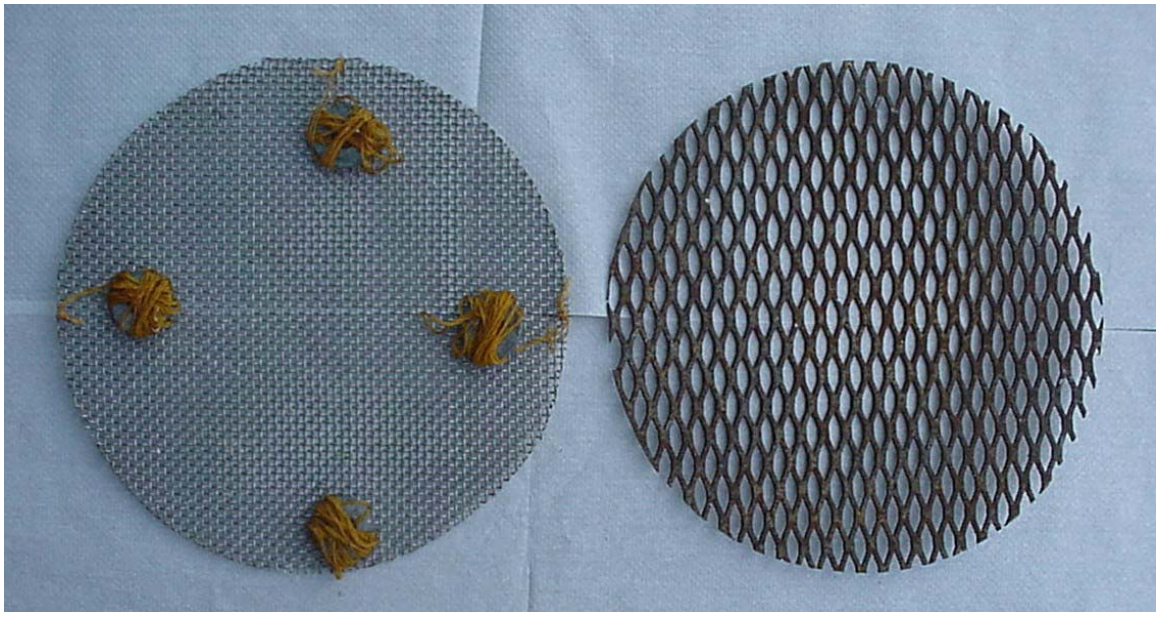

Fig. 4-3. Test screen (left) and supporting steel reinforcement (right).

Exploratory Testing

Before collecting data on the influence of water chemistry and precipitation on head loss, several exploratory tests were conducted to

- determine the limitations in experimental conditions (debris loading and/or flow velocity) that would not compromise the structural integrity of the test system and
- perfect the process for forming a uniform bed.

On the basis of the insights gained from these exploratory tests, a series of tests was conducted to measure the head loss.

Debris Quantity

Initial tests were performed using a theoretical bed thickness of 0.023 ft^3/ft^2. The theoretical bed thickness is calculated by dividing the fiber-sample mass by the as-manufactured insulation density and by the total flow path area. Theoretical thickness is commonly used as a basis for comparing the effects of bed compression under different particulate loadings and flow conditions. With such a small quantity of debris, it was difficult to consistently get a uniform bed. Past experience demonstrates that a small variation in the bed formation can influence the head-loss characteristics considerably. When the fiber quantity was doubled, a more uniform bed was formed and with less variation from one bed to the next. As a result, a theoretical bed thickness of 0.046 ft^3/ft^2 was used for most of the experiments.

The test system is designed to handle a maximum head loss of about 20 ft of water. The maximum quantity of NUKON™ that could be tested was limited by the corresponding head loss it would produce across the screen. With high head loss through the fibrous bed, the test section below the support screen may be subjected to negative pressure (suction), which may have negative consequences on the experiment or prevent the pump from operating correctly if the net positive suction head required (NPSHR) of the pump were exceeded.

Debris Addition

Because the distance between the top of the test system and the support screen is small (20 in.), the method for releasing debris into the test section has a strong influence on the uniformity of the fibrous bed. Experimentation with various methods demonstrated that maintaining a low approach velocity and adding the NUKON™ slowly produced the most uniform bed.

The method used for adding NUKON™ to the test system was as follows. The test section was filled with DI water to the level of the inlet pipe. The recirculation pump was turned on, and the flow control valve was set to an approach velocity of 0.1 ft/s in the test section. Half of the prepared NUKON™ was added to the test system and allowed to settle against the retaining screen; after it had settled against the screen, the remaining NUKON™ was added and allowed to settle against the screen. When the uniform bed was formed, the flow-regulating valve was adjusted to produce the desired flow rate for each experiment. The maximum approach velocity

in the test section was 0.51 ft/s, corresponding to a flow of 20 gal./min, which was the maximum reading on the flowmeter.

4.4.1 Validation of the Small-Scale Test Loop

Table 4-1 gives the range of specific test conditions studied for validation of the small-scale test system. For most tests, head-loss values were observed for 1 h. The pH level, approach velocity, and fiber quantity were varied. Experimental head-loss results obtained were compared with the head loss predicted by the parametric correlation published in NUREG/CR-6224 [9].

TABLE 4-1
TEST MATRIX FOR THE VALIDATION OF THE SMALL-SCALE TEST LOOP

Test ID	pH			Approach Velocity (ft/s)				Fiber Quantity (ft^3/ft^2)	
	7	8	9	0.3	0.36	0.38	0.4	0.023	0.046
1a	X			X				X	
1b			X	X				X	
1c		X		X				X	
1d			X	X				X	
2a	X				X				X
2b	X						X		X
3a			X		X				X
3b			X			X			X
4a	X			X					X
4b	X					X			X

The volume of water in the large-scale test system used in earlier experiments had sufficient mass (i.e., heat content) to maintain a constant temperature over the course of each experiment. However, the small-scale test loop had less thermal mass to resist temperature variations during the experiments. In addition, head loss occurred throughout the system, including the throttling valve used to control the flow rate; this head loss transferred energy to the water, which was manifested as an increase in temperature. The temperature rise during a typical experiment is shown in Fig. 4-4. On average, about a 16°C rise in water temperature occurred during a 1-h test run. This rise corresponds to a drop in the head-loss value of 0.3 ft of water. Figure 4-5 gives the head loss with time for test No. 2a in Table 4-2. The lower curve is based on the experimental values, and the other curve is obtained when normalized to an initial temperature of 27°C.

Head loss is a function of the flow temperature. NUREG/CR-6224 provided two parametric equations for the head loss in an incompressible pure fibrous bed: one equation at 60°F and the other at 120°F. The two equations are

$$\Delta H = [7.4\ U + 4.1\ U^2]\ \Delta L_o\ @\ 60°F \qquad (4\text{-}1)$$

and

$$\Delta H = [3.7\ U + 4.1\ U^2]\ \Delta L_o\ @\ 120°F\ , \qquad (4\text{-}2)$$

where ΔH is the head loss in feet of water, U is the approach velocity in feet per second, and ΔL_o is the theoretical bed thickness in inches.

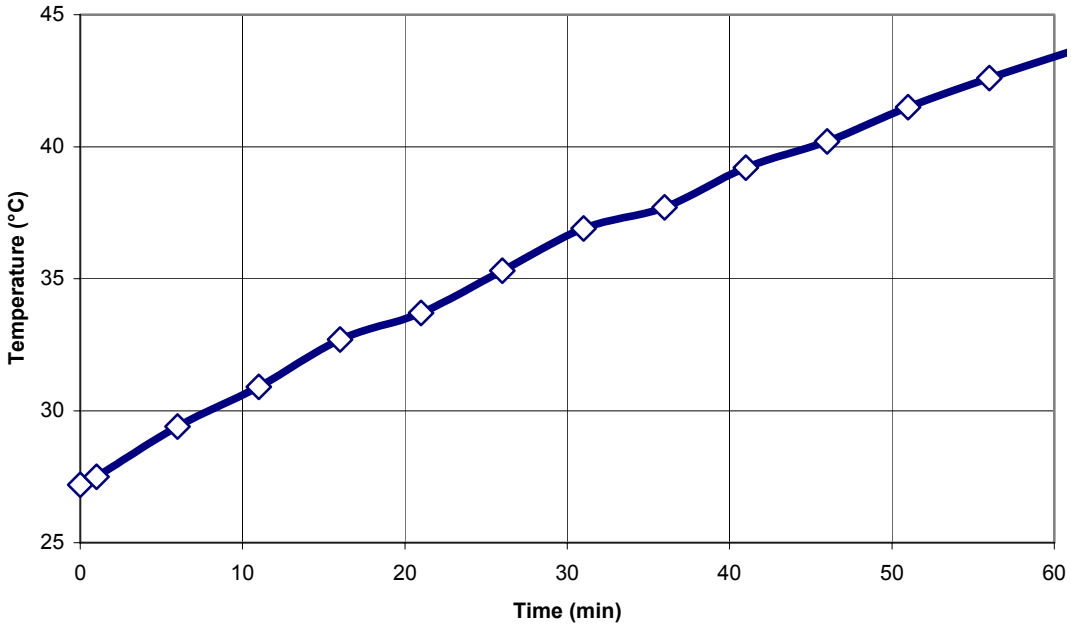

Fig. 4-4. Rise in flow temperature with recirculation time.

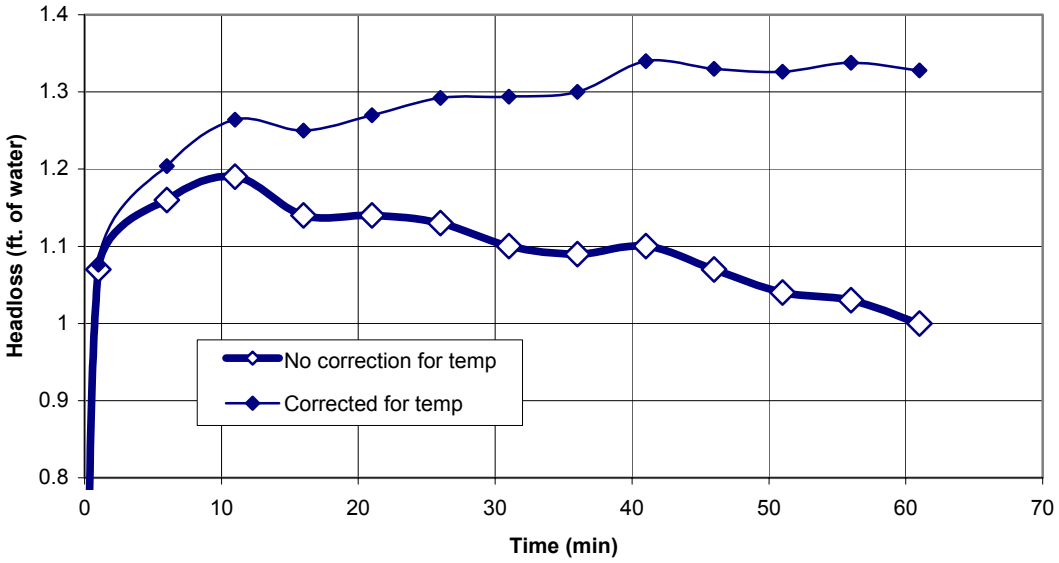

Fig. 4-5. Variation in head loss with time, with and without correction for temperature.

TABLE 4-2
VALIDATION TEST RESULTS FOR SMALL-SCALE TEST-LOOP

Test ID	Characteristics of the Test Regime	NUKON™ (g) - pH of Water	Velocity (ft/s)	Head Loss (ft H_2O)	Parametric (v = 0.5 ft/s and T = 60°F)	% Variation and Remarks
1a	@ 0.3 ft/s head loss = 0.34 ft, and the bed was uniform	2.2 - 7	0.3	1.36	1.17	+16
	@ 0.3 ft/s head loss = 0.51 ft, and the bed was uniform	2.2 - 7	0.3	1.53	1.17	+31
	@ 0.3 ft/s head loss = 0.35 ft, and the bed was uniform	2.2 - 7	0.3	1.37	1.17	+17
	@ 0.3 ft/s head loss = 0.2 ft, and the bed was nonuniform	2.2 - 7	0.3	1.22	1.17	+4.2
1b	@ 0.3 ft/s head loss = 0.3 ft, and the bed was uniform	2.2 - 9	0.3	1.32	1.17	+12.8
1c	@ 0.3 ft/s head loss = 0.46 ft, and the bed was uniform	2.2 - 8	0.3	1.48	1.17	+26
1d	@ 0.3 ft/s head loss = 0.38 ft, and the bed was uniform	2.2 - 9	0.3	1.40	1.17	+19.6
2a	T_0 = 27.2°C; T_f = 42.9°C; room temperature = 23.1°C; head-loss curve is given in Fig. 4-5	4.4 - 7	0.357	2.275	2.35	-3.2
2b	@0.40848 ft/s head loss = 1.12 ft, and bed was uniform	4.4 - 7	0.41	2.1	2.35	-10.6
	@0.40848 ft/s head loss = 1.61 ft, and bed was uniform	4.4 - 7	0.41	2.59	2.35	+10.2
	@0.40848 ft/s head loss = 1.62 ft, and bed was uniform	4.4 - 7	0.41	2.60	2.35	+9.6
	@0.40848 ft/s head loss = 1.79 ft in 15 min; bed was uniform on the day of the demonstration	4.4 - 7	0.41	2.55	2.35	+8.5
3a	ΔT = 24 to 36°C; head loss = 1.2 ft @0.38 ft/s in 45 min	4.4 - 9	0.36	2.02	2.35	-14
3b	ΔT = 24 to 36°C; head loss = 1.2 ft @0.38 ft/s in 45 min	4.4 - 9	0.38	2.2	2.35	-6.4
	ΔT = 28 to 41°C; head loss = 0.89 ft @0.36 ft/s in 45 min	4.4 - 9	0.38	1.99	2.35	-15.3
4a	ΔT = 33 to 44°C; head loss = 0.77 ft @0.32 ft/s in 45 min	4.4 - 7	0.32	2.19	2.35	-6.8
4b	Head loss is 1.14ft @ 0.38 ft/s in 45 min	4.4 - 7	0.38	2.28	2.35	-2.9
	ΔT = 33 to 42°C, head loss = 0.9 ft @0.38 ft/s in 45 min	4.4 - 7	0.38	2.02	2.35	-14

Tests 3–4 were performed in DI water.

Head loss through packed beds is the sum of two terms; the first term is proportional to the first power of fluid velocity, and the second is proportional to the square of the fluid velocity. The first term arises from viscous energy losses, and the second arises from kinetic energy losses. As a result, the first term is linearly proportional to fluid viscosity, which in turn is dependent on temperature, and the two parametric equations can be combined into a single equation that accounts for both temperature and velocity as

$$\Delta H = (k_1 \mu U + k_2 U^2) \Delta L_o \quad . \tag{4-3}$$

Comparison of this equation with the two parametric equations in NUREG/CR-6224 produces

$$\Delta H = (3.18 \times 10^5 \mu U + 4.1 U^2) \Delta L_o \quad , \tag{4-4}$$

where

ΔH = head loss (ft of water),
μ = viscosity (lb s/ft^2),
U = velocity (ft/s), and
ΔL_o = theoretical bed thickness (in.).

The relationship between temperature and viscosity is shown in Fig. 4-6. Figure 4-7 shows the head loss as a function of water temperature for different approach velocities, as calculated from Eq. (4-4).

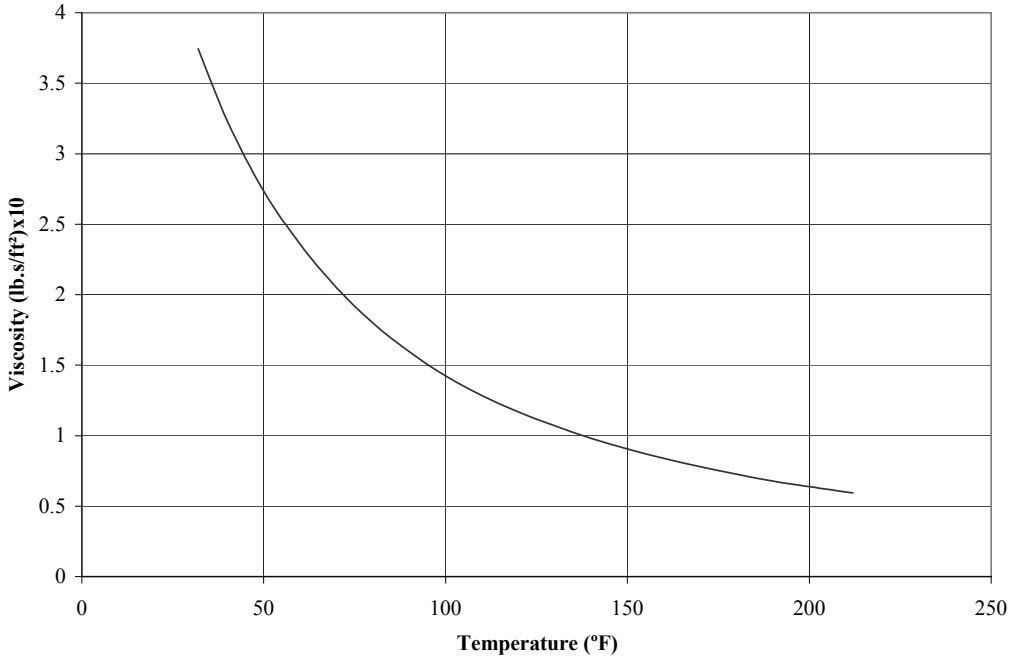

Fig. 4-6. Viscosity of water with temperature.

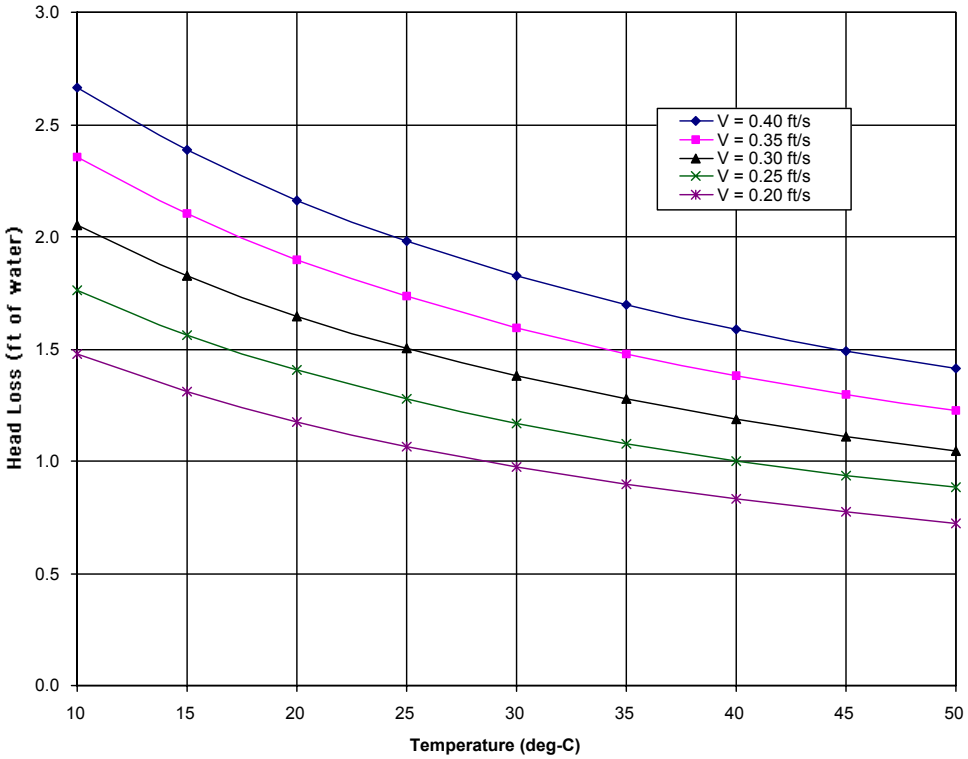

Fig. 4-7. Calculated head loss vs temperature at different approach velocities (bed depth = 0.4967 in.)

Experiments were also conducted with and without the top of the test section being open to evaluate the difference in the temperature rise and the amount of entrained air in the water. Temperature rise was observed with the top open and closed. The temperature rise is seen to be higher when the top is closed (see Fig. 4-8). With the top closed, the amount of entrained air was smaller than when the top was kept open.

During the initial head-loss tests, it was found that excessive head loss was generated when the metal precipitates were added to the water. As a result, modifications were made to the test system to provide for more reliable flow control. The modifications consisted of (1) replacement of the 0.75-in. hose to and from the pump with 1.25-in. smooth tubing, (2) relocation of the flow-regulating valve to be just upstream of the test section, and (3) installation of a slightly smaller pump. The installation of a smaller pump was anticipated to reduce the rate of temperature rise in the water; however, temperature still increased as a result of head loss throughout the system. The temperature reached a steady-state value of about 50°C to 55°C about 2.5 h after recirculation was started. After the modifications, water was recirculated for 2.5 h, before the addition of metal ion solutions to the test system to allow the tests to be done at a constant temperature.

At flow rate of 20 gal./min, the flow caused a vortex inside the test section, which affected the development of the fibrous bed. This circular motion of flow was eliminated by placing a baffle inside the test section.

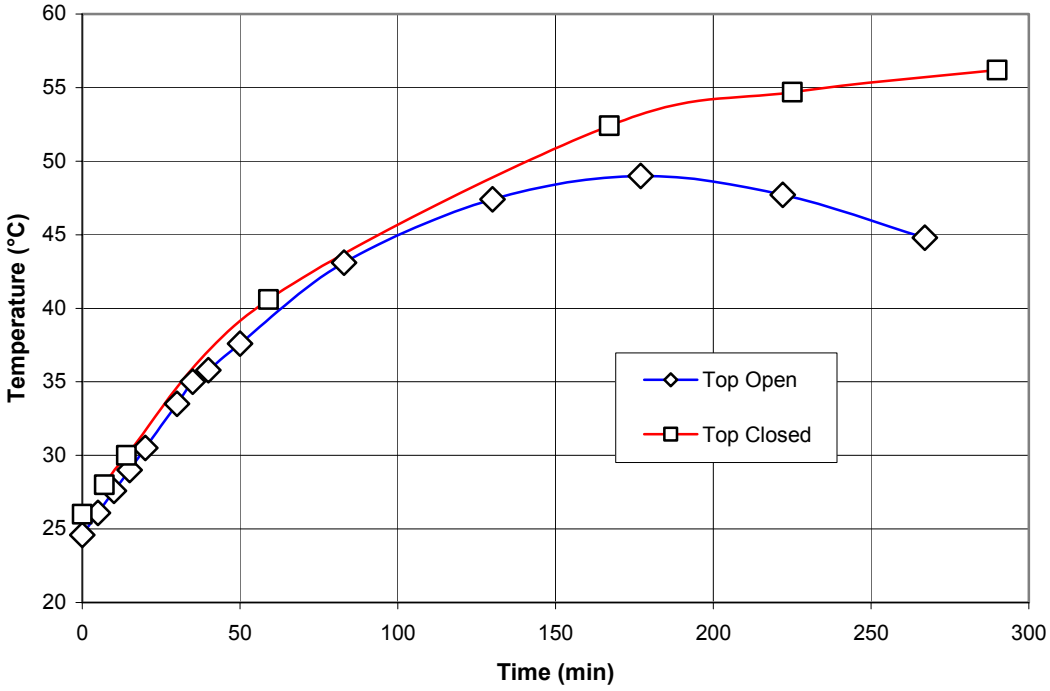

Fig. 4-8. Rise in flow temperature with the test section open and closed.

4.4.1.1 Observations

Validation test results are given in Table 4-2. The temperature, pH, velocity, and head-loss values given in this table were taken at the end of 1 h of recirculation. Values of head loss that were calculated with Eq. (4-4) for corresponding temperature and velocity values are also shown in Table 4-2 for comparison to the experimental values. The variation between the experimental and calculated values is less than 20% for all experiments, except two cases when the variation was closer to 30%. This level of variation is similar to that observed in the large-scale test system. The parametric head-loss equations reported in NUREG/CR-6224 were developed using the large-scale test system, and NUREG/CR-6224 reported that "the majority of the head-loss data obtained for NUKON™ can be predicted by these equations within ± 20 percent." These results demonstrate that the small-scale hydraulic test loop performed similarly to the large-scale hydraulic test loop. These results, along with the head-loss values that were corrected for temperature in Fig. 4-5, also suggest the validity of correcting head-loss values for temperature by using Eq. (4-4).

4.4.2 Effect of Water pH on Head Loss in a Fibrous Bed

The experiments used to validate the performance of the small-scale test system were performed at several pH values ranging from pH = 7 to pH = 9. These results are shown in Table 4-2. The results in this table suggest that changes in pH ranging from pH = 7 to pH = 9 do not have a substantial impact on the head loss through a fibrous bed over the duration of these experiments. Because initial indications showed that chemical effects on head loss due to metal precipitation had a much greater effect than pH changes on the fibrous bed, more extensive testing of this

experimental objective was not pursued. Results of the effects of metal precipitation on head loss through a fibrous bed are discussed in more detail in the following sections.

4.4.3 Head Loss Caused by Precipitation of Dissolved Metal

The purpose of this group of experiments was to determine whether precipitated aluminum, iron, and zinc compounds have an adverse effect on the generation of head loss through the bed of fibrous material captured by sump screens during a LOCA. Rates of corrosion of base metals that are necessary to produce the precipitates were not studied under this task; the ability of these metals to corrode under the conditions typical of a LOCA were studied separately and will be reported later in this document. To facilitate the rapid formation of metal precipitates, the metal ions were added as soluble salts, which is similar to the method where coagulants are added to water during municipal water treatment. Various metal salts were considered, with the resulting decision that the metal ions were added to the water as nitrate salts. Nitrate salts were selected because water chemistry modeling demonstrated that nitrates would have little or no impact on the distribution of the species of interest (borate and lithium in addition to the metals). Chloride salts were also considered but were rejected because chlorides are controlled tightly in the primary coolant and nitrates are controlled only to a lesser degree. It was determined that chlorides were less likely to be present in cooling water unless radiolytic decomposition of cable insulation material within the containment structure occurred. In addition, chloride will combine slightly more with zinc than with nitrate. Complexation increases the solubility of metals and reduces the formation of precipitates, and given that the objective is to form as much precipitate as possible to evaluate the effect of precipitates on head loss, chemicals that caused complexation were avoided as much as possible.

In addition to aluminum, iron, and zinc, the experiments also considered the addition of calcium to the pool water. Calcium was considered because of the possibility of calcium being introduced into the water from the erosion or corrosion of concrete.

Previous studies, as reported in Section 3.3, suggested that corrosion during a LOCA could produce a maximum soluble zinc ion concentration of 8.8×10^{-3} M and a maximum soluble aluminum ion concentration of 9.2×10^{-3} M. These values represent the corrosion of about 2000 lb of zinc and 1000 lb of aluminum and the dissolution of these metals into 1 million gal. (Mgal.) of water; these were considered to be the upper limits for the amount of metal that may corrode during a LOCA. Thus, the experiments considered a maximum concentration of 1.0×10^{-2} M for each of the metal ions of interest.

The use of phosphate and thiosulfate salts was considered because some facilities add one or both of these chemicals to the cooling water in the event of an accident. Phosphate and thiosulfate both are complexing agents that increase the solubility of metals and would reduce the production of precipitates in these experiments. These chemicals are not in universal use, and their absence is a more conservative evaluation of the effect of precipitation on head loss. As a result, neither phosphate or thiosulfate was used in these experiments.

The water used in the experiments was DI water that was supplemented to approximate the cooling-water composition. The primary additives in cooling water are boric acid and lithium.

Boric acid and lithium concentrations during a LOCA were presented in Table 3-3; the maximum values present during a LOCA were selected for these experiments to simulate maximum-concentration conditions. Due to a calculation error, 2000 mg/L of boric acid was added (3.3×10^{-2} M) rather than 2000 mg/L of boron (1.85×10^{-1} M). Water chemistry modeling, as well as confirmatory tests, demonstrated that this difference in boric acid concentration had no appreciable impact on the results of these experiments. Lithium was added at a concentration of 1.4 µg/L (2.0×10^{-4} M).

Experiments were performed at specific pH values. Sodium hydroxide (1 N NaOH) was added to increase the pH, and hydrochloric acid (1 N HCl) was used to decrease the pH.

The chemicals used in these experiments are shown in Table 4-3, and the matrix of experiments is shown in Table 4-4.

4.4.3.1 Solution Preparation

The water volume required to fill the test system was 10.4 L. Accordingly, the amount of chemicals needed to arrive at a particular concentration can be calculated. The required quantity of each chemical was weighed on an analytical balance and dissolved in distilled water to get the desired concentration.

To explain further, an example is given below.

To obtain a concentration of 1.0×10^{-2} M of aluminum ions, the desired molar concentration is multiplied by the molecular weight and the total volume of solution to be prepared.

Thus,

$$(1.0 \times 10^{-2} \text{ mol/L}) \times (10.4 \text{ L}) \times (375.13 \text{ g/mol}) = 39.11 \text{ g} \quad ,$$

i.e., to get a concentration of 1.0×10^{-2} M, 39.11 g of aluminum nitrate salt is dissolved in 1 L of DI water and added in the test system, where it is diluted to a total volume of 10.4 L. Chemicals

TABLE 4-3
CHEMICALS ADDITIVES AND THEIR CHARACTERISTICS

Chemical	Formula	Molecular Weight (g/mol)	Solubility (g/L)
Boric acid	H_3BO_3	61.83	63.5
Lithium hydroxide	LiOH	23.95	128.0
Sodium hydroxise	NaOH	34.99	Soluble
Iron nitrate nonahydrate	$Fe(NO_3)_3\ 9H_2O$	404.00	Soluble
Aluminum nitrate nonahydrate	$Al(NO_3)_3\ 9H_2O$	375.13	637
Zinc nitrate hexahydrate	$Zn(NO_3)_2\ 6H_2O$	297.47	1843
Calcium hydroxide	$Ca(OH)_2$	74.00	18.5

TABLE 4-4
TEST MATRIX FOR METALS ADDED DURING THE CHEMICAL PRECIPITATION HEAD-LOSS TESTS

Test ID	Added Metal Ion Concentration (M)			
	Aluminum	Iron	Zinc	Calcium
5a	1.0×10^{-2}	1.0×10^{-2}	1.0×10^{-2}	1.0×10^{-2}
5b	2.0×10^{-3}	2.0×10^{-3}	2.0×10^{-3}	2.0×10^{-3}
6a	1.0×10^{-2}			
6b	2.0×10^{-3}			
6c	1.0×10^{-3}			
6d	5.0×10^{-3}			
6e	2.5×10^{-4}			
6f	1.0×10^{-4}			
7a		1.0×10^{-2}		
7b		2.0×10^{-3}		
7c		1.0×10^{-3}		
7d		5.0×10^{-4}		
7e		1.0×10^{-4}		
8a			1.0×10^{-2}	
8b			2.0×10^{-3}	
8c			2.0×10^{-4}	
8d			5.0×10^{-5}	
9				1.0×10^{-4}
10a	2.0×10^{-4}			
10b	5.0×10^{-4}			
10c	8.0×10^{-4}			
10d			2.0×10^{-4}	
10e			4.0×10^{-4}	
10f			8.0×10^{-4}	

were added to 1 L of DI water before introduction into the test system to ensure that all chemicals were completely dissolved at the beginning of the test.

4.4.3.2 Test Procedure

The experiments were conducted according to the following procedure.

1. The test section was filled partially with DI water.

2. The background chemistry solution (containing boric acid and lithium) was added into the test system.

3. The pump was started and the flow was adjusted to a low approach velocity (4 gal./min, i.e., 0.1 ft/s).

4. Half of the prepared NUKON™ (approximately 2.2 gm) was added to the test system and allowed to settle against the retaining screen; after it had settled against the screen, the remaining NUKON™ (a total of 4.4 gm) was added and allowed to settle against the screen. The procedure of adding the NUKON™ in two batches was found to produce a more consistent fibrous bed.

5. Metal nitrate salt solutions were added to the test system. Precipitation occurred immediately upon mixing of the metal nitrate solution and the background chemistry solution in the test system because the boric acid buffered the solution at a pH value where aluminum, iron, and zinc are insoluble.

6. Additional DI water was added until the test system was full.

7. The pH was adjusted to the desired value.

8. The approach velocity was increased to the experimental value.

9. Head-loss readings were taken, along with temperature and time.

10. The pH of the solution was kept at the required value by adding an NaOH or HCl solution into the test system as necessary.

4.4.3.3 Observations

A large number of experiments, with varying concentrations of metal ions, were conducted according to the matrix shown in Table 4-4. A summary of all head-loss experiments with metal precipitates is presented in Table 4-5. The first two experiments (Tests 5a and 5b) involved the simultaneous addition of all metal precipitates (aluminum, iron, zinc, and calcium), whereas the remaining experiments were each done with only one metal ion present.

Head-loss values were found to be extremely high for the first experiments (with all metals present). In addition, the water velocity could not be maintained because of the additional head loss in the test system, and the tests had to be terminated after 12 to 15 min of recirculation. For these first two tests, the measured head loss ranged from 13 to 15 ft, as compared with a calculated value of 0.25 ft for a fibrous bed without precipitates at the measured velocity and temperature conditions using Eq. (4-4). The difference between the measured and calculated values represents a 50x increase in the head loss due to the addition of metal precipitates. Because the head loss with all metals simultaneously was so substantial, the remaining tests were conducted with only one metal each so that the effects of the additional metals could be isolated. In addition, the concentration of metal ions was gradually reduced in successive experiments until the head-loss values achieved were nearly equal to that for a fibrous bed alone.

TABLE 4-5
HEAD LOSS OF FIBROUS BED FOLLOWING THE PRECIPITATION OF METAL SALTS

Test ID	Metal	Conc. (M)	Test Duration (min)	pH	Velocity* (ft/s)	Temp* (°C)	Measured Head Loss* (ft)	Calculated Head Loss† (ft)	Ratio‡	Bed Morphology
5a	All	1.0×10^{-2}	15	~7.0	0.075	22	15.28	0.25	60.0	very shiny
5b	All	2.0×10^{-3}	12	~7.0	0.075	22	13.45	0.25	52.8	very shiny
6a	Al	1.0×10^{-2}	8	-	0.36	22	14.6	1.43	10.2	very shiny
6b	Al	2.0×10^{-3}	15	~7.0	0.075	32.2	17.18	0.2	85.1	very shiny
6c	Al	1.0×10^{-3}	60	7.13	0.13	41	6.8	0.31	21.9	very shiny
6d	Al	5.0×10^{-4}	60	~7.0	0.33	43.4	3.47	0.89	3.88	very shiny
6e	Al	2.5×10^{-4}	60	~7.0	0.38	41.6	2.23	1.09	2.05	shiny
6f	Al	1.0×10^{-4}	60	~7.0	0.31	45.1	1.55	0.81	1.91	shiny
7a	Fe	1.0×10^{-2}	60	-	0.24	26.3	8.33	0.81	10.3	shiny
7b	Fe	2.0×10^{-3}	60	~7.0	0.075	40	4.23	0.17	24.4	shiny
7c	Fe	1.0×10^{-3}	60	~7.0	0.35	36.7	5.82	1.06	5.49	shiny
7d	Fe	5.0×10^{-4}	60	~7.0	0.36	42.6	5	1.00	4.96	shiny
7e	Fe	1.0×10^{-4}	60	~7.0	0.33	43.4	1.74	0.97	1.80	shiny
8a	Zn	1.0×10^{-2}	10	~7.0	0.075	25	12.16	0.23	52.3	shiny
8b	Zn	2.0×10^{-3}	7	-	0.37	35	4.26	1.16	3.67	shiny
8c	Zn	2.0×10^{-4}	60	~7.0	0.38	44.5	3.26	1.05	3.12	shiny
8d	Zn	5.0×10^{-5}	60	-	0.35	40.3	1.0	1.00	0.99	shiny
9	Ca	1.0×10^{-4}	60	~7.0	0.40	45	0.9	1.1	0.81	dull
10a	Al	8.0×10^{-4}	60	~7.0	0.51	38	6.00	1.68	3.60	very shiny
10b	Al	5.0×10^{-4}	60	~7.0	0.51	46	6.01	1.52	3.95	very shiny
10c	Al	2.0×10^{-4}	60	~7.0	0.51	42	4.68	1.59	2.94	shiny
10d	Zn	8.0×10^{-4}	60	~7.0	0.51	44	7.04	1.56	4.50	shiny
10e	Zn	4.0×10^{-4}	60	~7.0	0.51	43	6.43	1.58	4.10	shiny
10f	Zn	2.0×10^{-4}	60	~7.0	0.51	45	4.5	1.54	2.93	shiny

Notes:
* Velocity, temperature, and measured head loss are reported for the end of the experiment.
† Calculated head loss is the value calculated using the parametric equations developed in NUREG/CR-6224, which gives the head loss for an incompressible pure fibrous bed of NUKON™ at the given temperature and water velocity (i.e., without metal precipitates).
‡ Ratio = measured head loss (including metal precipitates) divided by calculated head loss (fibrous NUKON™ only). The ratio provides a value for the increase in head loss resulting from the addition of metal precipitates to the fibrous bed.

The addition of aluminum was equivalent to concentrations ranging from 2.7 mg/L (1.0×10^{-4} M) to 270 mg/L (1.0×10^{-2} M). These values would be equivalent to the dissolution of 23 to 2300 lb of aluminum in 1 Mgal. of water. At concentrations of 54 mg/L (2.0×10^{-3} M), measured head loss was about two orders of magnitude higher than predicted by Eq. (4-4). In addition, the tests had to be terminated in 15 min or less and the water velocity was reduced due to the excessive head loss. With lower aluminum addition, the tests could be run for the full 60 min. At the lowest concentration, 23 lb/Mgal., the head loss was nearly double the value predicted by Eq. (4-4).

Similar results were observed for zinc addition. The addition of zinc was equivalent to concentrations ranging from 3.3 mg/L (5.0×10^{-5} M) to 654 mg/L (1.0×10^{-2} M), or concentrations of 27.5 lb/Mgal. to 5400 lb/Mgal. At concentrations above 2.0×10^{-3} M, tests were terminated in 15 min or less, with reduced water velocities due to excessive head loss. With lower zinc addition, the tests could be run for the full 60 min. At the lowest concentration, 27.5 lb/Mgal., the head loss was the same with or without the precipitate, according to the comparison of measured and calculated values, but the addition of 110 lb/Mgal. of zinc caused triple the head loss predicted by Eq. (4-4).

Head loss with iron does not appear to be quite as extensive as head loss with aluminum or zinc. All tests with iron could be run for the full 60 min, and the head loss did not exceed 10 ft at the end of any of the tests. The maximum increase in head loss with iron precipitates was 24.4 times the value predicted by Eq. (4-4), as compared with maximum values of 50 times to 85 times in the cases of zinc and aluminum, respectively.

Test groups 5 through 9 (see Tables 4-4 and 4-5) were conducted before modifications to the test system that provided more reliable flow control, as discussed previously. The remaining test groups were conducted after the modifications. The results of the experiments before and after the modifications are consistent with one another.

A graphical summary of the head-loss data with precipitates is shown in Fig. 4-9. A line showing head loss caused by the fibrous bed alone at 0.5 ft/s and 60°C is incorporated in the figure to compare the amount of additional head loss that can be caused by these precipitates at different concentrations. However, it should be noted that some of the highest head-loss values occurred at velocities significantly below the 0.5 ft/s value used for comparison with the fibrous bed. As a result, the difference between head loss with and without precipitates can be even more dramatic than that shown in Fig. 4-9. A second representation of the difference in head loss with and without precipitates is shown in Fig. 4-10. This figure shows the ratio of measured-to-calculated values of head loss (which represents the head loss with and without precipitates) as a function of the metal addition. At higher values of metal addition, the additional head loss caused by the addition of precipitates is substantial.

Figures 4-11 and 4-12 show the views of the fibrous beds coated with a precipitation of aluminum and iron, respectively, at different concentrations. Figure 4-13 shows the environmental scanning electron microscope (ESEM) of fibrous bed without any precipitation. Figures 4-14 through 4-16 show the ESEM views of the fibrous bed coated with different chemical precipitations.

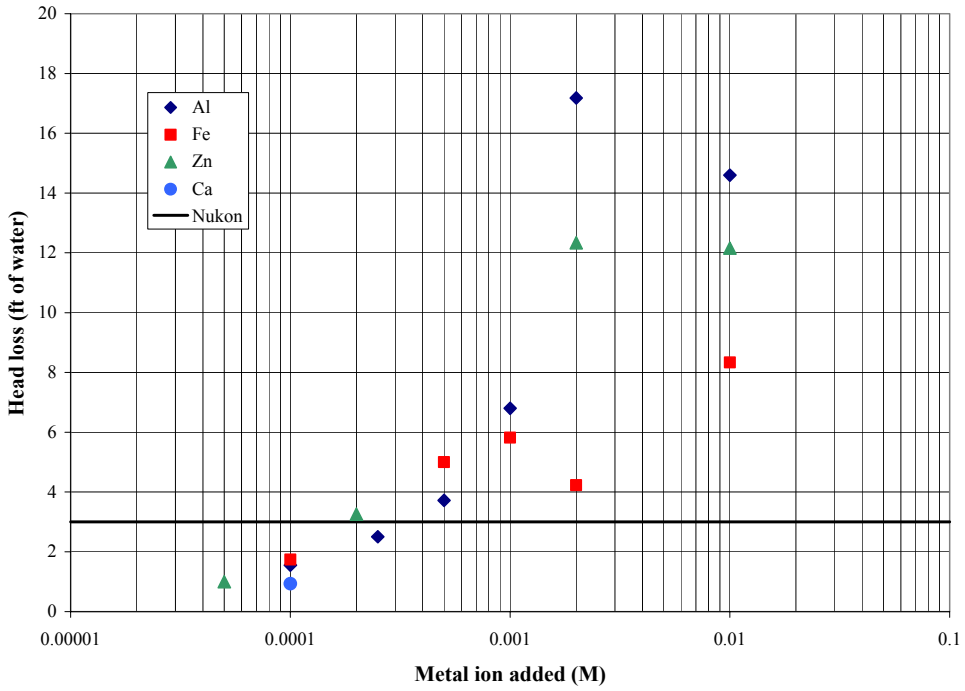

Fig. 4-9. Head loss vs material concentration.

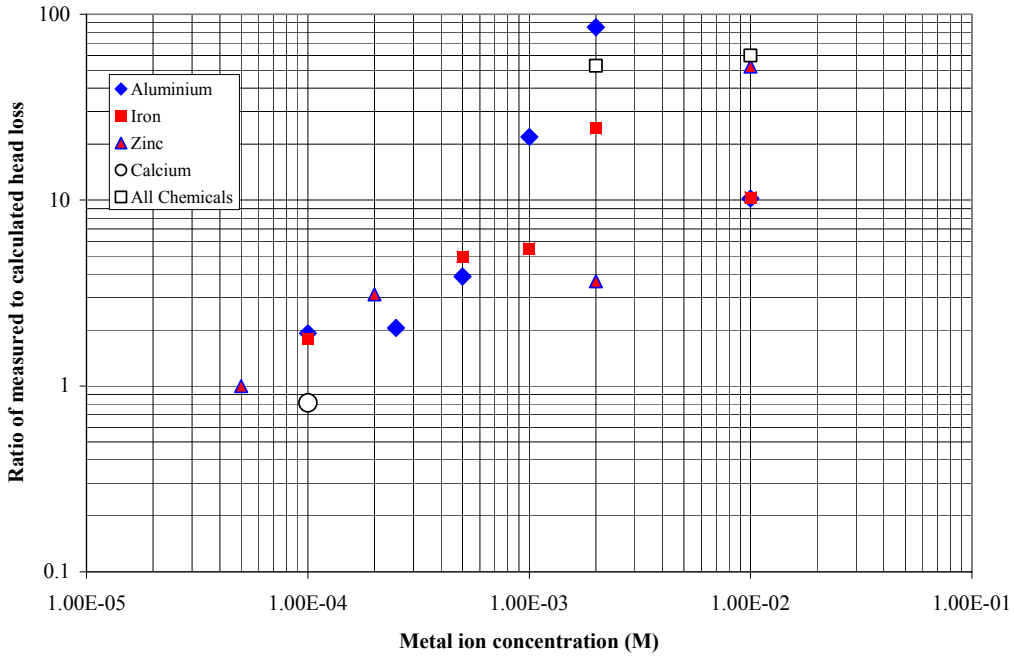

Fig. 4-10. Head-loss increase caused by metal precipitates.

Fig. 4-11. Bed with precipitates of aluminum nitrates at different concentrations.

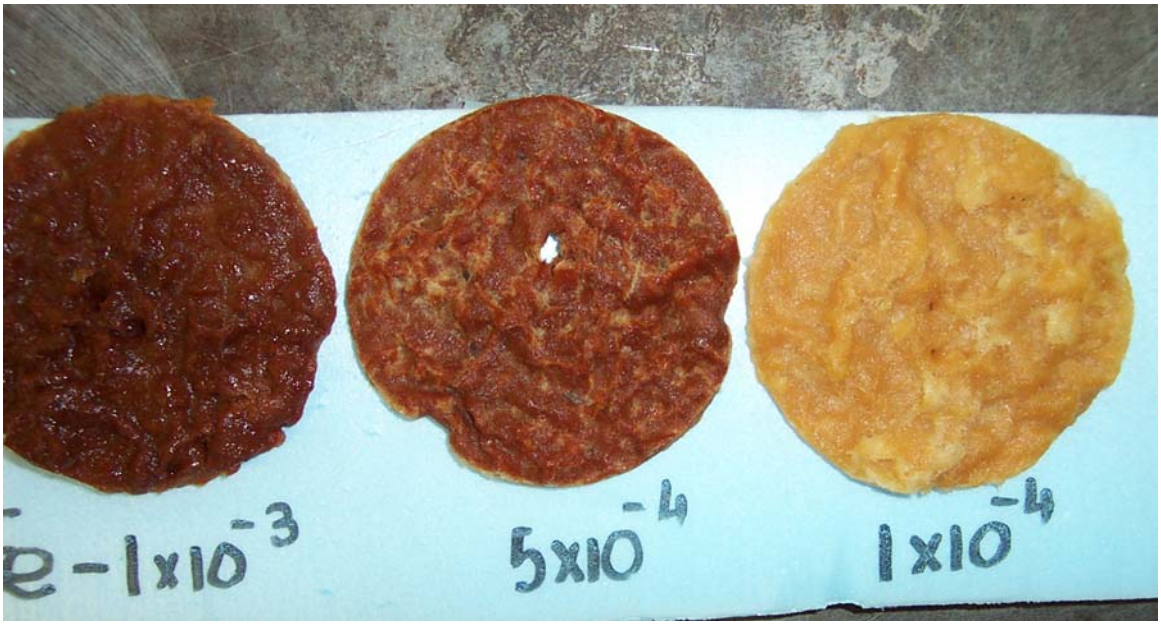

Fig. 4-12. Bed with precipitates of iron nitrates at different concentrations.

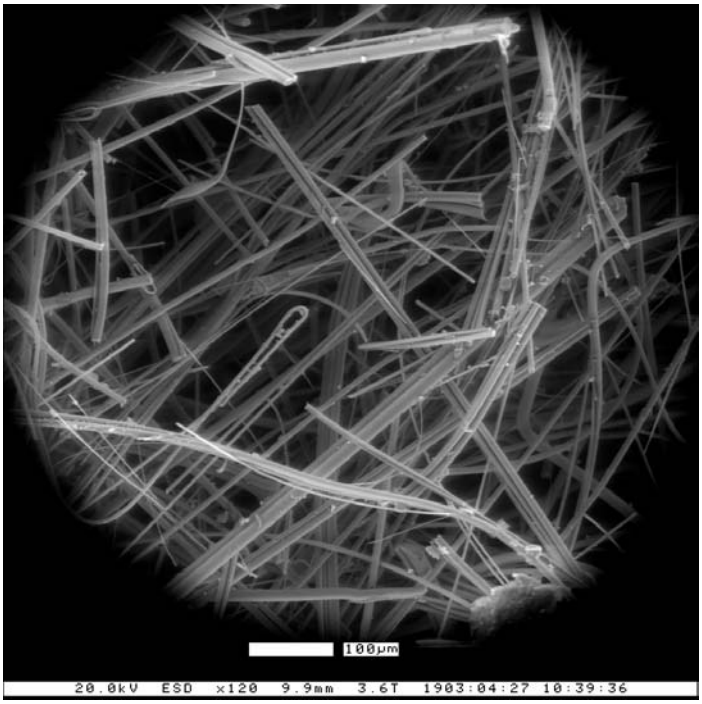

Fig. 4-13. ESEM of shredded NUKON™

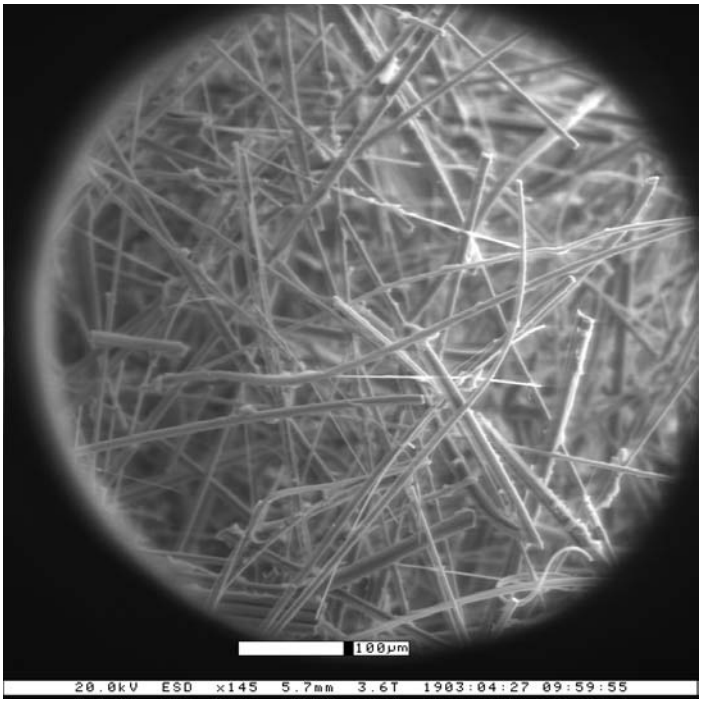

Fig. 4-14. ESEM of aluminum nitrate deposition on fibrous bed at a concentration of 2×10^{-3} M.

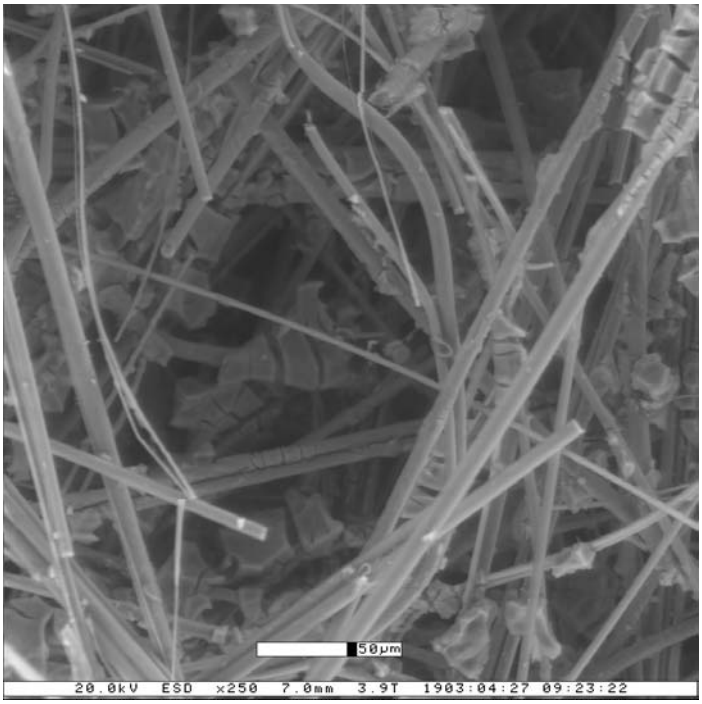

Fig. 4-15. ESEM of iron precipitation on fibrous bed at a concentration of 1×10^{-3} M.

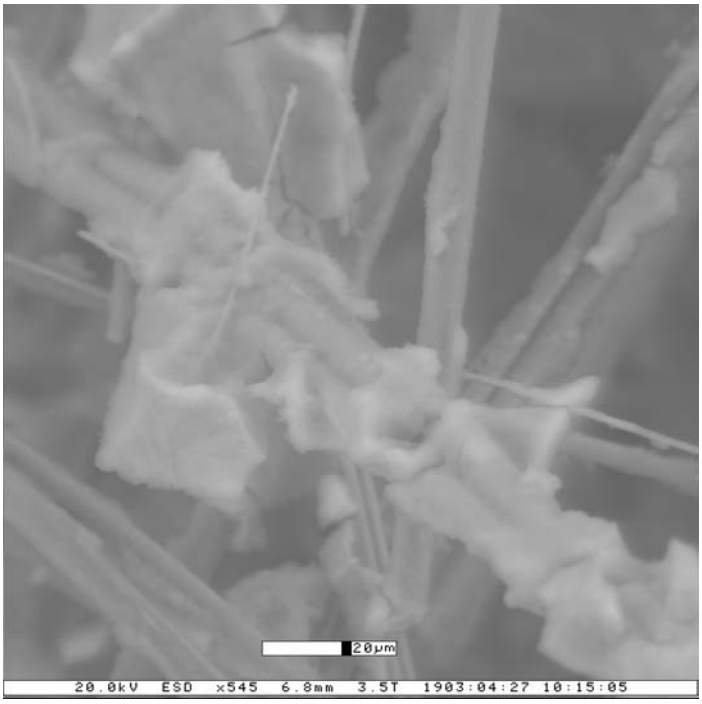

Fig. 4-16. ESEM of zinc precipitation on fibrous bed at a concentration of 2×10^{-3} M.

4.5 Long-Term Head-Loss Tests

4.5.1 Objective and Test Description

The objective of this test is to understand the head-loss characteristics of a fibrous bed when exposed to a prolonged buffer medium.

4.5.2 Test 1: NUKON™ Aged in Oven

4.5.2.1 Sample Preparation

A 4.4-g sample of NUKON™ was weighed, cut, and boiled in DI water in a beaker for 20 min. A solution of boric acid and lithium hydroxide was added in the same concentration that would be used during the test. The beaker was then left in the oven at 80°C for 5 days. After 5 days, the NUKON™, along with the water, was added into the test loop, and the test was performed.

4.5.2.2 Observation

The test was discontinued the next morning when the water level was found to be at the bed level. The head loss in 8 h, 12 min was found to be 4.6 ft, during which time the temperature rise was about 7°C. The head loss fell initially when the temperature rose, and afterward, the head-loss value remained constant. Figure 4-17 gives the long-term head-loss characteristics.

4.5.2.3 Repeat Test

The above test was repeated and continued for 10 h, 43 min, and the head-loss value dropped from 4.5 ft. to 3 ft. The bed was examined and found to be nonuniform, which had influenced the lower head-loss value. Figure 4-17 shows the head-loss variation with time.

4.5.3 Test 2: NUKON™ Aged at Room Temperature

4.5.3.1 Sample Preparation

A 4.4-g sample of NUKON™ was weighed, cut, and boiled in DI water in a beaker for 20 min. The beaker was then left at room temperature for 6 days. After 6 days, the NUKON™, along with the water, was added into the test loop and the test was performed. The test was discontinued the next morning when the water level in the test system dropped to just above the level of the fibrous bed; the cause for the loss of water in the system was not known. In a test period of 6 h, 12 min, the head loss changed from an initial value of 4 ft to 3 ft, during which time the temperature rose by about 10°C. The head loss fell initially with temperature but remained constant thereafter.

4.5.3.2 Observation

Table 4-6 gives the head-loss characteristics of NUKON™ after a prolonged exposure.

TABLE 4-6
HEAD-LOSS CHARACTERISTICS OF NUKON™ AFTER PROLONGED EXPOSURE

Exposure Condition	pH	Temp °C	Measured Head Loss (ft) and Time	Bed Morphology	NUREG/ CR-6224 Correlation for NUKON™	Ratio of Measured to Calculated Head Loss
Oven	7.1	49	4.42 in 8 h	Uniform	1.47	3.0
Oven (repeat test)	N/A	44	3.0 in 10 h	Nonuniform	1.56	1.92
Room temperature	7.05	22	2.99 in 6 h	Nonuniform	1.49	2.0

Figure 4-17 gives the long-term head-loss characteristics.

4.5.4 Discussion

The head loss decreased after the first hour of testing and remained constant thereafter for all the cases (Fig. 4-17). For all of the tests, the ratio of measured head loss to calculated head loss was found to be greater than one. It is recommended that more tests be conducted to arrive at a meaningful conclusion.

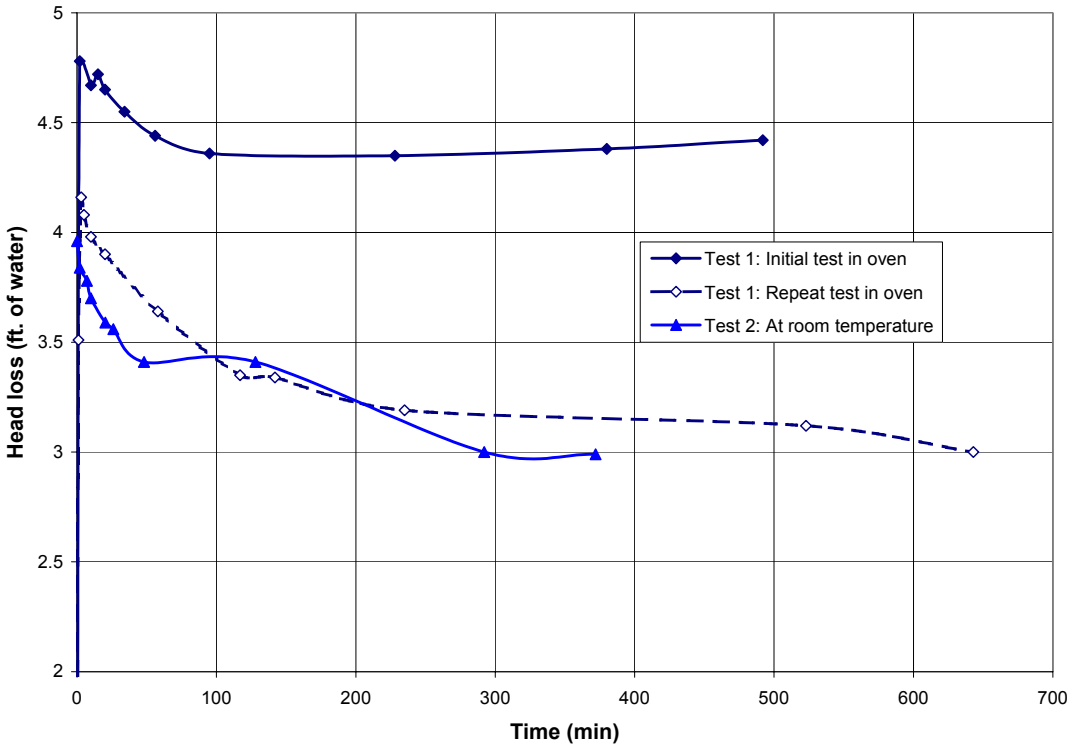

Fig. 4-17. Long-term head-loss test results.

4.6 Summary

A closed-loop vertical hydraulic test system was built for measuring the head loss across a debris-laden screen as a simulation of the screens on the sump for the recirculation pumps in a nuclear power plant. The purpose of these experiments was to evaluate the effects of solution chemistry on head-loss development. A similar but larger system had been used in earlier tests of the head loss caused by fibrous debris (NUKON™) and particulate debris (calcium silicate). The larger system had a capacity of about 110 gal. (420 L), but the system used in these tests had a capacity of 2.75 gallons (10.4 L), a 40x reduction in volume. The small system was designed and used in these tests for the following two reasons.

1. The chemicals needed for each test would have been expensive and the solutions difficult to prepare for a system with a capacity of 110 gal.

2. The disposal of large quantities of chemicals after each test would have been problematic.

The first set of tests was performed to verify that results generated with the small test system were comparable with results from the large test system and the parametric equations that were published in NUREG/CR-6224. The calibration and verification stage of the project addressed the following issues:

- calibration of the gauges and instruments,
- quantity of fibrous debris necessary to produce a uniform fibrous bed,
- temperature rise during recirculation pumping and methods to maintain constant temperature during the experiments,
- procedures to control the flow rate, and
- a procedure for adding debris to the test system to create a uniform bed.

As a result of preliminary testing, which demonstrated that increasing head loss across the debris bed would cause a reduction in the recirculation flow rate, the test system was modified to allow a constant velocity to be maintained. However, temperature variations during the experiments were more problematic. Because of the sustained recirculation of a small volume of liquid in the test system, pumping energy that was transferred to the water in the form of head loss caused a rise in temperature over the course of 1 to 2 h, at which time the temperature reached an equilibrium value. The temperature rise during this time was 20°C to 25°C. Experiments were initially done while the temperature was changing, and the head-loss results were normalized to a constant temperature value using the NUREG/CR-6224 head-loss correlation that provides a relationship between water temperature and head loss. The relationship between water temperature and head loss has been well known in filtration theory for many decades. Later experiments were done by adding debris to the test system after the equilibrium temperature had been reached so that the actual head-loss experiment was conducted at a constant temperature. Analysis of the data revealed that the experiments conducted with varying temperature were consistent with the ones done at constant temperature.

The calibration and verification test results confirmed that the head loss generated by a debris bed in the small test system was consistent with the large test system and the NUREG/CR-6224 correlation.

After the calibration and verification testing was complete, the primary focus of the experiments was on the additional head loss across an existing debris bed due to the capture of insoluble corrosion products that may precipitate after the corrosion of metals in the containment structure. The tests were done in chemical conditions that were representative of the chemical environment in the containment structure following a LOCA and included the addition of 3.3×10^{-2} M boric acid and 2.0×10^{-4} M lithium to deionized water. Precipitation was induced by adding metal nitrate salts to the water at quantities above the saturation limit for various metal precipitates. The first tests incorporated the simultaneous precipitation of aluminum, iron, zinc, and calcium metals, which were each added at a concentration of 1.0×10^{-2} M. High head loss was observed almost immediately, and the test had to be terminated within 15 min because the head loss had exceeded 15 ft and the recirculation flow rate had dropped to almost zero. Subsequent tests were conducted with only one metal precipitate at a time.

In all, more than 20 experiments were conducted with various concentrations of metal precipitates. The tests were reasonably consistent, despite the potential for wide variations resulting from test conditions that were difficult to control, such as the uniformity of the formation of the initial fibrous debris bed. The ability of a precipitate to cause additional head loss appeared at a concentration of about 1.0×10^{-4} M (equal to a concentration of 6.5 mg/L of zinc or 2.7 mg/L of aluminum). These concentrations correspond to less than 100 lb of metal dissolved into 1 Mgal. of water. The quantity of NUKON™ used for preparation of the fibrous bed was 4.4 g; therefore, the precipitate-to-fiber mass ratio at which additional head loss appeared was 0.015 for zinc. These results are significant because previous studies have reported that the sludge-to-fiber mass ratio at which additional head loss appears was 0.1 or higher. Additional head loss from precipitates of corrosion products may be significant at mass ratios on an order of magnitude lower than reported for particulate debris.

Higher quantities of metal precipitate consistently led to higher head loss. The head loss through a mixed bed of precipitate and fibers was about an order of magnitude higher than that through a fiber-only bed, when the metal concentration reached about 2.0×10^{-3} M. Results were similar, regardless of whether the tests were done at constant or varying temperature; repetitions of tests under identical test conditions produced repeatable results.

Physical examination of the beds after the tests revealed the presence of a sticky, gelatinous coating on the entire surface of the bed. This continuous gelatinous layer appeared to cause more physical resistance to water flow than mixed beds containing fibers and discrete particles. Examination of the beds by SEM showed that material adhered to individual fibers, although the gelatinous materials were desiccated by the high vacuum in the SEM.

Based on the observed results, the following conclusions can be made.

1. Head loss obtained from the small-scale test system for a fibrous debris bed without metal precipitates compares well with the NUREG/CR-6224 correlation.

2. High head loss can be caused by the capture of metal precipitates on a fibrous debris bed under the conditions used in these experiments. Additional head loss becomes apparent at precipitate-to-fiber mass ratios as much as an order of magnitude lower than for mixed beds containing particulates and fibers.

5.0 ZINC CORROSION TESTS

5.1 Background

As shown in Section 4, relatively small amounts of metal hydroxide precipitates can cause additional head loss through a bed of fibrous material captured on the recirculation screens during a LOCA. An important consideration is whether the corrosion of metal components in the containment structure can occur at a rate sufficient to cause precipitation.

Niyogi et al. [4] presented an equation for zinc corrosion that predicts a corrosion rate of 0.11 g/(m^2·h) at 80°C to 6 g/(m^2·h) at 22°C. The Finnish Centre for Radiation and Nuclear Safety (STUK) report [3] measured corrosion rates experimentally and found zinc corrosion rates ranging from about 0.05 to 11.27 g/(m^2·h) under a variety of experimental conditions.

5.2 Objectives

The objective of this group of tests was to measure the rate of corrosion of zinc in simple laboratory experiments. A series of immersion tests was used to measure the corrosion rate. The formation of corrosion products was observed during these tests. The corrosion products were examined and analyzed by light microscope, SEM, energy-dispersive spectrometry (EDS), x-ray diffraction, and acidification to determine the composition of the corrosion products. The immersion solutions were analyzed for zinc concentration to provide evidence for corrosion. In response to issues raised during the draft review meeting, a final group of experiments was done and the immersion solution was analyzed for silica concentration to evaluate the amount of silica present during the zinc corrosion tests.

5.3 General Procedures

Zinc samples were immersed for various time periods in aqueous solutions representative of the chemical composition of pool water during a LOCA. The zinc was carefully weighed before and after the immersion time, and the rate of corrosion was determined from the weight loss.

5.3.1 Sample Types

Experiments were performed using the following types of zinc samples.

1. Zinc granules (see Fig. 5-1). The zinc granules were 20 mesh, which has an average grain diameter of 0.85 mm and a surface area of 9.87×10^{-4} m^2/g (a 10-g sample has a surface area of about 98.7 cm^2). At a corrosion rate of 0.05 g/(m^2·h), a 10-g sample of material would lose about 0.12 g in 10 days, which is a measurable quantity with the procedures used in this study.

2. Zinc coupons—thin strips of metal commonly used in corrosion studies (see Fig. 5-2). The zinc coupons were 1.3 cm wide and 0.263 mm thick. Based on the measured thickness and the density of zinc metal, the coupons had a surface area of 1.07×10^{-3} m^2/g.

Fig. 5-1. Unreacted zinc granules (20 mesh).

Fig. 5-2. Unreacted zinc coupon (15.3 cm × 1.3 cm × 0.67 mm).

3. Dried and crumbled inorganic zinc paint primer, Dimetcote 6, obtained from Ameron International on 5/2/03 (see Fig. 5-3). This material was very brittle and crumbled under normal handling.

Fig. 5-3. Zinc primer before test.

5.3.2 Detailed Procedures

The corrosion tests were conducted according to the following procedures.

1. The granular zinc was rinsed and filtered through a 0.45-µm glass fiber filter to eliminate any fine material, dust, or other material that may be lost and measured as weight loss during the test.

2. Glass containers were filled with 1-L solutions containing 3.3×10^{-2} M boric acid and 2.0×10^{-4} M lithium hydroxide (see Fig. 5-4) and adjusted to the pH value selected for the experiment using either NaOH or HCl. The target pH values were typically either pH = 7.0 or pH = 9.0, although the pH was not controlled in some of the experiments. Some experiments were conducted with DI water instead of the solution containing boric acid and lithium.

3. Samples of zinc granules or zinc coupons were weighed to the nearest 0.0001 g and added to each container, and the containers were capped.

Fig. 5-4. Samples preparation in progress.

4. Some containers were left at room temperature. During these experiments, the room temperature in the laboratory varied from about 22°C to 25°C. Throughout the results sections of this report, the room-temperature experiments are reported as being conducted at 22°C. Other experiments were conducted at higher temperature (typically 80°C, although some experiments were also done at 40°C). These containers were placed in a constant temperature laboratory oven set to the desired temperature (see Fig. 5-5). For all jars, the volume of water was checked daily and distilled water was added if any water was lost from evaporation.

5. At the end of the experiment, the containers were taken out of the oven and allowed to cool to room temperature. When granules were used, each solution was filtered through a 0.45-µm filter (see Fig. 5-6). The filter paper was dried and weighed before filtration (see Fig. 5-7) and after filtration (see Fig. 5-8) to determine the net weight of granular zinc remaining after the corrosion test. The detailed procedures for determining the weight loss of each sample were performed according to Standard Method 2540-D [11]. The weight was recorded to the nearest 0.0001 g.

6. When the set of experiments included weight measurements after several different durations, each duration was determined with a separate experiment. In other words, granules or coupons were placed into separate jars, the sample from one jar was removed and weighed after the first day, the sample from a second jar was removed and weighed after the second day, etc. Samples were not returned to the immersion solution for multiple weight measurements.

Fig. 5-5. Samples being heat treated in the oven.

7. Corrosion rates were calculated from the weight of metal lost over the immersion period. The results from triplicate tests were averaged.

5.3.3 Tests Performed

The tests were grouped into sets with specific objectives. Each set of tests included 6 to 18 individual experiments. A total of six sets were conducted. The first set of tests examined the impact of temperature and pH on the corrosion rate of zinc granules. The second set evaluated the corrosion rate of different forms of zinc (i.e., granules, coupons, and paint chips). Remaining sets of tests evaluated the variation in corrosion over time and the corrosion rate in DI water as opposed to water that is similar to containment water during a LOCA. The results from each set of tests are described chronologically in the following sections. A summary describing the overall conclusions from these tests is provided at the end of this section.

5.4 Measurement of Zinc Corrosion Rates

5.4.1 Group 1 Tests – Effect of Temperature and pH

The first group of tests was carried out using 10-g samples of 20-mesh granular zinc. This group of tests was conducted to evaluate the effect of temperature and pH on zinc corrosion, with a matrix of four conditions being evaluated. The tests were done at pH = 7.0 and 9.0 and temperatures of 22°C (room temperature) and 80°C. The four test conditions were (1) 22°C,

pH = 7; (2) 22°C, pH = 9; (3) 80°C, pH = 7; and (4) 80°C, pH = 9. Each condition was tested in triplicate. Weight loss was measured after 11.75 days (282 h).

Fig. 5-6. Filtration in progress.

Fig. 5-7. 45-μm glass-filter paper being oven dried before filtration.

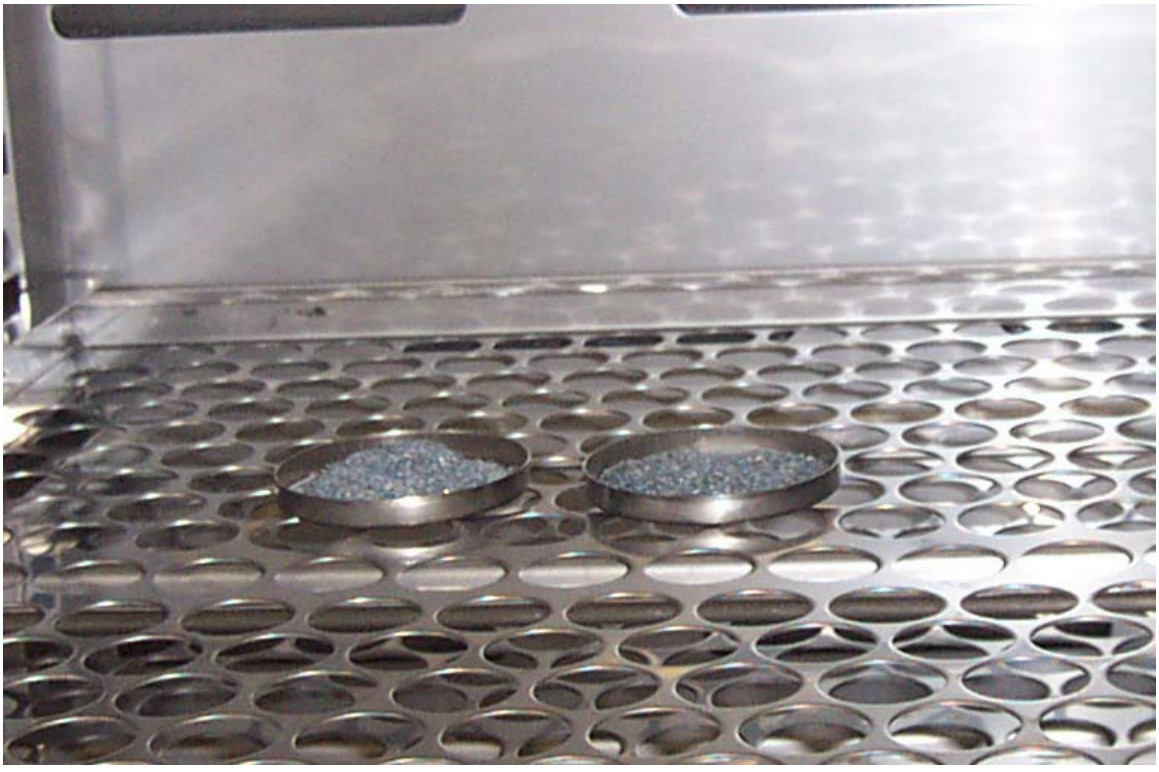

Fig. 5-8. After-filtration samples being dried.

5.4.1.1 Observations and Discussion

Table 5-1 gives the corrosion rate of zinc granules tested under various pH and temperature conditions. A total of 11 leaching tests, with 4 test conditions each, were conducted in triplicate (the tests at 80°C and pH = 9.0 were done only in duplicate because of the loss of one sample). Each test had about 10 g of zinc and 1 L of water and was kept in its jar for 282 h.

All of the tests showed signs of corrosion, and both qualitative and quantitative evidence for corrosion was observed. Figures 5-9 and 5-10 show the zinc granules after the tests.

TABLE 5-1
WEIGHT-LOSS MEASUREMENTS AND CORROSION RATES FOR THE FIRST GROUP OF ZINC CORROSION EXPERIMENTS

Test No.	Material	Solution Chemistry*	Temp (°C)	Time (h)	Beginning Weight (g)	Final Weight (g)	Weight Change (g)	Corrosion Rate (g/m^2 h)
1-1	granules	pH = 7.0	22	282	10.00	9.9543	-0.0457	0.0164
1-2	granules	pH = 7.0	22	282	10.00	9.9527	-0.0473	0.0170
1-3	granules	pH = 7.0	22	282	10.00	9.9497	-0.0503	0.0181
						Average:	-0.0478	0.0172
						Std. dev:	0.0023	0.0008
1-4	granules	pH = 9.0	22	282	10.00	9.9803	-0.0197	0.0071
1-5	granules	pH = 9.0	22	282	10.00	9.9603	-0.0397	0.0143
1-6	granules	pH = 9.0	22	282	10.00	9.9645	-0.0355	0.0128
						Average:	-0.0316	0.0114
						Std. dev:	0.0105	0.0038
1-7	granules	pH = 7.0	80	282	10.00	10.0035	0.0035	-0.0013
1-8	granules	pH = 7.0	80	282	10.00	9.9691	-0.0309	0.0111
1-9	granules	pH = 7.0	80	282	10.00	10.0051	0.0051	-0.0018
						Average:	-0.0074	0.0027
						Std. dev:	0.0203	0.0073
1-10	granules	pH = 9.0	80	282	10.00	10.0487	0.0487	-0.0175
1-11	granules	pH = 9.0	80	282	10.00	10.0507	0.0507	-0.0182
						Average:	0.0497	-0.0179
						Std. dev:	0.0014	0.0005

* Solution chemistry was $[H_3BO_3] = 3.3 \times 10^{-2}$ M, $[Li^+] = 2.0 \times 10^{-4}$ M; the pH was adjusted to value shown.

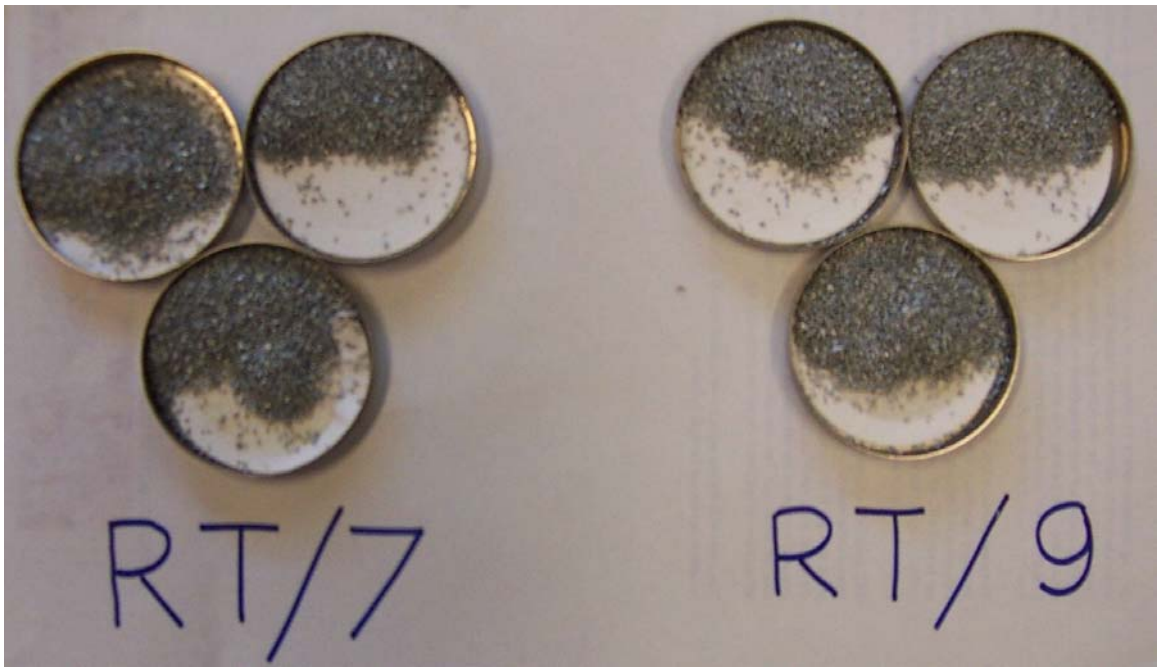

Fig. 5-9. Zinc granules after exposure at room temperature (RT) for 7 days at pHs of 7 and 9.

Fig. 5-10. Zinc granules after exposure in oven (O) for 7 days at pHs of 7 and 9.

The zinc immersed at 22°C and pH = 7.0 quantitatively had the most weight loss. The samples lost an average 47.8 mg (standard deviation = 2.3 mg). This corresponds to a corrosion rate of

0.012 g/(m^2·h). For comparison, the corrosion rates in the STUK report [3] ranged from about 0.01 g/(m^2·h) to 11.27 g/(m^2·h). The rates measured in this study are on the low end but within the range of values observed in the previous study. Zinc concentration in the water was also measured. In this set of tests, the measured zinc concentration was 10 to 14 mg/L, suggesting that there was some unaccounted loss of zinc. The unaccounted loss of zinc could be due to measurement errors or to the adsorption of zinc on the walls of the bottles or other surfaces.

The zinc immersed at 22°C and pH = 9 had less weight loss (averaging 31.6 mg) and less zinc in solution, suggesting that the corrosion rate at pH = 9.0 is lower than the corrosion rate at pH = 7.0. Because higher zinc corrosion was observed at pH = 7.0, subsequent tests were done only at pH = 7.0.

The jars in the oven at 80°C could not be analyzed quantitatively. Almost all of the jars exhibited negative weight loss (i.e., they gained weight). All jars except one contained a black material in addition to the original metallic zinc. It is assumed that the black material is a corrosion product that has a higher molecular weight than the original zinc. The black material is a coating on the zinc granules, and the material can be easily scraped off to reveal metallic zinc underneath. The zinc concentration in the water in the 80°C jars was about 1 to 3 mg/L for the pH = 7 jars and about 0.1 mg/L for the pH = 9 jars.

These experiments demonstrated the corrosion of zinc under the chemical conditions typically found during a LOCA, in both quantitative and qualitative terms. Quantitatively, the zinc-granule weight loss during the experiments was a quantitative measure of zinc corrosion. In a qualitative sense, the aqueous zinc concentrations and the development of the black material on the zinc granules are evidence of corrosion. Together, these observations suggest that zinc corrosion under these conditions is a true phenomenon.

5.4.2 Group 2 Tests – Effects of Material Configuration

The objective of this set of tests was to obtain the corrosion rates for other potential sources of zinc present in a containment structure. Three types of zinc sources were used. The sources were (1) zinc granules, (2) zinc coupons, and (3) inorganic zinc primer. Because the first group of experiments demonstrated higher corrosion rates at pH = 7.0, all of these tests were done near this pH value and not at pH = 9.0. The test protocol included tests at room temperature (22°C) and 80°C, but problems with the temperature setting on the laboratory oven prevented those experiments from being successful; therefore, the results of the 80°C test are not reported. Weights were measured after 3 and 7 days.

5.4.2.1 Observations

Table 5-2 gives the corrosion rates for zinc granules and coupons. Corrosion rates for the zinc primer could not be calculated because the surface area of the material was not known. Samples were analyzed for weight loss after 3 days of immersion and after 7 days of immersion. For both granules and coupons, the rate of corrosion was greater during the first 3 days than the average over the 7-day period. These results are expected; the corrosion rate is expected to be highest

TABLE 5-2
WEIGHT-LOSS MEASUREMENTS AND CORROSION RATES FOR THE SECOND GROUP OF ZINC CORROSION EXPERIMENTS*

Test No.	Material	Temp (°C)	Time (h)	Beginning Weight (g)	Final Weight (g)	Weight Change (g)	Corrosion Rate (g/m^2 h)
2-1	coupon	22	72	3.6692	3.6629	-0.0063	0.0224
2-2	coupon	22	168	3.6498	3.6405	-0.0093	0.0142
2-3	granules	22	72	10.0071	9.9798	-0.0273	0.0384
2-4	granules	22	168	10.0058	9.9775	-0.0283	0.0171
2-5	paint chips	22	72	9.9986	10.0054	0.0068	N/A†
2-6	paint chips	22	168	4.9999	5.0899	0.0900	N/A

* Solution chemistry was $[H_3BO_3] = 3.3 \times 10^{-2}$ M, $[Li^+] = 2.0 \times 10^{-4}$ M; the pH was not adjusted or measured but subsequently was determined to be about pH = 6.6.

† Corrosion rates for paint chips could not be determined because the exposed surface area could not be determined.

when the samples are immersed in water containing no zinc and should slow down as the zinc concentration in the water increases, which decreases the driving force for zinc dissolution. Corrosion rates for granules and coupons were similar to each other at both 3 and 7 days for the samples immersed at room temperature. The corrosion rate after 3 days was 0.038 $g/(m^2 \cdot h)$ for the granules and 0.022 $g/(m^2 \cdot h)$ for the coupons. After 7 days, the corrosion rate was 0.017 $g/(m^2 \cdot h)$ for the granules and 0.014 $g/(m^2 \cdot h)$ for the coupons. Figures 5-11 through 5-17 present images of the samples after the exposure.

5.4.3 Group 3 Tests – Corrosion as a Function of Time

The objective of the third set of corrosion tests was to evaluate the change in the rate of corrosion over time. Mass transfer rates are typically dependent on the deviation from equilibrium conditions. The concentration of zinc in solution is zero at the beginning of the corrosion tests but increases as corrosion proceeds. As a result, it can be expected that the fastest rate of corrosion will correspond to the beginning of the corrosion test and that the rate will decline as the zinc concentration in solution approaches the saturation concentration. All experiments in this set were done at 80°C. Tests 3-1 through 3-9 were done without pH adjustment for consistency with the second set of tests, and the measured pH in each of the solutions was pH = 6.6. The pH was adjusted to 7.0 in tests 3-10 through 3-18. The purpose of conducting tests with and without pH adjustment, even though the measured pH was similar, was to determine whether the addition of acid or base for pH adjustment had an impact on the corrosion rate. Samples were analyzed for weight loss after 1, 3, and 7 days, and all experiments were done in triplicate. To minimize the effect of zinc saturation of solution, the sample sizes were limited to about 1 g.

Fig. 5-11. Zinc granules after 3 days in oven at 105° C and at room temperature at a pH of about 7.

Fig. 5-12. Zinc coupons before and after exposure at room temperature and in oven.

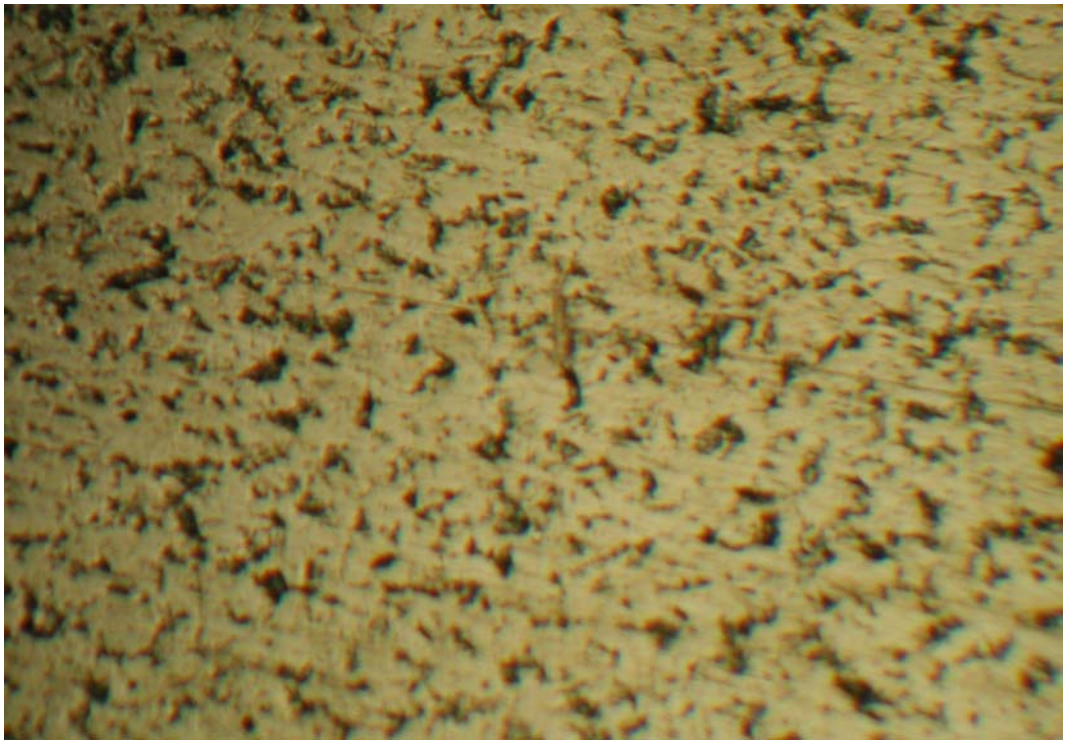

Fig. 5-13. Zinc coupons before exposure.

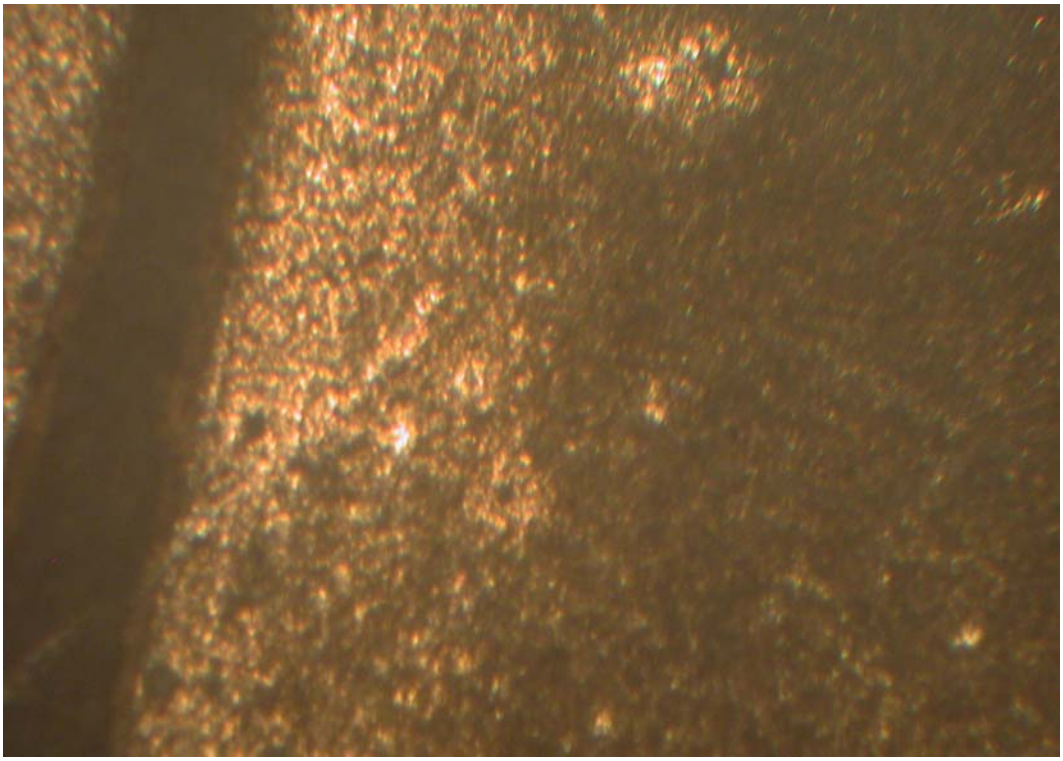

Fig. 5-14. Zinc coupons after exposure in oven at 80° C for 7 days at a pH of 7.

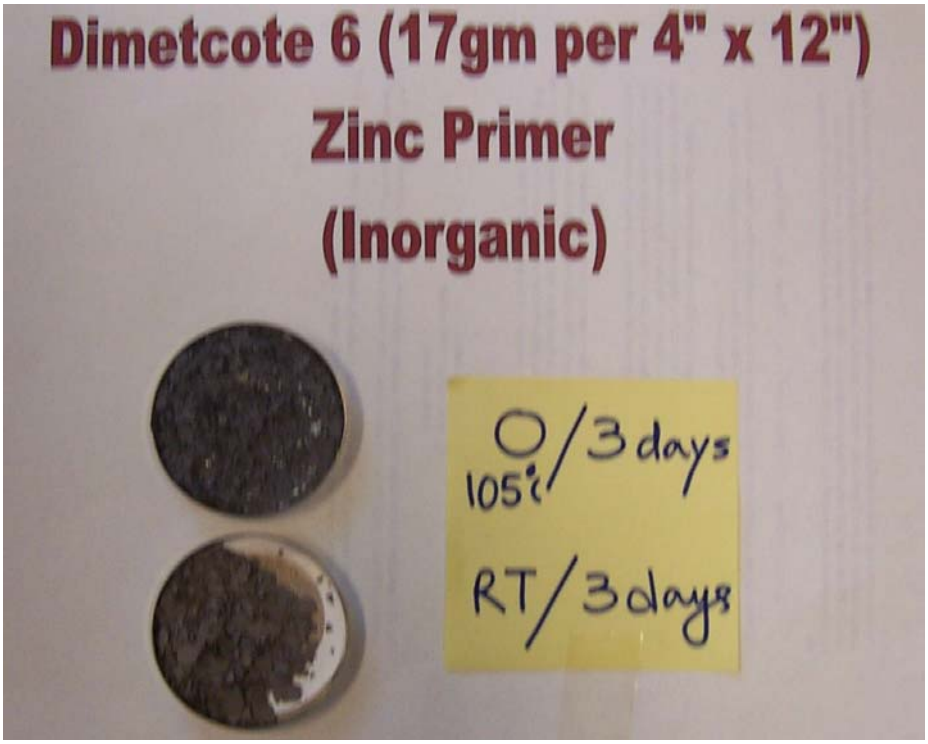

Fig. 5-15. Zinc primer after exposure for 3 days in oven at 105° C and at room temperature.

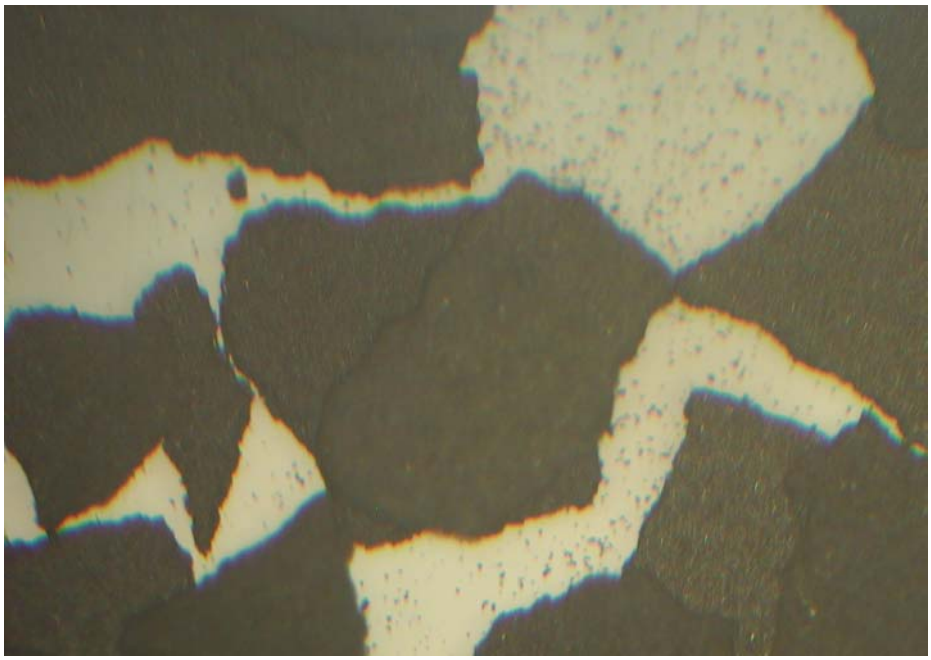

Fig. 5-16. Zinc primer before exposure.

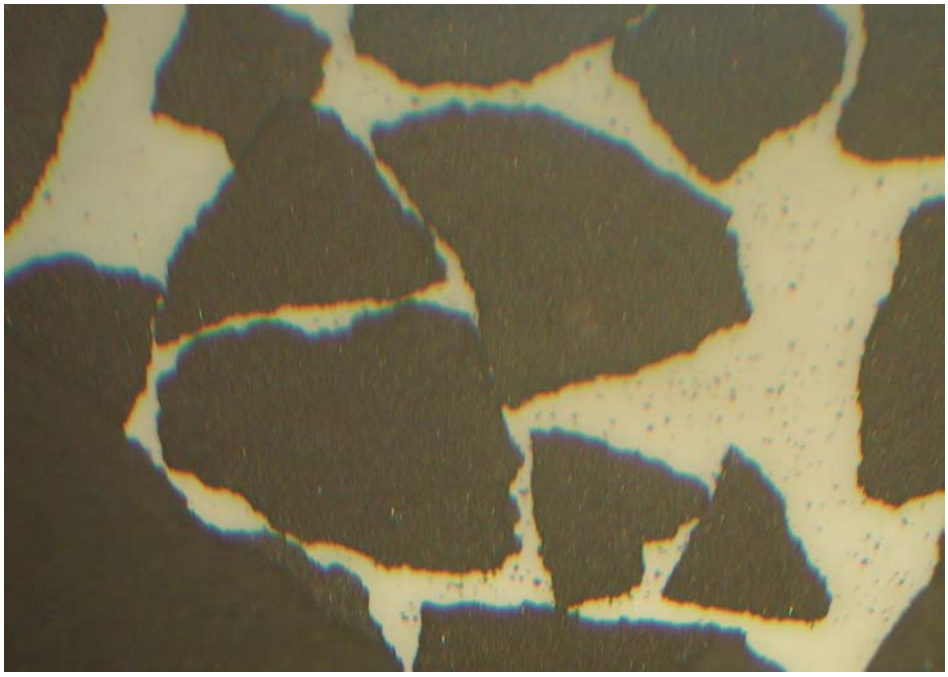

Fig. 5-17. Zinc primer after exposure in oven at 80° C for 7 days at a pH of 7.

5.4.3.1 Observations

The results for the third group of experiments are shown in Table 5-3. The small sample size and short test duration resulted in small values for weight change during each experiment. The average change in weight for each group of three tests ranged from 0.8 mg to 1.4 mg, which is too small to give reliable corrosion rates without large experimental errors. Nevertheless, the highest corrosion rates measured in these tests was 0.031 g/(m^2·h), which is similar to earlier measured corrosion rates. As expected, the corrosion rates decreased as time increased, with the average corrosion rate for three samples at pH = 6.6 being 0.031 g/(m^2·h) after 1 day, 0.016 g/(m^2·h) after 3 days, and 0.0049 g/(m^2·h) after 7 days. No significant differences were observed between the samples with and without pH adjustment.

5.4.4 Group 4 Tests – Corrosion in DI Water as a Function of Time

The fourth set of corrosion experiments evaluated the change in the rate of corrosion over time and the difference in the rate of corrosion in DI water vs earlier tests, which were done in chemical solutions representative of containment water. All experiments in this set were done at 80°C using zinc granules and in triplicate. Samples were analyzed for weight loss after 1, 3, and 7 days.

TABLE 5-3
WEIGHT-LOSS MEASUREMENTS AND CORROSION RATES FOR THE THIRD GROUP OF ZINC CORROSION EXPERIMENTS*

Test No.	Material	Temp (°C)	Time (h)	Beginning Weight (g)	Final Weight (g)	Weight Change (g)	Corrosion Rate (g/m^2 h)
3-1	coupon	80	24	1.0071	1.0064	-0.0007	0.0272
3-2	coupon	80	24	1.1980	1.1968	-0.0012	0.0391
3-3	coupon	80	24	1.4076	1.4066	-0.0010	0.0278
					Average:	-0.0010	0.0314
					Std. dev:	0.0003	0.0067
3-4	coupon	80	72	1.0057	1.0037	-0.0020	0.0259
3-5	coupon	80	72	1.2041	1.2032	-0.0009	0.0097
3-6	coupon	80	72	1.4129	1.4116	-0.0013	0.0120
					Average:	-0.0014	0.0159
					Std. dev:	0.0006	0.0088
3-7	coupon	80	168	1.0255	1.0245	-0.0010	0.0054
3-8	coupon	80	168	1.2103	1.2095	-0.0008	0.0037
3-9	coupon	80	168	1.4055	1.4041	-0.0014	0.0056
					Average:	-0.0011	0.0049
					Std. dev:	0.0003	0.0010
3-10	coupon	80	24	0.7866	0.7880	0.0014	-0.0695
3-11	coupon	80	24	1.1130	1.1133	0.0003	-0.0105
3-12	coupon	80	24	1.6036	1.6042	0.0006	-0.0146
					Average:	0.0008	-0.0316
					Std. dev:	0.0006	0.0330
3-13	coupon	80	72	0.7848	0.7838	-0.0010	0.0166
3-14	coupon	80	72	1.0997	1.0980	-0.0017	0.0201
3-15	coupon	80	72	1.6207	1.6204	-0.0003	0.0024
					Average:	-0.0010	0.0130
					Std. dev:	0.0007	0.0094
3-16	coupon	80	168	0.7785	0.7778	-0.0007	0.0050
3-17	coupon	80	168	1.0993	1.0978	-0.0015	0.0076
3-18	coupon	80	168	1.6249	1.6233	-0.0016	0.0055
					Average:	-0.0013	0.0060
					Std. dev:	0.0005	0.0014

* Solution chemistry was $[H_3BO_3] = 3.3 \times 10^{-2}$ M, $[Li^+] = 2.0 \times 10^{-4}$ M; the pH was not adjusted in experiments 3-1 to 3-9 and was pH = 7.0 in experiments 3-10 to 3-18.

5.4.4.1 Observations

The results from the fourth group of corrosion experiments are shown in Table 5-4. After 1 day, the zinc-granule samples lost an average of 20.3 mg, corresponding to a corrosion rate of 0.086 g/(m^2·h). This corrosion rate is higher than that measured in chemical solutions representative of containment water, but not by a dramatic amount. The higher corrosion rate may be due to the short duration of this test. The zinc-granule samples that were weighed after 3 days of immersion had no weight change on average. Thus, the weight loss that apparently occurred during the first day was cancelled by an equivalent weight gain during the second and third days, suggesting that the solution became saturated with zinc, leading to the precipitation or formation of a corrosion product with a higher molecular weight than the zinc metal. After 7 days, the zinc-granule samples had gained an average of 16 mg, suggesting the continued formation of higher molecular-weight corrosion products.

TABLE 5-4
WEIGHT-LOSS MEASUREMENTS AND CORROSION RATES FOR THE FOURTH GROUP OF ZINC CORROSION EXPERIMENTS*

Test No.	Material	Temp (°C)	Time (h)	Beginning Weight (g)	Final Weight (g)	Weight Change (g)	Corrosion Rate (g/m^2 h)
4-1	granules	80	24	10.0031	9.9962	-0.0069	0.0291
4-2	granules	80	24	10.0081	9.9749	-0.0332	0.1400
4-3	granules	80	24	10.0097	9.9888	-0.0209	0.0881
					Average:	-0.0203	0.0858
					Std. dev:	0.0132	0.0555
4-4	granules	80	72	10.0077	9.9968	-0.0109	0.0153
4-5	granules	80	72	10.0024	10.0133	0.0109	-0.0153
4-6	granules	80	72	9.9995	10.001	0.0015	-0.0021
					Average:	0.0005	-0.0007
					Std. dev:	0.0109	0.0154
4-7	granules	80	168	9.9958	10.0069	0.0111	-0.0067
4-8	granules	80	168	10.0031	10.015	0.0119	-0.0072
4-9	granules	80	168	10.0052	10.0303	0.0251	-0.0151
					Average:	0.0160	-0.0097
					Std. dev:	0.0079	0.0047

* Solution chemistry was DI water.

5.4.5 Group 5 Tests – Corrosion in DI Water as a Function of Time at Room Temperature

The fifth group of corrosion tests evaluated corrosion zinc coupons in DI water at room temperature as a function of time. Samples were analyzed for weight loss after 1, 4, 5, 6, and 7 days.

5.4.5.1 Observations

The results from the fifth group of corrosion experiments are shown in Table 5-5. All coupons exhibited a gain in weight after immersion in DI water. The coupon immersed for 1 day increased in weight by 0.3 mg, and the coupons immersed for 4 to 7 days increased in weight by between 2.5 mg and 3.5 mg. These results suggest that the coupons were coated with a corrosion product in less than 4 days and that little or no further deposition of corrosion products occurred after 4 days.

TABLE 5-5
WEIGHT-LOSS MEASUREMENTS AND CORROSION RATES FOR THE FIFTH GROUP OF ZINC CORROSION EXPERIMENTS*

Test No.	Material	Temp (°C)	Time (h)	Beginning Weight (g)	Final Weight (g)	Weight Change (g)	Corrosion Rate (g/m^2 h)
5-1	coupon	22	24	3.5755	3.5758	0.0003	-0.0033
5-2	coupon	22	96	3.5699	3.5734	0.0035	-0.0096
5-3	coupon	22	120	3.5873	3.5899	0.0026	-0.0057
5-4	coupon	22	144	3.7090	3.7125	0.0035	-0.0061
5-5	coupon	22	168	3.6874	3.6897	0.0023	-0.0035
5-6	coupon	22	168	3.6940	3.6965	0.0025	-0.0038

* Solution chemistry was DI water.

5.4.6 Group 6 Tests – Repeated Corrosion Tests as a Function of Time

A final group of zinc corrosion tests was performed to determine whether the rate of weight loss could be sustained over several days. In earlier tests, some samples exhibited an increase in weight due to the deposition of corrosion byproducts that had a higher molecular weight than the original zinc. The existence of these corrosion byproducts raised questions about whether corrosion rates measured as weight loss were accurate or whether the weight loss due to corrosion was partially offset due to the deposition of higher weight corrosion byproducts, resulting in a lower weight-loss measurement (and, correspondingly, a lower corrosion rate). The deposition of corrosion byproducts (identified as weight gain) generally occurred under (1) higher temperature conditions, which cause higher corrosion rates and lower zinc solubility; (2) higher pH conditions, which cause lower zinc solubility; or (3) longer time durations, which cause more corrosion. All of these conditions can lead to a situation where the solution was

saturated or supersaturated with zinc corrosion products, which can then lead to precipitation and deposition of corrosion products onto the original zinc granules. Accordingly, the final group of tests were run at pH = 7.0, room temperature, and shorter durations to minimize saturated conditions. All tests were done in triplicate. Additional tests in this group were run at 40°C in an attempt to determine an Arrhenius constant that could be used to predict corrosion rates at higher temperatures.

5.4.6.1 Observations

The results from the sixth group of corrosion experiments are shown in Table 5-6. At room temperature, the coupons lost an average of 9.9 mg after 2 days and 17.1 mg after 4 days. These weight-loss measurements correspond to a corrosion rate of 0.055 g/(m^2·h) averaged over 2 days and 0.046 g/(m^2·h) averaged over 4 days. The continued loss of weight between the second and fourth days suggests that deposition of higher molecular-weight corrosion products had not yet started and that the corrosion rates measured by weight loss were representative of the true corrosion rates present under these experimental conditions. The observed corrosion rates were somewhat higher than those observed in earlier tests but are consistent with the observation that the corrosion rate decreased as the zinc concentration increased in solution (at the same experimental conditions, the corrosion rate was 0.017 g/(m^2·h) averaged over 11.75 days in the first group of tests).

Similar corrosion rates were initially observed for the coupons immersed at 40°C. These coupons lost an average of 10.4 mg after 2 days, corresponding to a corrosion rate of 0.057 g/(m^2·h). After 4 days, however, the average weight loss had increased only marginally to 10.9 mg, causing the corrosion rate to drop to 0.030 g/(m^2·h). The lack of continued weight loss between the second and fourth days suggests that the solution had reached saturated conditions, which limited the corrosion of zinc without the formation of corrosion products.

The zinc concentration in solution was measured after a number of the experiments. In the first several sets of experiments, relatively poor correlation was observed between the mass lost by the granules or coupons and the mass of zinc measured in solution. The poor correlation may have been due to adsorption of zinc onto the glass bottles or other apparatus used in the experiments or the fact that corrosion products had deposited on the granules or coupons, thus interfering with the weight-loss measurements. However, for the final group of experiments, a good correlation between weight-loss measurements and zinc concentration in solution was observed. The correlation between these values is shown in Table 5-7. With only a few exceptions, the mass lost by the coupons was nearly identical to the mass of zinc measured in solution. The weight lost by the coupons and the zinc concentration in solution are two independent measurements that provide evidence of similar corrosion rates, thus giving confidence that the method used to measure the corrosion rates provides an accurate value.

TABLE 5-6
WEIGHT-LOSS MEASUREMENTS AND CORROSION RATES FOR THE SIXTH GROUP OF ZINC CORROSION EXPERIMENTS*

Test No.	Material	Temp (°C)	Time (h)	Beginning Weight (g)	Final Weight (g)	Weight Change (g)	Corrosion Rate (g/m^2 h)
6-1	coupon	40	48	3.4539	3.4403	-0.0136	0.0769
6-2	coupon	40	48	3.4752	3.4679	-0.0073	0.0410
6-3	coupon	40	48	3.8883	3.8780	-0.0103	0.0518
					Average:	-0.0104	0.0566
					Std. dev:	0.0032	0.0184
6-4	coupon	40	96	3.4306	3.4190	-0.0116	0.0330
6-5	coupon	40	96	3.4963	3.4880	-0.0083	0.0232
6-6	coupon	40	96	3.8794	3.8666	-0.0128	0.0322
					Average:	-0.0109	0.0295
					Std. dev:	0.0023	0.0055
6-7	coupon	22	48	3.4408	3.4298	-0.0110	0.0625
6-8	coupon	22	48	3.4763	3.4666	-0.0097	0.0545
6-9	coupon	22	48	3.7284	3.7194	-0.0090	0.0472
					Average:	-0.0099	0.0547
					Std. dev:	0.0010	0.0077
6-10	coupon	22	96	3.4526	3.4348	-0.0178	0.0504
6-11	coupon	22	96	3.7159	3.6979	-0.0180	0.0473
6-12	coupon	22	96	3.9052	3.8897	-0.0155	0.0388
					Average:	-0.0171	0.0455
					Std. dev:	0.0014	0.0060

* Solution chemistry was $[H_3BO_3] = 3.3 \times 10^{-2}$ M, $[Li^+] = 2.0 \times 10^{-4}$ M, pH = 7.

TABLE 5-7
COMPARISON OF MASS OF ZINC LOST FROM COUPONS AND GAINED BY SOLUTION

Sample ID	Mass of Zinc Lost from Coupons (mg)	Mass of Zinc Gained in Solution (mg)	Zinc Recovery (%)
6-1	13.6	13.2	97
6-2	7.3	7.3	100
6-3	10.3	10.0	97
6-4	11.6	11.2	97
6-5	8.3	7.4	89
6-6	12.8	12.1	95
6-7	11.0	8.6	78
6-8	9.7	7.6	78
6-9	9.0	4.2	47
6-10	17.8	17.8	100
6-11	18.0	17.1	95
6-12	15.5	0.6	4

5.5 Identification of the Zinc Corrosion Products

Several analyses were performed to attempt to identify the chemical composition of the black material formed on the zinc granules during the immersion tests. These analyses included

1. visual observation with a light microscope and an SEM,

2. elemental composition as identified by EDS, which is an analytical technique available in conjunction with the SEM;

3. percent zinc content of the corrosion product, determined by acidification and aqueous zinc analysis; and

4. composition as identified by x-ray diffraction.

5.5.1 Description of the Scanning Electron Microscope

A systematic analysis of the black coating on the zinc granules was conducted using a SEM. The electron microprobe generates a beam of high-energy electrons, which are focused by a column of lenses onto the surface of a specimen. The electrons originate from a hot cathode consisting of a hairpin tungsten filament held at an electrical potential of 10,000 to 30,000 volts, with respect to an anode at ground or zero potential. The electrons are drawn from the filament, accelerated through a hole in the anode, and focused by several electromagnetic lenses as they travel at nearly the speed of light down the electron column. The beam is focused by the lenses into a tiny spot, usually 1 μm or less in diameter, at the surface of the sample. The beam electrons interact with the atoms of the sample, thus producing signals that contain different types of information.

Low-energy electrons, called secondary electrons (SE), are knocked from the surface of the sample and carry information about the sample-surface topography. High-energy electrons can be scattered back from the atoms within the sample and are referred to as "backscattered electrons" (BSE). Both types of electrons are collected by detectors around the sample chamber and can be used to form images. The number of BSEs produced by the sample increases with the atomic number (Z) of the sample. Therefore, the BSE images carry information about the chemistry of the sample; higher atomic numbers will appear brighter and lower atomic numbers will appear darker. As an example, alumina (average Z = 10.6) will appear somewhat brighter than silica (Z = 10.8) and both will be significantly darker than iron oxide (Z = 20.6).

In addition to the electrons emitted from the sample, the interaction of the beam with the atoms of the sample will also produce x-rays. The x-rays have an energy and wavelength characteristic of the element that produced them. A sample containing magnesium, silicon, and iron will have x-ray peaks of 1.254 kiloelectronvolts (keV) for magnesium and 1.74 keV for silicon. These peaks are called K_α peaks. Iron will have two peaks: a K_α at 6.403 keV and a K_β at 7.057 keV. Increasingly higher atomic numbers will have more and higher energy peaks because the number of electrons surrounding the nucleus increases as the atomic number increases. For example, uranium will have several K peaks: the K_α at 98 keV; a group of L peaks, with the main peak (L_α) at 13.6 keV; and a number of M peaks, with the main peak M_α at 3.17 keV. However, the number of x-ray peaks generated will depend on the accelerating voltage of the electron beam, and for the most part, only the M family of peaks for uranium would be visible.

Several types of detectors measure the x-rays emitted from the sample. An EDS uses a solid-state diode to measure the characteristic energy level of the x-rays and then plots a spectrum of the energy. The spectrum is represented as a histogram, plotted from 0 to a higher energy level, usually 10 or 20 keV. The x-rays appear as peaks at their representative energies, and the greater the concentration of a particular element in the sample, the higher the peak. Wavelength-dispersive spectrometers (WDS) measure the wavelength and intensity by mirroring x-rays off of a curved crystal and focusing them onto a Geiger-counter type of detector. In either case, the number of x-rays produced by each element is proportional to the concentration of that element in the sample. The x-rays can be quantitatively analyzed by counting the number of x-ray photons emitted from the sample over a short period of time, i.e., 10 to 30 s, and this number is then compared with the number of x-rays emitted from a standard of known composition, under the same instrument conditions. The concentration is determined from the ratio of the x-ray intensities in the sample and a standard. Although both systems can be used to measure the number or intensity of x-rays, the WDS is more precise and has a lower detection limit. The EDS generally provides a detection limit of tenths of a percent by weight, while the WDS can measure on the order of 10 ppm or 0.001 wt %.

In addition to chemical quantification of x-rays, an image can also be formed of the various x-rays where they emanate from the sample. A digital computer system moves the beam along the sample, stops it for a short period to collect x-rays, and then moves it to the next spot. All of the spots where information is collected, called "picture elements" or "pixels," are equally spaced along the width and height of the image. The center of each pixel represents a square on an image so that all the data from the point where the beam stops momentarily will be contained in a single pixel. The size of each pixel on the image depends on the magnification. For example,

if an image is 128 pixels wide, at a magnification of 100 times, each pixel is 9.4 μm square. Therefore, the resolution of the image is 9 μm; features smaller than that will not be observable. Increasing the magnification will result in better or higher resolution. However, the ultimate resolution that can be obtained on an x-ray image depends on the element being mapped; the average best resolution for x-rays is about 1 to 2 μm. An image (also referred to as an x-ray map) is collected for each element of interest. Because the x-ray intensity is proportional to the concentration of an element, the image will be brighter in areas of higher concentration of that particular element and darker where the element concentration is low or nonexistent. The various maps may be digitally overlaid onto each other to see where concentrations of elements coincide. For example, overlapping concentrations of silicon, aluminum, and potassium might indicate the presence of a K-feldspar.

5.5.2 Visual Observations of the Zinc Granules

Zinc granules were examined by light microscope and SEM before and after immersion. Figures 5-18 through 5-20 show light microscope images of samples of the zinc granules before and after exposure to higher temperatures. Before immersion, the granules are a light-gray color and have a shiny appearance. After immersion, some exposed granules are a light-gray color, whereas others have a dull-black appearance. The light-gray granules do not appear to be as shiny as the

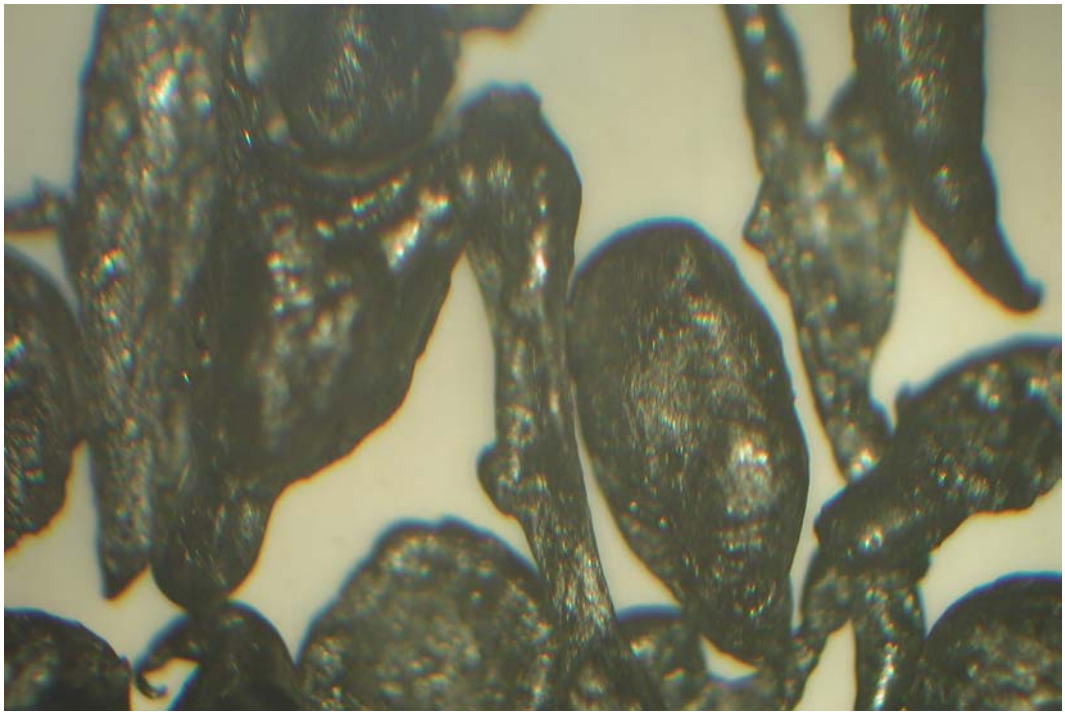

Fig. 5-18. Zinc granules before exposure under optical microscope (magnification 49).

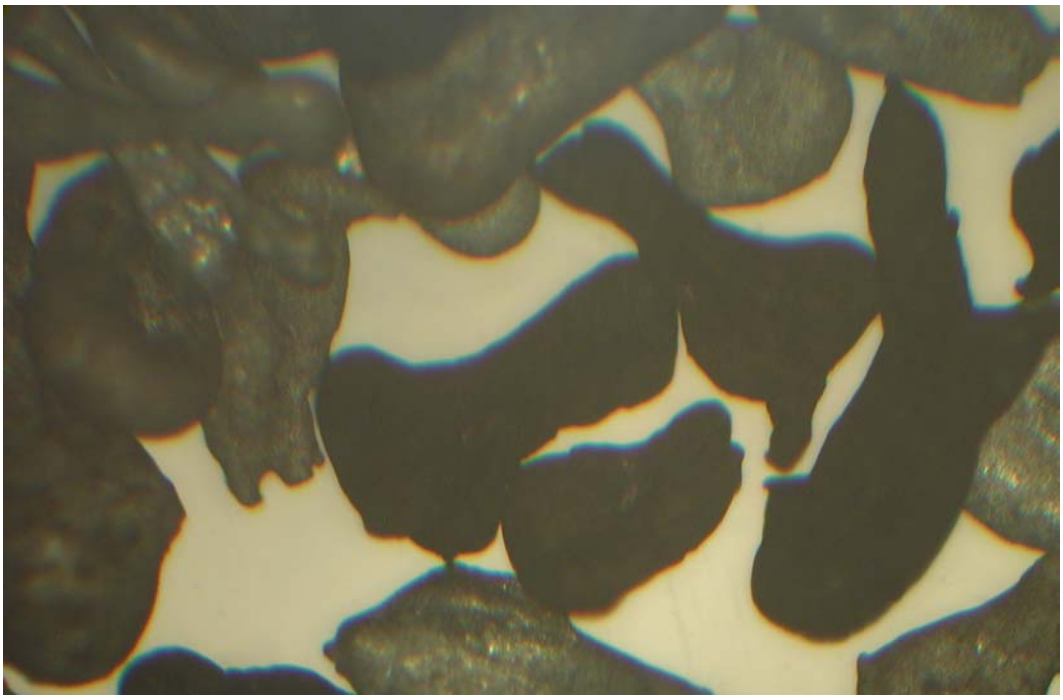

Fig. 5-19. Zinc granules after exposure (oven at 80° C for 3 days) under optical microscope (magnification 49).

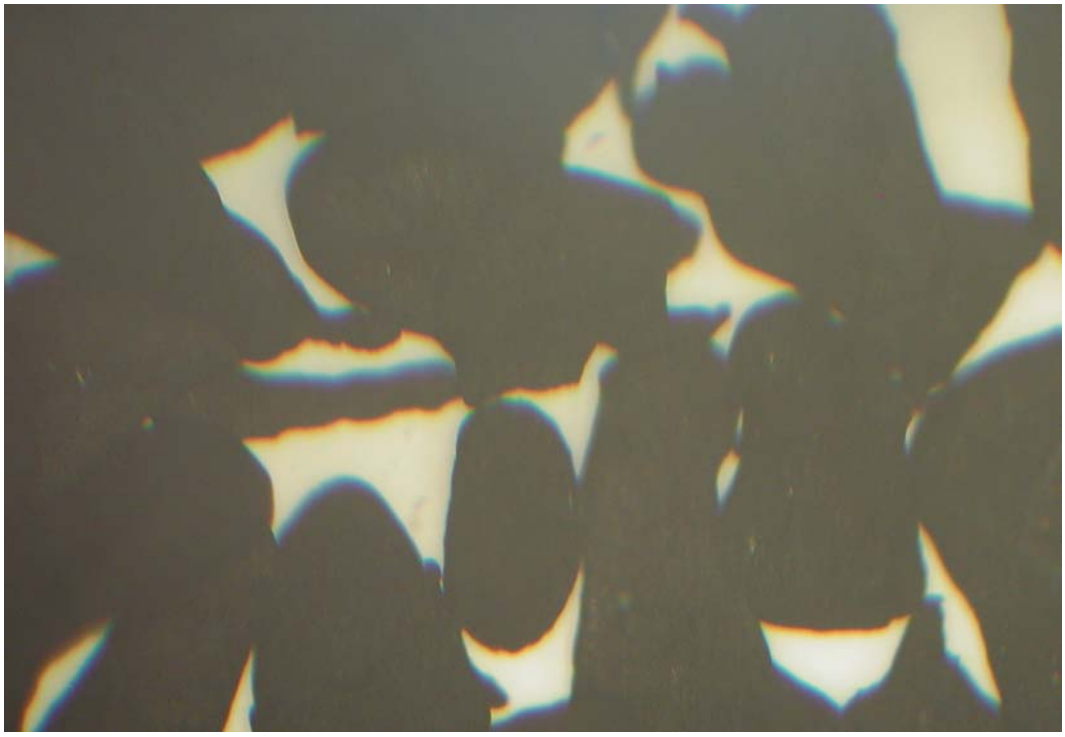

Fig. 5-20. Zinc granules after exposure (oven at 105° C for 3 days) under optical microscope (magnification 49).

granules before immersion, but the color is similar. The granules appear to be entirely gray or entirely black, with no gradation of color on individual granules. It appears that some granules are completely coated with a black corrosion product, whereas others are not coated. These results suggest that zinc dissolved into solution and then formed a corrosion product on the granules. The corrosion product initially formed only on some of the granules. Additional formation of corrosion products occurred on granules that were already partially coated because those granules had nucleation sites where additional precipitation could occur with lower energy than the formation of fresh precipitates on uncoated granules. If the reaction had proceeded as a surface reaction without the dissolution of zinc ions in solution, the granules would have been expected to have a more uniform appearance. These images suggest that the corrosion proceeded by releasing zinc ions into solution followed by formation of a zinc precipitate rather than as a chemical reaction that proceeded at the surface of the granules.

Figures 5-21 and 5-22 show SEM images of the structure of the corrosion products on a granule coated with black material. Several different structures were observed. Several locations seem blocky or nodular, whereas other locations have a spiky, plate-like appearance. The spikes in Fig. 5-22 have flat surfaces about 2 μm long, 1 μm wide, and 0.4 μm thick. These structures appear to be significantly different from the structure of metallic zinc granules, which can be seen at some underlying locations on the granule.

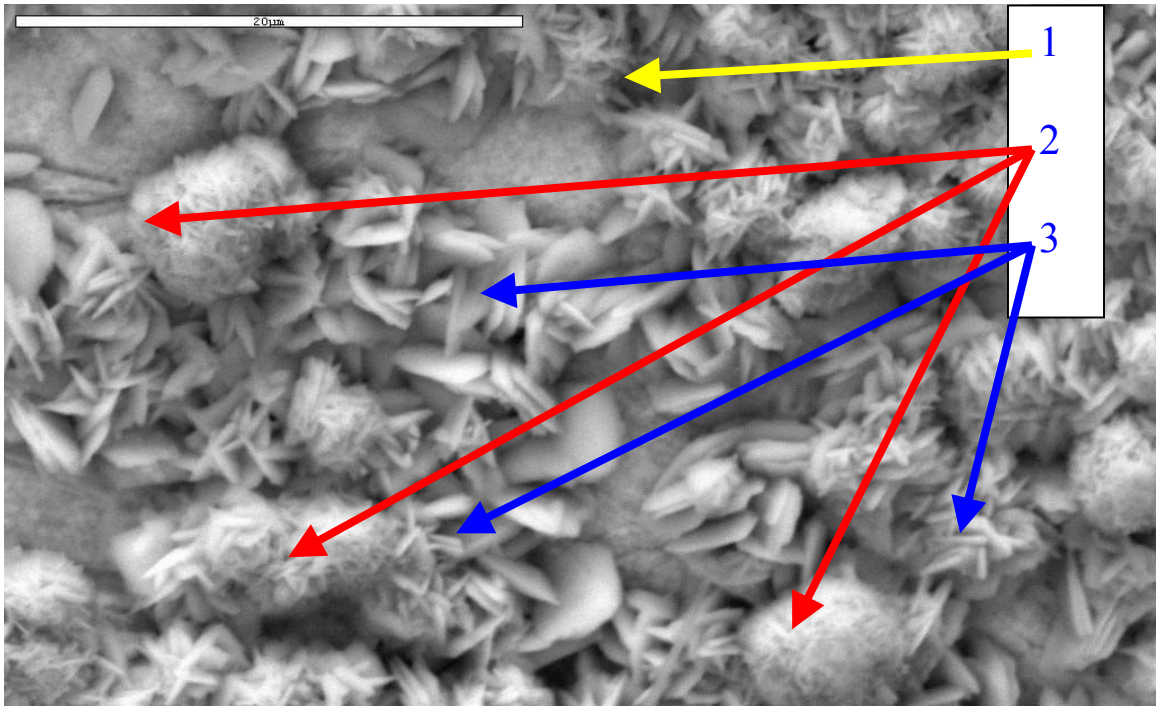

Fig. 5-21. SEM picture of the zinc granules of Fig. 5-20.

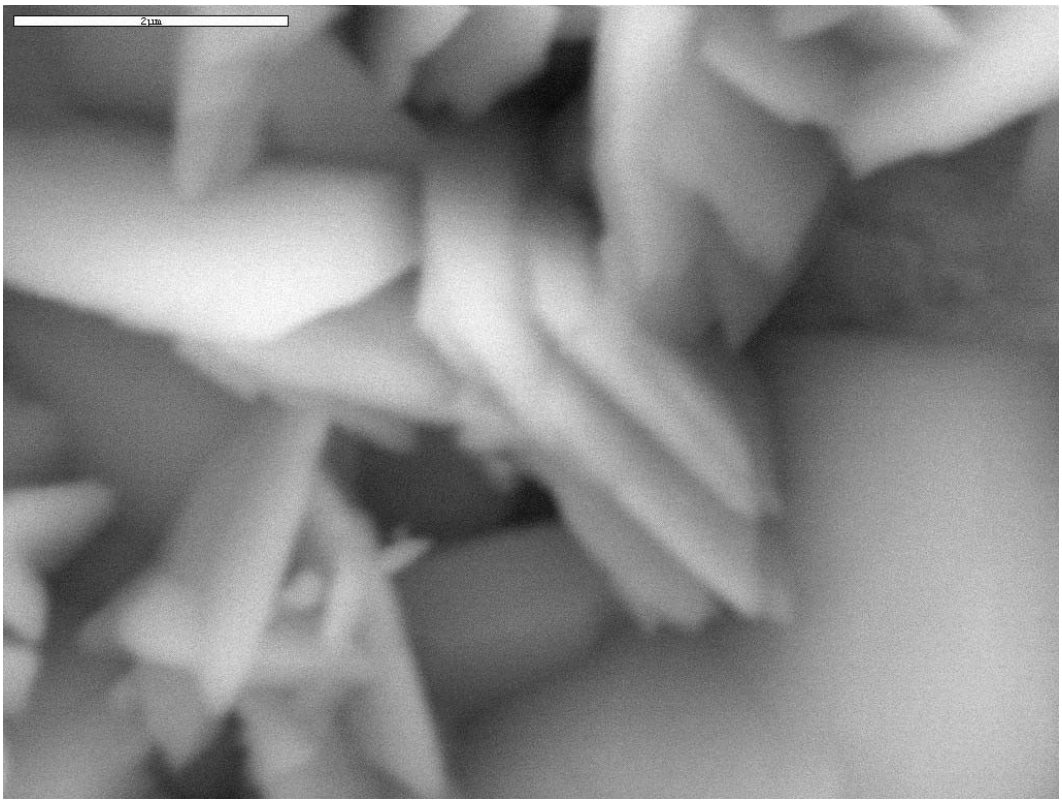

Fig. 5-22. Magnified view of the spikes seen in Fig. 5-21.

5.5.3 Elemental Composition as Identified by Energy-Dispersive Spectrometry

The chemical composition (percent weight of elements) of the various structures on the granule coated with black material can be determined by EDS. These EDS results are given in Figs. 5-23 through 5-25. The chemical compositions, given by EDS, for the different structures on the granule surface are given below.

Fig. 5-21	SEM	Composition (% weight)				
Location No.	Fig. No.	Carbon	Oxygen	Aluminum	Silicon	Zinc
1	5-23	3.1	6.03	0.23	0.76	89.88
2	5-24	9.85	20.77	0.24	10.59	58.55
3	5-25	5.93	17.74	0.49	11.85	63.99

The location identified as No. 1 in Fig. 5-21, which was assumed to be the underlying metallic zinc granule, appeared to be about 90% zinc, with small amount of oxygen and carbon, which may be due to nearby corrosion products. Locations 2 and 3 in Fig. 5-21, which were assumed to be corrosion products, contained significantly less zinc (about 60%) and significantly more carbon and oxygen.

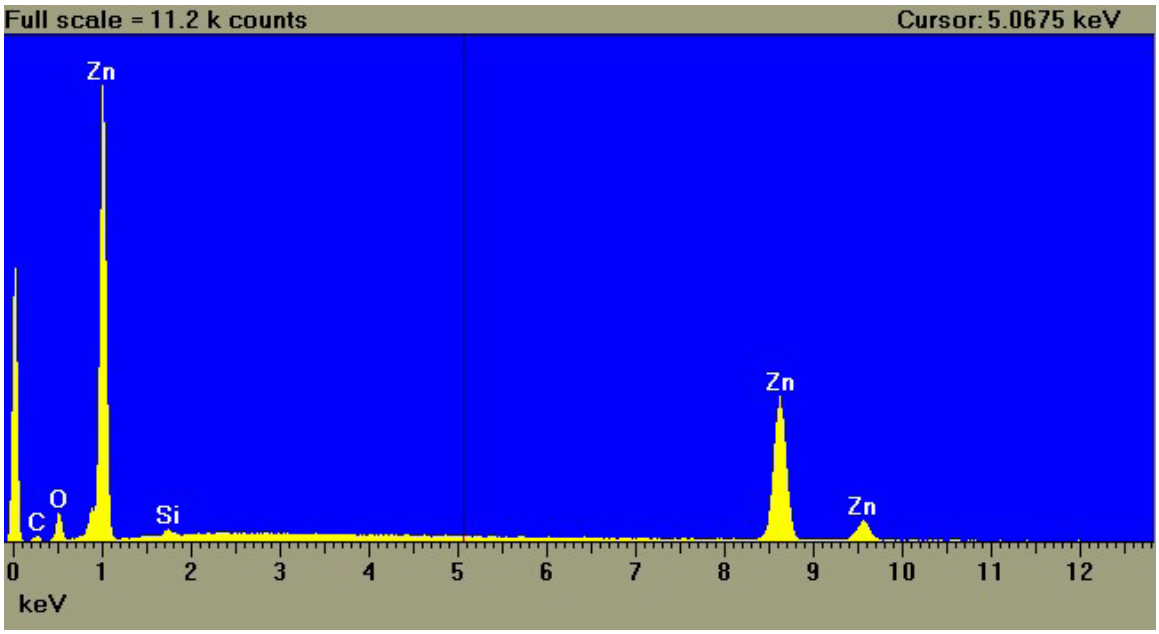

Fig. 5-23. Chemical analysis of zinc granule at a location where there is no corrosion product (location 1 of Fig. 5-21.)

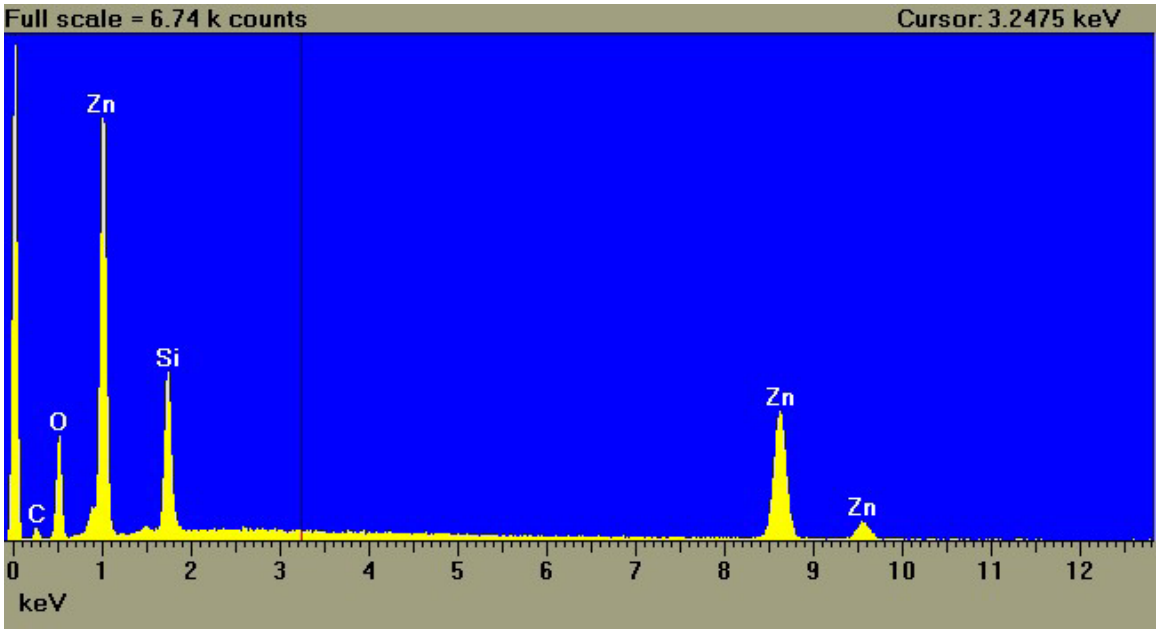

Fig. 5-24. Chemical analysis of zinc granule at a location where corrosion forms a blocky structure (location 2 of Fig. 5-21.)

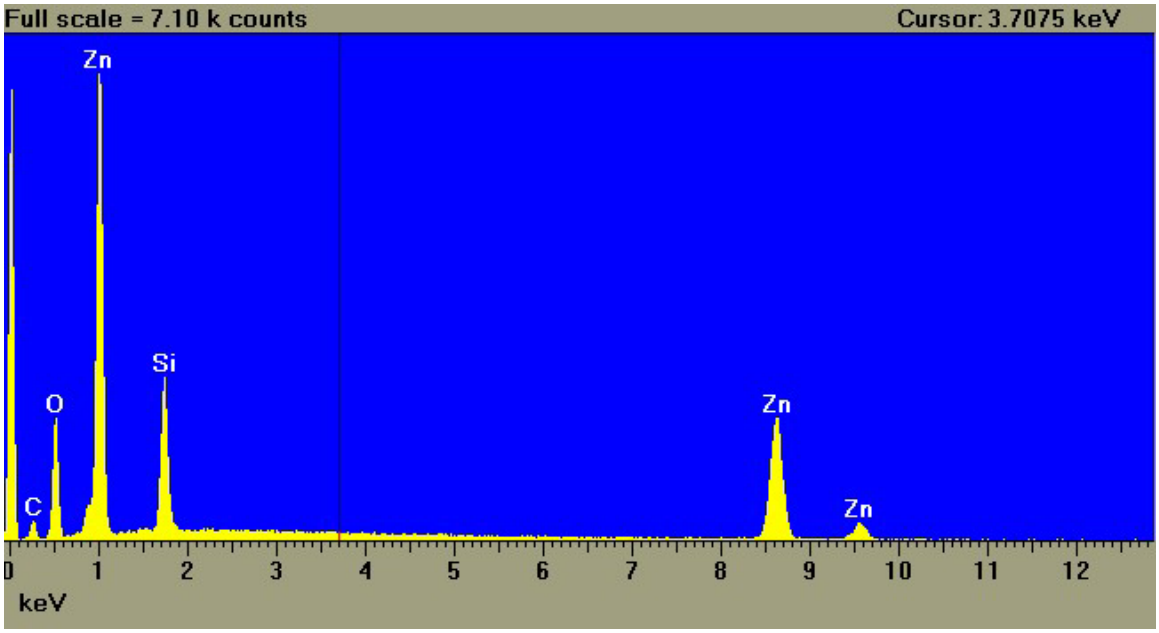

Fig. 5-25. Chemical analysis of zinc granule at a location where corrosion forms a sharp needle-like structure (location 3 of Fig. 5-21.)

5.5.4 Zinc Content by Acidification and Mass Balance Analysis

The black corrosion product was present as a coating on metallic zinc granules. Acidification and weight analysis were performed to determine the amount of corrosion product formed in comparison with the zinc weight loss and to provide a separate measurement of the zinc content of the corrosion product. The analysis was conducted with 0.7389 g of the corroded zinc granules taken from one of the corrosion tests. The sample was acidified with 10 ml of 1% HCl, and the black coating dissolved almost immediately (within 10 s). The sample was then rapidly doused with water to prevent dissolution of the underlying metallic zinc. The sample was filtered, dried, and weighed according to the procedures discussed above, and the sample weight was found to be 0.7220 g, indicating a weight loss of 0.0169 g during acidification. The diluted acid was analyzed and found to contain 0.0106 g of zinc. Comparing these two weight measurements indicates that the material dissolved during acidification was about 62.7% zinc by weight and about 37.3% other elements. The elemental composition determined during SEM imaging gives the zinc content in the block precipitates as 58.55% (see Fig. 5-24) and in the spiky precipitates as 63.99% (see Fig. 5-25), giving an average of 62%. Stoichiometrically, the elemental composition of $Zn_5(CO_3)_2(OH)_6$, the precipitation product predicted by water-quality modeling, is 60% zinc, 4% carbon, 35% oxygen, and 1% hydrogen. Thus, the zinc content determined during SEM imaging and by acidification produced very similar results, and both support the possibility that the corrosion product formed during the corrosion tests was $Zn_5(CO_3)_2(OH)_6$.

5.5.5 Chemical Composition Determined by X-Ray Diffraction

X-ray powder diffraction is primarily used as a method for determining what crystalline phases are present in a specimen. The ideal powder specimen contains a large number of randomly oriented crystallites of all phases present within it to the x-ray beam. The incident beam will generally penetrate a few tens of microns into the specimen so that surface and subsurface phases will contribute to the diffraction pattern. The diffraction beam is then measured as a series of peaks and intensities that may be used to "fingerprint" particular phases that are present, based on their unique crystalline structure. The success of the method in determining the phases that are present in the sample is a function of the abundance of randomly oriented crystallites of each phase being present in the area of the specimen that is irradiated by the incident beam.

The sample was examined using a binocular microscope prior to any preparation for analysis. The material consists of granular, elongate (up to 3 mm), dark-gray-to-black rounded granules that are very globular when viewed with the microscope. There are some white patches that may be coating the granules or "shining through" from below the dark surface. Much of the surface shows a translucent honey-brown reflectivity. There are reasonably abundant holes in the surface of the granules that suggest that they may be partially hollow.

The granules could not be ground into a powder using either an agate mortar and pestle or a Diamonite (synthetic alumina) mortar and pestle; however, the grinding produced some gray powder on the surface, thus resulting in a slight lightening of the gray color. Reexamination under the binocular microscope revealed that the granules were indeed hollow and appeared to be a thin shell of malleable metal that was torn open in some spots by the attempted grinding.

The attempt to powder the sample further was abandoned. A quantity of the material was mounted on a Plexiglas specimen holder for analysis, using petroleum jelly as a binder to hold the granules in place.

Parameters for data acquisition were as follows: K-α X-radiation; x-ray tube acceleration voltage 40 kV; and tube current 35 mA. The specimen was run over an angular range of 10^o to 70^o 2θ at a scan rate of 0.5 ^{o}/min, for a total scan time of about 2 h. DataScan 3.1 software from Materials Data Incorporated (MDI) was used for data acquisition, and Jade 5.0 (from MDI) was used for data analysis and presentation. The database contains x-ray diffraction pattern data for more than 99,000 inorganic compounds. Intensity- 2θ variation is given in Fig 5-26.

5.5.5.1 Discussion of the Results

It is noted that on the raw data plot, there is a significant "hump" in the background pattern in the 2θ angular region between 10^o and 20^o. This hump is not related to the specimen but is an artifact of the Plexiglas specimen holder that is used in the instrument.

The most prominent peaks in the pattern are the four located at 36.5^o, 39.2^o, 43.5^o (resolved as two peaks), and 54.4^o 2θ (also resolved as two peaks). The phase indicated by these peaks is zinc metal, and it appears to be the dominant phase in the sample. The diffraction pattern is compared

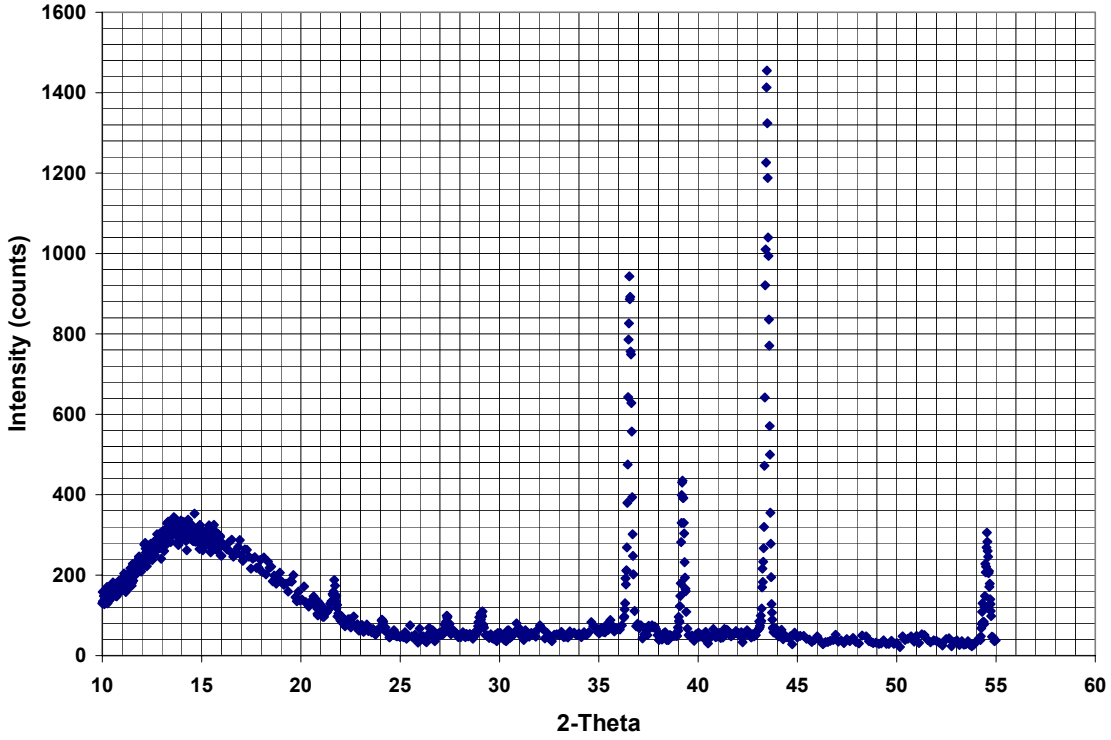

Fig. 5-26. X-ray diffraction analysis.

with the possible compounds ZnO, $Zn(OH)_2$, $Zn(CO_3)$, $Zn_5(CO_3)_2(OH)_6$, and $Zn(BO_2)_2$; none could be identified conclusively. The only possible exception to this is zinc oxide, which shows a slight correspondence with some "wiggles" in the background.

The peaks unmatched by metallic zinc are at 21.7°, 24.1°, 27.3°, 29.0°, and 29.1° 2θ; these represent one or more other crystalline phases present in the sample. It should be noted that, because x-ray powder diffraction with a diffractometer requires a large amount of small crystallites that is randomly oriented, any preferred orientation of the specimen could result in relative peak intensities that do not match that of the "standard" pattern. In some cases, the preferred orientation can result in the absence of the peaks, which would be present in a randomly oriented specimen. An insufficient number of crystallites could also result in a pattern in which the contribution from the phase in question could not be differentiated from the background noise in the pattern.

An automated search/match on the pattern, unconstrained by chemistry limitations, yielded a match to potassium uranium oxide (K_2UO_4). The match is quite good to four peaks above this phase or to one that is unidentified in the database but very similar structurally.

5.5.6 Summary of Identification of Zinc Corrosion Products

The formation of a corrosion product that is about 60% zinc by weight supports the experimental observation of weight gain during some of the tests. At pH = 7.0, where zinc is more soluble, the

zinc appears to have dissolved from the zinc-granule surface and remained in solution, resulting in a net loss of weight during the corrosion tests. However, at pH = 9.0, the $Zn_5(CO_3)_2(OH)_6$ is near its minimum solubility point; thus, any dissolution of metallic zinc from the granule surface would have formed $Zn_5(CO_3)_2(OH)_6$ instead of remaining in solution as Zn^{2+} ions. Because the $Zn_5(CO_3)_2(OH)_6$ is only 60% zinc by weight, the replacement of metallic zinc with $Zn_5(CO_3)_2(OH)_6$ would have resulted in the observed weight gain. The lower zinc concentration measured in solution after the corrosion tests is also consistent with the lower solubility at pH = 9, as predicted by the water-quality modeling.

5.6 Analysis of Silica Content in Immersion Solutions

The elemental composition of EDS identified the presence of silica on the granules used during the zinc corrosion tests. Several questions were raised during the review of the draft report: (1) What was the source of the silica because silica was not intentionally added to the water during the experiments? (2) Does the presence of silica significantly alter the corrosion rates of zinc in containment pool water? (3) Is the presence of silica representative of chemical conditions that may be present in containment water? To answer these questions, additional experiments were conducted.

Several sources of silica were considered, including leaching from the borosilicate glass bottles used in the experiments, contamination from the chemicals, and contamination from the laboratory DI water. To identify the source of silica, a final group of experiments was conducted using polypropylene (PP) bottles instead of glass bottles for the immersion tests. In addition, a set of metal-free bottles was prepared, in which DI water without metal was placed in the PP bottles, carried through the test procedure, and analyzed for silica concentration.

The presence of silica in the laboratory experiments may actually be consistent with the conditions inside the containment structure during a LOCA. Dust and debris inside containment may contain silica that could be dissolved into solution. More importantly, the NUKON™ insulation around the pipes is made of fiberglass, which contains a significant amount of silica. To determine whether silica could leach out of NUKON™ in a reasonable amount of time, NUKON™ was added to a set of jars filled with synthetic containment water, and the silica concentration in the water was measured after several days.

5.6.1 Observations

One liter of DI water was placed into each of two PP jars. After 4 days of storage in a 40°C oven, the silica concentration of the water was analyzed. The silica concentration in each jar was measured in triplicate and found to be 3.48 mg/L in the first jar and 4.13 mg/L in the second jar. These results indicate that the laboratory DI system was one source of silica in the previous tests.

The water in six of the jars in the sixth group of corrosion tests was analyzed for silica concentration. The six jars selected for analysis were the jars that had been held for 4 days prior to analysis of zinc corrosion. The jars each contained water with boric acid and lithium that had been adjusted to pH = 7.0. Three of the jars were stored at room temperature, and three were stored at 40°C. All jars showed evidence of silica in amounts higher than the concentration in the

DI water. Silica concentrations ranged from 5.2 to 22.3 mg/L. Higher concentrations of silica corresponded to greater amounts of NaOH and HCl used to adjust the pH to 7.0. For instance, in tests 6-2 and 6-4, an excess of NaOH was used in adjusting the pH, leading to a pH value greater than 7.0, and HCl was used to bring the pH back down to 7.0. The water in these jars had silica concentrations of 18.5 and 22.3 mg/L, respectively. These results indicate that the chemicals used to adjust the pH contained trace amounts of silica, which were introduced into the sample jars when the pH was adjusted.

Three additional jars were prepared with about 1.5 g of NUKON™ in 1 L of water (containing boric acid and lithium) in each jar. The pH in each jar was adjusted to a value of between 9.7 and 10.2. The jars were stored in the oven at 40 °C for 4 days and then analyzed for silica. Each silica analysis was performed in triplicate. The silica concentrations ranged from 30.4 to 37.0 mg/L, thus indicating that silica leaching from NUKON™ under high pH and moderate temperature conditions is likely.

5.7 Summary of Zinc Corrosion Tests

Corrosion tests were conducted by immersing zinc materials in aqueous solution for a period of several days and measuring the change in weight after the immersion period. Tests were done with zinc granules, zinc coupons, and crumbled inorganic zinc primer. Most tests were done with solutions representative of the water in the containment pool during a LOCA (NaOH, 3.3×10^{-2} M H_3BO_3 and 2.0×10^{-4} M lithium), although some tests were also done in DI water. Experimental variables included pH, temperature, and duration.

The tests that were the most successful in establishing a corrosion rate were the ones conducted at a pH = 7.0 and room temperature. A general trend can be established that the average corrosion rate decreased as the duration of the experiment increased. Measured corrosion rates ranged from 0.055 g/(m^2·h) averaged over 2 days to 0.017 g/(m^2·h) averaged over 11.75 days.

Piippo et al. [3] measured zinc and aluminum corrosion rates using electrical resistance measurements with several test solutions. These solutions included (1) distilled water that had been adjusted to pH values of 8.0 and 10.0 using LiOH and maintained in either aerated or deaerated conditions and (2) a 0.1-M borate buffer solution at pH 9.2. The tests were done at temperatures ranging from 50°C to 130°C. For purposes of comparison, the test conditions in the current experiments are most closely comparable with the borate buffer solution used by Piippo. In the borate solution, Piippo measured zinc corrosion rates of 0.05 g/(m^2·h) at 50°C, 0.03 g/(m^2·h) at 70°C, and 0.04 g/(m^2·h) at 90°C. Piippo also referenced data from van Rooyen [12] and Loyola and Womelsduff [13], which also experimentally evaluated corrosion rates of zinc in water containing borate. The results in [12] and [13] were relatively consistent with Piippo's results. The results of the current study, with corrosion rates of 0.055 g/(m^2·h) at 22°C and 0.057 g/(m^2·h) at 40°C, are very compatible with rates measured in previous studies.

Piippo measured much higher zinc corrosion rates under other experimental conditions. For most aqueous solutions, the corrosion rate increased by at least an order of magnitude when the temperature increased above the normal boiling point of water. In the borate solution, Piippo measured a zinc corrosion rate of 4.45 g/(m^2·h) at 110°C and 1.26 g/(m^2·h) at 130°C. However,

the highest measured zinc corrosion rate in the Piippo report was a value of 11.27 g/(m^2·h), which was measured in a deaerated DI solution at 170°C, after the test materials had been exposed to hot steam at 300°C.

Tests at higher temperatures or higher pHs were less successful in producing quantitative corrosion rates. Many of the tests at these conditions resulted in a gain of weight over the test duration, thus indicating the formation of a corrosion product with a higher molecular weight than the original material. In addition, many of these tests resulted in the formation of a black coating on the zinc granules and coupons, which could be scraped off. The black coating and the increase in weight, which indicates a corrosion product, are qualitative indicators of corrosion.

Several attempts were made to identify chemical and physical characteristics of the corrosion products. Visualization with a light microscope demonstrated a change in appearance after immersion, with the zinc granules exhibiting a shiny, light-gray appearance before immersion and either a dull light-gray or dull black appearance after immersion. SEM imaging identified the formation of a platelet structure, which was not characteristic of the original zinc material. Elemental composition by EDS and zinc content by mass balance both suggested that the corrosion material was about 60% zinc. Chemical composition by x-ray diffraction suggested the presence of zinc oxide but could not conclusively identify other zinc compounds. EDS identified the other elements present as oxygen (18% to 20%), silica (10% to 12%), carbon (6% to 10%), and aluminum (trace). No evidence of the presence of boron or lithium was observed. One of the species predicted by water-chemistry modeling to precipitate is $Zn_5(CO_3)_2(OH)_6$. The elemental composition of this compound is 60% zinc, 35% oxygen, 4% carbon, and 1% hydrogen. It is possible that the EDS analysis detected a combination of this compound, background metallic zinc, and other compounds that formed on the granules, including some silica-containing compounds.

Silica was determined to be present during the corrosion tests and was found to be present in the DI water and in the chemicals used to adjust the pH. However, it was also determined that silica can leach from NUKON™ under chemical and temperature conditions representative of the containment water during a LOCA; therefore, the presence of silica in these tests cannot be considered to be a mitigating factor. In fact, the presence of silica in the tests is consistent with the chemical conditions expected during a LOCA.

6.0 CONCLUSIONS AND RECOMMENDATIONS

6.1 Principal Results of the Study

The research conducted in this study regarding the potential effects of chemistry on debris generation and head loss experienced during a PWR LOCA represents the first investigation of its kind sponsored by the NRC in the context of GSI-191. The broad issue of "potential chemical effects" includes, but is not limited to, the following list of candidate concerns:

1. metal corrosion in both spray and immersion environments;
2. plausible mechanisms for the formation of "gelatinous material";
3. degradation of unqualified paints;
4. leaching of zinc from inorganic coatings;
5. long-term chemical degradation of fibrous debris beds;
6. accurate descriptions of time-dependent pool pH and temperature;
7. benefits or detriments introduced by the use of phosphate complexing agents;
8. sensitivities of water chemistry to the presence of silicates introduced by dirt in containment, leaching from fiberglass, ablation of concrete, or dissolution of calcium silicate insulation materials;
9. ultimate saturation of silicates with subsequent precipitation;
10. time scales for adverse chemical reactions and head-loss effects in the context of plant accident response; and
11. interactions between any and all of the above concerns.

Research documented here has attempted to survey a number of these concerns and to generate data that establish a technical basis for deciding whether chemical reactions and water chemistry conditions play an important role in debris generation and sump-screen head-loss phenomena. All previous GSI-191 research on debris transport and head loss was conducted over relatively short durations using room temperature water and no control of water pH (presumed neutral). The initial objective was to assess the potential for chemically-induced corrosion products to impede the performance of ECCS recirculation after a LOCA in PWR plants. A comprehensive understanding of any single concern listed above or a knowledge base of all issues and their interactions will require additional study.

From this initial list of candidate concerns, it has been determined that

1. temperature-dependent corrosion of metal can occur at temperatures and pH typical of immersion in post-LOCA accident environments;

2. precipitation of dissolved metals in excess of their relatively low solubility limits can produce transportable gelatinous material that causes significant pressure drops across a fibrous debris bed;

3. dissolved zinc can be leached from zinc-based coating debris typical of that generated in the zone of influence near a high-pressure pipe break;

4. silica can be leached from typical fiberglass insulation debris and, because of its prevalence in containment, may be an important constituent of the chemical system under consideration.

However, it must also be acknowledged that, although the necessary chemical conditions and plausible reaction mechanisms may exist to form a gelatinous precipitant, the implied progression from metal corrosion to ultimate precipitation and head loss was not demonstrated conclusively. The philosophy applied in this study has been first to understand the separate effects important for each step of the accident scenario before attempting to conduct and interpret the results from a large-scale integrated test. The potential for chemical precipitation represents a unique challenge to existing and future sump-screen designs than previously investigated under GSI-191. Alternative chemical reactions were noted, such as the formation of crystalline corrosion deposits under somewhat atypical quiescent immersion conditions; thus, as yet, there is no firm causal relationship between corrosion and precipitation. In conjunction with the head-loss data reported here, industrial experience with metallic coagulation agents and silica-based gels and coprecipitants confirms that chemical precipitation is not a desired outcome for ECCS sump pool chemistry.

If it is assumed that it is possible to gradually approach the solubility limit of dissolved metals in a well-mixed containment pool, then the time needed to reach saturation becomes a critical parameter in the systems analysis of the accident sequence. At this juncture, important chemical transitions will occur. Formation of flocculent precipitants is one possible outcome with detrimental effects. Formation of crystalline surface deposits may also represent a large quantity of previously unconsidered and undesirable particulate if it were shown to be frangible in turbulent flow conditions. The saturation time definitely depends on the amount of exposed surface area, the pool dilution volume, and the corrosion rate. For this reason, a great effort was made to validate metal corrosion rates reported in the literature. Carefully controlled immersion tests finally yielded repeatable data for corrosion of zinc at 22ºC (room temperature) and 40ºC. The respective time-averaged values of 0.04 and 0.06 $g/m^2/h$ agree well with literature values reported for similar immersion conditions.

The biggest impediment to accurate measurements of metal corrosion rates, at high temperature in particular, proved to be the low solubility limit of these metals in solution. Initial attempts to derive time-averaged corrosion rates based on sample weight-loss rates and dissolved zinc concentration measurements showed decreasing rate estimates as the duration of the experiment increased. In fact, at high temperatures, the samples quickly began to gain weight and to turn black, thus suggesting the formation of a higher molecular-weight corrosion product (the black crystalline product discussed in Section 5). Several attempts were made to adjust the averaging time, the exposed surface-to-volume ratio, and the temperature to avoid confounding rate estimates with the approach to saturation. In retrospect, use of an agitated or circulating

immersion medium may have eliminated high local concentrations near the sample surface that could have initiated crystal growth. In the uniform thermal environment of the oven, minimal convection currents may have permitted stratified concentrations, even at elevated temperatures.

Other aspects of the initial test matrix were not investigated as thoroughly as were corrosion and head loss. For example, zinc leaching from inorganic paint chips was observed and documented; however, because of the difficulty in estimating exposed surface areas of the crumbled samples, no rates were quantified. The importance of this additional source of dissolved zinc depends greatly on the comparison between the exposed area of galvanized metals in containment and their combined spray/immersion corrosion rates vs the amount of paint debris generated near a high-pressure pipe break. Because paint damage near steam jets has been observed and because no data exist to characterize the size distribution and surface area of this debris type, it would be conservative to assume that all of the zinc in the damage region is available for dissolution in the pool.

Similarly, the leaching of silica from fiberglass debris was observed; however, no rates were quantified. The ultimate importance of this contribution would depend on the presence of other dominant sources, such as calcium silicate insulation and ablated concrete, as compared with the amount of fiberglass debris generated in the LOCA. The Chemical Test Peer Review Panel emphasized the importance of sump pool chemistry in the presence of silica. Silica has the potential to reduce the solubility of metals, participate in many coprecipitation reactions, and ultimately reach its own saturation limit with subsequent preferential precipitation within a fiberglass debris bed itself.

6.2 Suggestions for Future Work

Given the limited duration of this investigation and the potential complexity of chemical systems that may exist in the post-LOCA accident environment, it is not surprising that a number of issues remain unresolved and that additional information is desired. The following discussion focuses on lessons learned during the recent experimental investigation. Additional chemical concerns listed at the beginning of this section may be equally deserving of further study; however, the necessary background does not yet exist to help direct suitable recommendations.

- The single most beneficial exercise needed to allay (or solidify) concerns regarding chemical precipitation is an integrated corrosion and head-loss test that combines realistic galvanized coatings and/or aluminum alloys with a fibrous debris bed in a circulating system of representative chemistry and temperature. A series of integrated tests would alleviate criticisms of the current work regarding the use of atypical metal samples and quiescent immersion conditions. Time-dependent measurements of head loss across the debris bed would be monitored for any gradual or abrupt changes signifying the transition from soluble to insoluble corrosion products. The proper suite of analytic tests and sufficient laboratory experience is now available to design, execute, and interpret tests of this nature. Integrated testing has been endorsed by both the Chemical Test Peer Review Panel and the ACRS.

- The second most beneficial experiment needed to tighten the present understanding of systems response and time scales to pool saturation is to measure the corrosion rate of typical galvanized material under well-oxygenated spray conditions. Some as-yet unidentified experiments may also be reported in the literature regarding spray or high-humidity corrosion for common metals. Good estimates of spray corrosion rates and exposed surface areas are critical to accurate estimates of saturation time. The issue of preexisting surface oxidation should also be examined in a study of this nature. In fact, the contribution of surface oxidation may be necessary to define the initial chemical conditions for an integrated test that represents continual immersion in a flowing system.

- Further investigation of silicate chemistry is needed to determine its influence on metal solubility in the context of ECCS sump pool chemistry. For chemical systems dominated by a debris source such as calcium silicate, the real potential for silicate saturation must be considered. Recent head-loss tests using calcium silicate as a particulate source have not considered the potential chemical effects that may drive head-loss behavior for saturated systems. The Chemical Test Peer Review Panel first emphasized the potential importance of silica as a candidate for chemical concerns. Silica will participate actively in many precipitation and surface-deposition processes.

- Although the head-loss behavior of metal precipitants has been investigated, predictive correlations of pressure drop are still needed as a function of precipitant quantity. Correlations of this kind may be derived using data in this report; however, systematic tests would be needed for additional validation under a variety of composition, mass, velocity, and temperature conditions. The composition of observed metal precipitants is also speculative at this time. Although equilibrium chemistry considerations suggest metal hydroxides or silicates, no analytic techniques have been applied to confirm this speculation.

- As additional physical data become available to describe the chemical conditions of the sump pool, the preliminary work presented here on systems safety considerations should be developed in tandem to both benefit from the new data and help direct and prioritize research investments. Systems studies are the analytic analogy to integrated experimentation, where the interactions of all potentially important parameters can be examined and understood in detail. A systematic, integrated analysis perspective will ultimately be needed to validate any mitigation strategies that are proposed to counter legitimate adverse chemical effects.

- Although pH and temperature are important aspects of the physical chemistry, the ultimate influence of these factors will be driven more by uncertainties and variabilities in the accident history than by a lack of understanding of their direct effect on chemical reactions. In general, zinc solubility will decrease with both temperature and pH; thus, in some respects, the current tests performed at relatively low temperatures and neutral pH levels have been nonconservative. On the other hand, potential problems revealed under the current test conditions more conclusively demonstrate the plausibility of important chemical interactions. More detailed parametric analyses of the accident history may reveal critical time frames where it

may be beneficial to have better information on corrosion and the combined solubility of various metals as a function of pH and temperature.

- Although some aspects of the current work are not definitive, the combination of industrial experience and separate-effects testing validates the potential for adverse chemical effects to induce additional head loss across preexisting fibrous debris beds. As more information is added to the knowledge base, there may eventually be a need to formulate and test chemical mitigation strategies. Among the potential concepts are coating systems to reduce corrosion, buffering or complexing agents to increase solubility of metals, seeding agents or catalysts to scavenge adverse products before they reach the screen, and certainly more traditional concepts for active screen protection, such as moving scrapers and sacrificial screen areas. As always, mitigation strategies must be carefully integrated with all current plant safety systems to ensure that unintended problems are not introduced.

- The knowledge base can always be expanded by conducting corrosion and head-loss tests with other metals, such as copper, lead, aluminum, and iron. Samples of these metals should be representative of structural and manufacturing materials present in containment.

7.0 REFERENCES

1. H. P. Hermansson and S. Erixon, "Chemical Environment for Strainers at Loss of Coolant Conditions in a PWR," Swedish Nuclear Power Inspectorate (SKI) Report 98:12 (February 1997).

2. K. W. Ross, D. V. Rao, and S. G. Ashbaugh, "GSI-191: Thermal-Hydraulic Response of PWR Reactor Coolant System and Containments to Selected Accident Sequences," United States Nuclear Regulatory Commission report NUREG/CR-6772, Los Alamos National Laboratory report LA-UR-01-5661 (August 2002).

3. J. Piippo, T. Laitinen, and P. Sirkiä, "Corrosion Behaviour of Zinc and Aluminium in Simulated Nuclear Accident Environments," Finnish Center for Radiation and Nuclear Safety report STUK-YTO-TR 123, (February 1997).

4. K. K. Niyogi, R. R. Lunt, and J. S. Mackenzie, "Corrosion of Aluminum and Zinc in Containment Following a LOCA and Potential for Precipitation of Corrosion Products in the Sump," United Engineers and Constructors, Inc., Proceedings of the Second International Conference on the Impact of Hydrogen on Water Reactor Safety held in Albuquerque, NM on Oct. 3-7, 1982, NUREG/CP-0038, pp. 401-423.

5. R. Kallstrom, H. P. Hermansson, and C. Norrgard, "The Effect of Chemicals on Strainer Filtration. Final Report: Laboratory Tests at Various pH Levels," Swedish Nuclear Power Inspectorate report (January 1995).

6. I. Vicena, V. Gubco, J. Batalik, J. Murani, M. Davydov, O. I. Melikhov, V. N. Blinkov, Y. Armand, and J. M. Mattei, "Experiments on the risk of sump plugging on French PWR," Proceedings of the Conference EUROSAFE 2002 – International Forum for Nuclear Safety, 4-5 Nov. 2002, Berlin, Germany.

7. W. D. Shults, Oak Ridge National Laboratory, Analytical Chemistry Report to J. A. Daniel, GPU Service Corporation (September 14, 1979).

8. J. D. Allison, D. S. Brown, and K. J. Novo-Gradac, "MINTEQA2/PRODEFA2, A Geochemical Assessment Model for Environmental Systems: Version 3.0 User Manual," United States Environmental Protection Agency Environmental Research Laboratory report EPA/600/3-91/021 (March 1991).

9. G. Zigler, J. Bridaeu, D. V. Rao, C. Shaffer, F. Souto, and W. Thomas, "Parametric Study of the Potential for BWR ECCS Strainer Blockage due to LOCA Generated Debris," United States Nuclear Regulatory Commission report NUREG/CR-6224, Science and Engineering Associates, Inc. Report No. 93-554-06-A:1 (January 1994).

10. M. T. Leonard, D. V. Rao, A. K. Maji, and A. Ghosh, "GSI-191: Experimental Studies of LOCA-Generated Debris Accumulation and Head Loss with Emphasis on the Effects of

Calcium Silicate Insulation," Los Alamos National Laboratory report LA-UR-03-0471 (January 2003).

11. Standard Methods for the Examination of Water and Wastewater, prepared and published jointly by the American Public Health Association, American Water Works Association, and Water Environment Federation, Washington, DC (1999).

12. D. van Rooyen, "Hydrogen Release Rates from Corrosion of Zinc and Aluminum," BNL-NUREG-24532 informal report, pp. 1-37 (May 1973).

13. V. M. Loyola and J. E. Womelsduff, "The Relative Importance of Temperature, pH, and Boric Acid Concentration on Rates of H_2 Production from Galvanized Steel Corrosion," Sandia National Laboratories report SAND82-1179, United States Nuclear Regulatory Commission report NUREG/CR-2812 (November 1983).

14. D. V. Rao, B. Letellier, C. Shaffer, S. Ashbaugh, and L. Bartlein, "GSI-191 Technical Assessment: Parametric Evaluation for Pressurized Water Reactor Recirculation Sump Performance," Los Alamos National Laboratory report LA-UR-01-4083, Volume 1 of United States Nuclear Regulatory Commission report NUREG/CR-6762, "GSI-191 Technical Assessment" (August 2002).

15. W. Serkiz, "Containment Emergency Sump Performance," United States Nuclear Regulatory Commission report NUREG-0897 Rev. 1 (October 1985).

16. J. C. Griess and A. L. Bacarella, "Design Considerations of Reactor Containment Spray Systems – Part III. The Corrosion of Materials in Spray Solutions," Oak Ridge National Laboratory report ORNL-TM-2412 Part III (December 1969).

17. Wm. B. Cottrell, "ORNL Nuclear Safety Research and Development Program Bimonthly Report for July-August 1968," Oak Ridge National Laboratory report ORNL-TM-2368 (November 1968).

18. Wm. B. Cottrell, "ORNL Nuclear Safety Research and Development Program Bimonthly Report for September-October 1968," Oak Ridge National Laboratory report ORNL-TM-2425 (January 1969).

19. NRC-SER-URG, "Safety Evaluation by the Office of Nuclear Reactor Regulation Related to NRC Bulletin 96-03 Boiling Water Reactor Owners Group Topical Report NEDO-32686, 'Utility Resolution Guidance for ECCS Suction Strainer Blockage,'" Docket No. PROJ0691 (August 20, 1998).

20. NEDO-32686, Rev. 0, "Utility Resolution Guidance for ECCS Suction Strainer Blockage," Boiling Water Reactor Owners Group (November 1996).

21. Surry Power Station Units 1 and 2 Updated Final Safety Analysis Report, Rev. 33, Virgina Electric and Power Company.

22. Comanche Peak Steam Electric Station Final Safety Analysis Report, Amendment 97, TXU Energy (February 2001).

APPENDIX A

PEER-REVIEW-PANEL MEMBER COMMENTS

On September 15, 2003, a peer review panel meeting was convened in Albuquerque, NM at the University of New Mexico where the chemical test experiments were conducted. The purpose of this meeting was to review the Los Alamos draft report on the effects of chemical reactions on debris bed head loss. The peer review panel members consisted of:

Professor Peter Griffith, Massachusetts Institute of Technology
Dr. Edward J. Lahoda, P.E., Westinghouse Electric Company
Professor Adrian Hanson, New Mexico State University

Also in attendance at the meeting were the following:

Tsun-Yung Chang, NRC/RES/DET
Bruce Letellier, Los Alamos National Laboratory
Kerry Howe, University of New Mexico
Ashok Ghosh, University of New Mexico
Arup Maji, University of New Mexico
Russ Johns, Los Alamos National Laboratory
James Lime, Los Alamos National Laboratory

Following the review meeting, a tour of the experiment facility and a demonstration of how a head-loss test was conducted were given. The report review of the panel members are given in this appendix as follows:

Review of:

"Small Scale Chemical Experiments: Effects of Chemical Reactions on Debris-Bed Head Loss", LA-UR-6415, by R C Johns, K J Howe, A K Ghosh, August 2003

Peter Griffith
26 September 2003

Introduction

In-so-far as this draft report included neither an abstract nor conclusions, it is difficult to judge whether the objectives of the program have been met. I assumed when the draft report was sent to me, that the missing sections would be handed out at the meeting. That didn't happen, so I'm going to start this review by suggesting some changes that can lead to a tighter report. The authors are certainly free to ignore any suggestions as they see fit. They know more about the program than I do. Some of these suggestions can be justified by the data that has been taken while some are harder to justify, but they do show what kind of changes need to be made if this work is to be useful.

I'll start with suggestions for this report that can be adopted without much

further work. I'll then proceed to suggestions for further work

I do not regard this work as complete so this report should really be treated as a progress report, subject to revision as more is learned.

Recommendations for this report

1) Say a single LB LOCA transient should be selected for each plant that is to be examined. It should be chosen at best estimate conditions and all complicating factors such as products from fires or core damage should be ignored for the present. (I suspect that many plants will pass without much trouble if this is done.)
2) Say the system chemistry should be simplified so that calculations needed for evaluating possible fixes can be handled more easily. Focus on the most important chemical parameters and freeze the secondary variables at conservative values. Specifically, I suggest the following;
   a) Replace the variety of metals that are in the pool by an equivalent quantity of zinc. (I believe Figure 4-9 of the draft report can be used to justify what is selected.)
   b) Choose a single representative value for the pH for the transient. A value of 8.0 seems reasonable.
   c) The system temperature should be allowed to vary over the transient but a single value should be chosen for each segment of the transient. (See comment 4.) This temperature would be interpreted as both the pool temperature and the temperature of the atmosphere in the containment. The LOCA calculation would have this temperature as one of its outputs.

d) The atmosphere in the containment should be assumed to consist of steam, at its appropriate partial pressure, and the air originally in the containment.

3) Say that all the floc that makes it to the screens is trapped on them. (This was apparent in the demonstration but is not mentioned in the report.)

   I think it is true and simplifies subsequent calculations if it is.

4) Improve or replace the time-line given on Figure 2-1. There is too much detail in the blowdown phase and not nearly enough in the later phases, where the processes important to screen blockage, take place. Perhaps the time-line format of Appendix C should be adopted. In any case, add more information. Put in the system temperature for each phase of the transient. Put in the water level and the pump and spray flow rates. A lot more detail in the period from 0.25 hours to 24 hours is needed.
5) Go back through the experiments and extract the most important finding for each set of experiments and make it into a conclusion. Edit the suggested conclusions so you are comfortable with them. That we need more information about a certain topic is a perfectly acceptable conclusion.
6) Reduce the head loss results of Figure 4-9 to a form of flow resistance which can easily be used by someone trying to evaluate the safety of a plant. As the results are presented now they are in a form peculiar to the apparatus used by you. I also suspect that most to your data is not in the range of pressure drops or mass velocities of interest to a user. I suspect that they are too high. Extrapolate right down to zero or a very low flow rate. Don't ask the user to extrapolate or reduce your data, do it for him.
7) To the extent that you can, discuss and justify the system simplifications that I have suggested in the light of the experiments that you have run. If you can't justify them, change them.
8) Create a new section which is, in essence, an example calculation. It should include the debris transport and trapping processes in a simplified way, but with realistic values for the parameters. Cite other sources if they are needed to justify the choice of values. Use the same values of the system variables that you use in your-time line. Show how the information you are presenting can be used to solve a problem. Whether the plant selected passes or fails doesn't matter, it is only an example. The values of the variables selected should be in a realistic range however. This overview will help us to focus an the most important uncertainties in the future work.
9) Run some replication experiments to give the readers a feel for the precision of the reported results. The data reported on Figures 4-9 and 4-10 is most significant in this regard. Complete this report before running any brand new experiments, however.
10) Re-organize the report so that anything that you can turn into a conclusion is included as a conclusion and is described in the body of the report. If you cannot use it for a conclusion, try to put it in an Appendix. As it is, the report rambles. Anything you can do to tighten it up will help.
11) Go through the report and sort out all the acronyms and make sure they are included in the list.

Suggestions for future work.

1) Run some zinc corrosion experiments at the appropriate temperature and pH. These are needed to confirm or disprove the corrosion rate results reported by the Finns in Reference (3) of the draft report.
2) Run an experiment to see whether the concerns of Ed Lahota about the effect of silicon on floc formation are justified. These experiments should be run at more prototypical flow rates and head losses. This is important because the flow resistance of the floc does not remain constant with pressure drop at low pressure drops. At low flows, the flow resistance tends to drop too.
3) Run a very low flow rate experiment. At large times after the accident, the amount of water needed to keep the core cool is very low. Even a degraded screen might work well be able to provide all the water that you need.
4) Run an experiment specifically to find out at what fiber loading the screen performance degrades. Early in the transient, there will be very little dissolved metal in the water. When the demand for water is high, early in the transient, the screens might work fine because the metal hasn't had a chance to dissolve yet. Late in the transient the demnd for water is low. The system might work well enough if the water supplied to the core is controlled to meet the demand.
5) The screens that were tested in these experiments had very small holes in them. The bridges that the fibers formed were hard to push through. If the holes are big enough, I don't think that would be the case. Find out how big the holes have to be to form a blockage that can be dislodged by the driving pressure.
6) Sooner or later I think we will need suitably scaled experiment that uses prototypical water chemestry, protypical water mass velocities and prototypical pool depths. Different screen designs can be tested and we will be able to see whether, if the pool depth is increased gradually, the amount of fiber that makes it to the top of the screen is so small, that the screen performs satisfactorily. The experiment would be tall and slender in order to keep the overall flow rate reasonable. I think prototypical fiber loadings in the water need to be maintained for this experiment.

(The following are additional comments received from Professor Griffith on 10/1/03.)

Date: Wed, 01 Oct 2003 13:46:07 -0700
To: TYC@nrc.gov
From: peter griffith <pgrif@MIT.EDU>
Subject: additional remarks

Additional remarks on the "Small scale chemical experiments: Effects of chemical reactions on debris-bed head loss"

My suggestions here are not so much for more experiments as for more focus for the experimental program. Ultimately we need two things; first, a way of evaluating existing plants which shows whether we have a problem, and second, a fix for those that don't pass. I think a modest extension of the work that has already been completed will give us what we need to evaluate current plants. Additional work should mostly be directed toward the second goal, though anything we learn can help on both goals.

I am not certain that the chemistry of all the subject plants is similar enough so that a single standard chemistry specification can be constructed, but I think it is within reach because we should not be reaching for the extremes on this problem. I believe we should choose a prototypical zinc loading and convert the other metals into zinc equivalents using the data already collected. For the other components, like silicon and carbon, some additional experiments are needed but not exhaustive ones. We should stick to typical rather than conservative values. We should also pick a prototypical temperature and a reasonable pH for any additional experiments.

I'd continue by freezing the debris formation and transport numbers based on current NRC information but use best estimate values. (I know this isn't how you usually operate but the accident we are examining is not very likely. I think the practical operation of "risk informed regulation" should be use best estimate rather than conservative values for very unlikely accidents.) We should now turn our attention to the scenario.

Go through the scenario, step by step, and identify a stage, apiece of equipment and an action that is common to all plants for the chosen accident scenario. If we have to intervene it should be in a way that is common to all plants, and should involve a fix that can be applied to all plants. This may not be possible, but it's worth a serious try. If we can't find a general fix, we'll have to go the plants one by one.

One obvious way to intervene would be to alter the system chemistry in some way, perhaps by releasing a chemical. I'm opposed to this because it will involve putting in another system which will probably never be used but will have to be built, licensed, maintained, and tested for the remaining life of the plant. An attractive fix would involve only changes in the operation of the plant or passive systems like a better screen or a paint job on the offending parts. In any case I'd like to see any further experimental work be such that it can be used to identify or contribute to a solution to the problem. I'm

sure a screen redesign using a traveling screen can be designed to solve the problem but I'd much rather stick to a passive solution.

In a general way I'd like to see a standard chemistry for this transient defined and typical values for debris formation and transport and, water depths and flow rates, selected as soon as possible. Plants can then be screened to see if there is a problem. Soon after that is finished, there should be a meeting with plant owners and operators to get on the table their ideas on the ways to solve this problem. A whole raft of solutions exist for the problem plants and I think we've scarcely touched them. There are so many ways to intervene that it would be a mistake to proceed with the limited view point that we now have. We need the inputs from all the specialties involved in the design and operation of the plants.

From: Science and Technology Department
Phone: 412-256-2238
Date: September 29, 2003
Subject: Review of Small-Scale Experiments: Effects of Chemical Reactions on Debris-Bed Head Loss
To: T. Y. Chang (USNRC)

cc: R. C. Johns
K. J. Howe
A. K. Ghosh
B. Letellier
A. K. Maji
P Griffith
A. Hanson
J. F. Lime
J. Goossen (WSTD)

Summary

As part of the review of the test work presented in "Small-Scale Experiments: Effects of Chemical Reactions on Debris-Bed Head Loss", I reviewed the document cited in this report (ref. 3, "Corrosion behaviour of zinc and aluminium in simulated nuclear accident environments" by Piipo et al. This document clearly demonstrates the need for additional work to better determine the source terms for further experiments and accident modeling. For instance, tests in this reference showed that >70% of the zinc and >60% of the aluminium corrosion products were held up on the corroded surfaces. These phenomena would result in a dramatic decrease in fines available for plugging the Nukon fiber material. Also, temperature was shown to dramatically affect the corrosion rate of the zinc and less so the aluminum. The quoted rate in the UNM test report of 11.3 $g/m^2/hr$ was obtained at 110°C, whereas the long term pool temperature is estimated at about 63°C. The rate obtained in this paper at 63°C was about .04 $g/m^2/hr$, a reduction of over 2 orders of magnitude. Finally, this same article provided references that used actual galvanized steel that showed the corrosion rate was even somewhat lower than that of pure zinc. Therefore, I conclude that the kinetics of corrosion of target metals such as Zn galvanized metals and Al as well as non metals such as Si and Ca need to be incorporated into a time/temperature/chemical environment/location dependent model to more correctly determine the source terms for potentially troublesome species in future test programs. In addition, time/temperature/chemical environment/location dependent models are also required for precipitation to determine a reasonable rate of formation of solids within the screened materials in order to correctly evaluate the effect of these fines under accident conditions.

I have reviewed the draft of the report on the effects of chemical additions on the pressure drops in the screens of PWRs. Contingent on the satisfactory completion of verification tests, I agree with the broad conclusion that further work may be required to determine the likelihood of significant added pressure drops due to the addition of Zn, Al and Fe to a preformed mat of Nukon on a 1/8" mesh screen. I recommend that this supplementary work include the addition of silica and other components found in galvanized products to the current cation mix to determine their effect on pressure drop. This conclusion is presented with the caveat discussed in the first paragraph above.

The low temperature zinc metal corrosion study appears to report reasonable results. However, the higher temperature tests appear to be compromised by the solubilization of silica from the container. I recommend the performance of replacement tests at a temperature of 63°C in plastic containers that have been cleaned to remove any residual silica contaminants. Supplementary work that measures the corrosion rate in actively oxygenated, stirred tests using zinc galvanizing material partially covering a steel substrate as used in operating plants is recommended. This is to address my concern that tests with pure zinc may be unrepresentative of the actual galvanizing material. Note that the low Zn corrosion rates that were obtained at the higher temperature due to silica contamination may in fact be closer to the truth than the pure Zn corrosion rates. Note also that some of the Zn may or may not be contributed by way of the sprays that contain NaOH. In this case, the corrosion rate of the Zn could be significantly different and much of the corroded Zn that is formed may stay attached to the original metal surface.

The review of this test report is presented below in two sections. The first is of the pressure drop work and the second is of the zinc corrosion work. If there are any questions, please contact me.

Edward J Lahoda
Chemical Engineering Group Lead
Westinghouse Science and Technology Department
1344 Beulah Road
Pittsburgh, PA 15235-5083
lahodaej@westinghouse.com

Test Report Review

As a general comment, I prefer to include tables and figures into the text. It makes it easier on the reader to follow what is going on.
Section 8.0 – See my comments on the suggestions for longer term programs for each section below.

Pressure Effects of Zn Fe, and Al Additions

Below are my comments on this report and test program to determine if the addition of Zn, Fe and Al to a bed of Nukon glass fibers results in added pressure drop. My comments are divided into two areas; the current report and the next round of the experimental program.

Comments of the Current Report

Pg. 2, Para. 2 – Indicate what pH is expected for the spray water and the pool water to provide some perspective for your test conditions. This will allow the applicability of the experimental data to actual PWRs to be evaluated.
Pg. 5, Para 2 – Indicate composition of mineral wool and fiberglass
Pg. 5, Figure 2-1. This figure is not adequately discussed. I would recommend that it be combined with Table 2-1 and Appendix C to provide a more comprehensive picture of the time/temperature/chemical environment that is the basis for your tests.
Section 2 – Context for the Experiments – I would suggest that the assumptions you made to define your test conditions be listed in a list format. For instance, are you trying to simulate the pool conditions after 15 minutes or after 24 hours? Finally, I would suggest putting section 2-1 at the beginning of Section 2 and the resulting experimental conditions with the assumptions made at the end of the section.
Section 3 Background – Suggest combining with Section 2.
Pg. 10, Para. 5 – CAT and SAT and numerous other acronyms are not listed in your table of abbreviations up front.
Pg. 11, Table 3-2 – It would be helpful to include major chemical components as part of this table.
Section 3.4 – This section discusses the solubility of the various cations in the solutions on a uni-cation basis. Since you are operating above these solubility limits because you want to form solids, I don't see the relevance of the discussion. In addition, as I indicate below, a mix of cations is likely to give different precipitates than the uni-cation case covered in this section. Therefore, these results are probably not even relevant to an actual analysis. I would therefore delete this section.
Section 4.3 – Did you calibrate the flow and pH devices? If so, then please include calibrations in appendix. If not, do so. Include all pressure calibration measurements in appendix.
Section 4.3 – Please include the specifications for the chemicals used in the experiments in the appendix.
Section 4.3 – Include labeling of lid and vortex suppressor in Figure 4.2.
Section 4.3 – What is the size of the support screen? Is this prototypic of the screens found in actual nuclear plants? What is the net % flow area? What is the pressure drop with no Nukon as a function of flow rate? Of temperature? If the screen area is not prototypic, perhaps the support and top screen should be varied to achieve the same net flow area as in actual plants.
Section 4.3 – The pressure gauges are located at the elbows which is not normally the recommended location. What effect does this have on your pressure indications? Were the pressure drops corrected for this? If so, what was the adjustment and why is that adjustment appropriate?

Section 4.4.3.2 – Most of your tests were conducted in the 40 to 50°C range. The long term pool temperature is estimated at 63°C. It was assumed that the lower temperature was less conservative so that if the test showed a problem there, then there would be a problem at the higher pool temperature. This is not necessarily the case. At a lower temperature, the precipitation reaction is likely slower which could lead to formation of material in the Nukon versus on top of the Nukon. In addition, the viscosity effect would tend to give a larger pressure drop at the lower temperature. While you cannot correct for the reaction rate (except to run future tests at the higher temperature), you can correct for the viscosity. I would recommend it.
Section 4.5.2 – Although you boiled the Nukon, it was boiled in water rather than in the more caustic borated solution. Even the small amount of silica you would have obtained may have been the reason why the Al seemed to be much more effective at blocking the Nukon than either the iron or Zn. Future testing may want to consider this as a test.
Table 4-5 – Indicate the data that is not included in Figures 4-9 and 4-10. Discuss the reasons for not plotting this data.
Figures 4-9 and 4-10 – Include only the data from the experiments that met the test requirements of time and temperature. Provide a fitting curve for each type of data.

Suggestions for Additions to a Long-Term Testing Program

1. The effect of silica has not been included in the testing so far. Future tests need to be carried out using silica levels representative of those that will be found in the pool water that will be leached from concrete and insulation materials. This recommendation is based on the fact that Na-Al-Si gels can be formed due to the very low K_{sp} even though Si and Al based solids are not formed. In addition, these Na-Al-Si gels have very large volumes due to their large numbers of waters of hydration.
2. Depending on the type of galvanizing used in PWRs, lead and other components normally found in hot dipped galvanized coatings should be added to the pool water inventory and tested for contributions to pressure drop.
3. Tests of precipitation from a mix of cations and anions should be pursued more vigorously. This is due to the fact that co-precipitated cations/anions may have significantly different properties than the precipitates formed from single species. The Na-Al-Si system cited above is one example where the K_{sp} of the mixture is much lower than the K_{sp} of any individual component. In addition, one could expect the formation of flocs that would accumulate on top of the Nukon and result in lower pressure increases compared to the tendency for the formation of very small or gelatinous materials within the Nukon.
4. Tests to determine likely silica levels need to be conducted. These tests should be run at the high caustic levels found in the spray system as well as the lower caustic level found in the long term pool liquid inventory.
5. Account needs to be taken of the likely levels of CO_2 that will be found in the spray water and adsorbed from the concrete and air in containment. If a fire scenario is assumed, additional levels of CO_2 will be found in the pool water which will act to form Ca and Zn precipitates.
6. Account needs to be taken of any mercury (Hg) that may be carried into the pool water. This is due to the catalytic affect that Hg has on dissolving Al based materials.
7. The kinetics of corrosion of target metals such as Zn and Al as well as non metals such as Si and Ca as well as precipitation need to be included in an overall analysis to determine a reasonable rate of formation of solids within the screened materials. The kinetics need to be included within the framework of the time/temperature/chemical/location likely to be found during any LOCA accident. If the type of LOCA changes the time/temperature/chemical/location, then a different

overall model is required since this may change the potential for precipitate formation. Note that there may be a variety of different conditions, depending on what type of LOCA is considered (Large, Medium or Small Break or RCP Seal).

8. Multiple tests need to be run at all points but in particular at the conditions that lead to excessive pressure drop. At this time, there is no indication of the repeatability of any of the tests.
9. Measurement of the delta P at constant flow during the pressure drop tests will likely yield useful data as to the rate of formation of deposits. This will be especially true for those precipitating systems such as Na-Al-Si that tend to form very high levels of super saturation and then rapidly deposit.
10. Correlation of pressure drop test using the porosity parameter is recommended. This is based on the assumption that the inter-bed formation of precipitates will be the controlling pressure increase factor. Estimation of the change in porosity with time can be done using a combination of kinetic models for precipitation and assuming even distribution of the precipitate on the available fiber surface area. If the mechanism for pressure buildup is by the formation of a separate bed on top of the Nukon, then this approach can still work except that that the porosity will remain constant while the bed thickness will increase. Implicit in this recommendation is the need to develop a repeatable method for determining bed porosity.

Corrosion Rate of Zinc

Below are my comments on this report and test program to determine the corrosion rate of pure zinc metal. My comments are divided into two areas; the current report and the next round of the experimental program.

Comments of the Current Report

5.5.5.1 – You do not discuss the significance of the Si in the deposit. To me, this is a key item. It indicates that the silica that comes into the system (in this case from the bottle) will react to coat and protect the Zn metal.

Figures 5-19 to 5-21 – What is your explanation of the differences in these figures?

Suggestions for Additions to a Long-Term Testing Program

1. An effort to identify the type of zinc that is commonly found in PWRs needs to be carried out. This is due to the variation in composition of galvanized coatings. For instance, electro-plated coatings tend to be almost 100% zinc whereas hot dipped coatings tend to have significant levels of Pb and Sn as well as Zn.
2. When conducting Zn corrosion tests, the tests should be carried out with representative galvanizing coatings on steel. In addition, these test coupons should have a portion of the steel exposed to the solution to allow the galvanic effects to be included in the test. The environment of these tests should include agitation and aeration, as well as aeration and spray. The amount of material that remains on the surfaces should also be recorded since it will not participate in the screen plugging mechanism.
3. Corrosion/leach tests also need to be carried out on zinc-rich primer coating commonly used in PWR's. Specifically, the primer in question is Carboline's Carbo-zinc CZ-11. This product is typically used on metals with a top coat of Carboline's Phenoline 305. The Phenoline product provides a protective top coat that is readily decontaminable. That is, it does not readily allow water to penetrate to the primer and substrate. The composition of a cured film of CZ-11 is:

- Zinc at least 80% by weight
- Ethyl silicate no more than 20% by weight
- Nominal dry film thickness (per manufacturer's specification) is 3 to 5 mils. Although it may occasionally be found in the un-topcoated condition inside PWR containments, it is generally topcoated with Carboline's Phenoline 305 product.

4. All corrosion test data needs to be repeated to determine the statistics on any given data point.
5. Corrosion tests need to be carried out in the environment that is expected to be seen by the base metals. For example, the high temperature tests reported in this draft of the report indicate negative corrosion rates due to the presence of silica in the solution. Similar passivating effects may be found during a LOCA and will likely change the corrosion rates found using pure solutions and could dramatically reduce the source term for particulate forming materials. Expected temperature is another environmental factor that needs to be carefully considered during testing in order to obtain truly representative results.

U.S. Nuclear Regulatory Commission
Division of Engineering Technology
Office of Nuclear Regulatory Research
ATTN: Dr. T.Y. Chang
Project Manager
RES/DET/ERAB
Mail Stop T-10D20
Washington, DC 20555-0001 September 30, 2003

General Comments
The report is a well written draft. It is clear from the work presented that metal dissolution, precipitation, and removal on the sump screen, is a potential problem in a LLOCA. There are a number of areas that are troubling. I will try and point out the issue that I find troubling as I have pondered the results. I will start with some general comments, followed by some precipitation, headloss comments, then corrosion, and final a suggestion regarding further efforts.

As a side note, and contract issues may prevent this, but it seems that there is a significant body of information out on this project. It appears that the investigators have performed as they agreed to, but the complexity that has emerged warrants additional work. If it is reasonable, you might consider titling this a Phase I Final Report or something else that will flag for the reader that there is additional work begging to be performed.

Review
It would help to understand the initial context of the problem and would help in discussion of the data in making the argument that corrosion by-products are potentially a major concern in the large break scenario. There was an overview graphic in the power point presentation that would be very helpful for the reader. The graphic was a three part graphic that showed: a cartoon of a generic power plant in a birds-eye view, a line drawing of a large break locus in the context of the power plant, and a detail showing a screen. This was later supported by a photo of a screen that might also be included in the report. The report is lacking any “intuition builders”. These images would assist the reader in establishing context.

At the end of Section 2.0, there is a time line for a LLOCA. This is just sort of hanging there. It is suggested that this be integrated with flow information, pH information, screen cake (fiberglass) build up data. This suggested figure, which I would envision as consisting of a number of horizontal information bars all correlated with the time line, would then become a vehicle for discussion of the data later in the report. It would reference where all of the pivotal events happened relative to each other. It isn’t really important that it be representative of all plants as long as it provides the reader with a rational progression through the LLOCA in the context of the additional data being presented. For instance, the time line allows you to discuss, based on your best range of estimates, when metal dissolution will reach critical saturation and start raising concern over plugging due to floc growth. This potential headloss and the related time frame can then be compared to the rapid onset of the low headloss induced by insulating material. There does need to be a conclusion section that suggests potential solutions that need to

be further considered. Peter mentioned a couple associated with modifing screen geometry and modifying the NRC pump survivability philosophy. There is also the potential for installing some type of a back-flush vacuum system at the screen face, similar to a backwash on a continuous duty granular media filter. This device might be something that would slow the pumps, initiate a back spray, and vacuum up the solids that where re-suspended from the screen. Ed seemed to indicate that there might be strategies that would provide a chemical solution to the problem rather then a mechanical solution. These and other reasonable solutions should be listed, discussed, and prioritized to give the industry some insight into how the problem might be addressed.

The report as it stands demonstrates that there is a clear potential problem under extreme (to the point of unrealistic) conditions, but it would be helpful if the investigators did a little brainstorming at the end of the report to suggest to the industry how the magnitude of the concern in a real scenario might be better understood. This will be addressed a little more in the long-term comments.

Short Term Comments
Precipitation Filtration Comments
Page 5 of the draft Paragraph 1, there is a mention of coagulation tendency for iron oxides and fiber at a pH <4. It might be useful to mention to the reader that $Fe(OH)_3$ in this pH range tends to be "+" charged while the fibers will very likely continue to be negatively charged. This can be merely asserted at this point and then demonstrate this to the reader later during the discussion of Al and Fe on page 7. I believe it would be a good thing to expand the discussion given there to include a little chemistry background that might help the reader understand what they are observing. It is suggested that this would also be the place to cover Si chemistry, both dissolution from fibers and impact on precipitations.

Page 5 of the draft Paragraph 3
There is mention of "long-term headloss". Need a brief discussion of what this means. It would be nice to tie the discussion into Figure 2-1, and put the time frame in the context of the LLOCA.

Since water chemistry and fiberglass are being discussed, this might be a good place for a discussion of silica solublization and potential for gel formation. The details can be discussed later, say around page 7 the middle of the page. Massey (1990, page 251) states that, dissolution of silicates in a strong base solution breaks down into smaller more soluble species. The constituents of such a solution are very complex, a recent NMR study identified the presence of at least 22 different anions. Water glass has been used for years to modify solubility and corrosion in municipal water systems. I believe this appears to be an area, which needs to be further considered.

For the authors convenience, I might suggest that LANL has a silica chemistry resource, Dr. Peter Worland.

Again, Figure 2-1 needs to be expanded and integrated. It should be possible to integrate the information in the appendix either into the figure or into the discussion of the figure.

Page 7 of the draft Paragraph 4
The last sentence in this paragraph is the 3rd time you have asserted that a high pH is essential in preventing coagulation and deposition of fines and particles. It would be nice to present a little substantiation for this statement. Present the anticipated zero point of charge (ZPC) for the fiberglass. This information may be useful later in understanding some of the other results. Then discuss the impact of pH on the hydroxide floc. It should be noted that if there is enough material in solution, sweep floc will form. Sweep floc is less efficient as a coagulant at high pH, but only marginally less efficient. The mass of material sweeping through the water column is important, the charge is secondary.

It should also be recognized that, if the pH is being controlled to limit coagulation/flocculation, formation of many of the coagulating species is driven by hydroxide /metal ratios (Hanson and Cleasby, 1990, Clark, M.M., R. Srivastava , and R. David, 1993). Controlling the system based on pH ignores the fact that the pKw is sensitive to temperature. As the temperature increases, the pH for a constant pOH will be reduced. I am not clear on what is being accomplished in this system with the pH adjustment, but I suggest that someone who is familiar with the system take a look at the temperature corrections to pKw, they can be critical in some reactions.

Page 7 of the draft Paragraph 5
This paragraph along with the ZPC info for fiber glass in the previous paragraph make a good lead in to some chemistry information regarding precipitation of Al, Zn, and Fe. It is also a good opportunity to discuss reaction mechanisms on floc characteristics, and pH/surface charge information. This information will assist your audience in understanding your results. You appear to be covering this back in Section 3.4 on Page 14. That is fine, but it really needs to be beefed up.

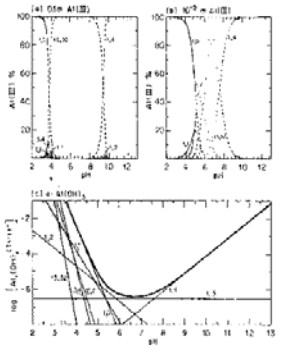

Figure 39. Distribution of hydrolysis products (n,p) at $I \to 1$ m and 25 °C in (a) 0.1 m Al(III), (b) 10^{-2} m Al(III), and (c) solutions saturated with α-$Al(OH)_3$. The dashed curves in (a) and (b) denote regions supersaturated with respect to α-$Al(OH)_3$; the heavy curve in c is total concentration of Al(III)

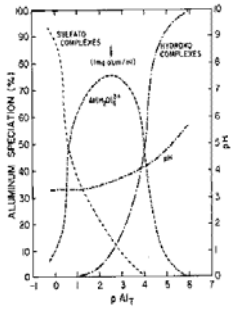

Figure 25. Species composition of aluminum sulfate solutions

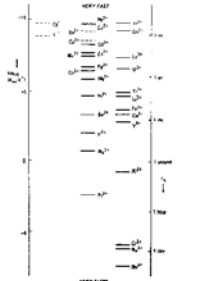

Figure 41. Rate constants for water exchange, and mean residence times for water molecules in primary hydration shells, for 3+ and 2+ metal ions, at 298 °K. Octahedral species are indicated by thick lines, non-octahedral species by thin lines. Dashed lines denote estimates derived from rate constants for complex formation

The figures shown here are examples of the type of information that your readers may be interested in. The figure on the left(Baes and Mesmer, The Hydrolysis of Cations, Al Page 122, Fe page 237, Zn, Page 294, Si Page 337) illustrates a thermodynamic equilibrium representation similar to MINTEQ, but for a single component system. This

type of figure is available for iron, aluminum, and zinc in this reference and demonstrates a number of things that might be of interest to a reader. The two plots on the top of the figure show the metal polymer chemistry shifts for aluminum as the concentration of aluminum changes in the system. It also shows the reader which species are expected to be in the solid phase and which are expected to be dissolved. This is especially important since most of the species that are supposed to be solid below a pH of 6.8 are in fact soluble polymers because of kinetic considerations. More on that in the next paragraph. The minimum in the solubility envelope is in fact the theoretical zero point of charge. The species to the left of the minimum are positively charged and the species to the right are negatively charged. This probably explains where the keeping the pH elevated inhibits destabilization of debris. I am not familiar with that literature, but I am a bit concerned that they have neglected the impact of sweep floc. A very useful sister diagram to present flocculation mechanisms and their impact on screen plugging would be Amitharaja's flocculation diagrams for iron and aluminum. These show regions of adsorption/destabilization, sweep floc, and mixed mechanism flocculation. The figure in the middle (Charley O'Melia) demonstrates how the speciation relative to various complexes is a function of metal concentration, and in some concentration ranges a strong function of concentration. This figure does not show silica, but it shows sulfate, hydroxides, and water (aqua-metal ion). The figure on the far right(Ions in Solution), shows the 1/2 time of water in the hydration sheath for various eight atom metal polymers. It gives an indication of which metal chemistry reactions will dominate in a competition. If this information is combined with information regarding associative and dissociative reaction mechanisms, it is clear that Zn and Fe, which can both react dissociatively and which both have a very short 1/2 time of water in the hydration shell, will tend to react quickly and come to equalibrium quickly. This will tend to form smaller floc for these two, which under some circumstances may provide better fibre bed penetration and thus cause a lower head loss for those precipitates then the precipitates of aluminum hydroxide. Again, some of this can be seen by comparing the Amitharaja flocculation diagrams for Al and Fe. Note that the sweep floc for Fe extends to very low pH values compared to aluminum. A direct reflection of these kinetic issues. I suspect these same kinetic issues may be important is determining headloss build up in the LLOCA scenario if realistic concentrations, flow rates, and times are maintained in the reactor system. The figure below (Dentel, 1987) is another issue that would bear presentation and discussion. It represents a conceptual model of metal reactions in solution after

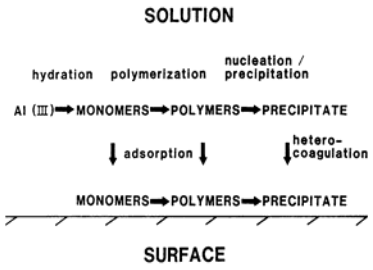

Figure 45. Schematic representation of the various pathways followed by aluminum hydroxide species in solution or at a surface in contact with the solution

injection of a an aqua-metal ion. It shows that there is a competition between polymerization, surface adsorption, and precipitation. This along with the time scale information for each of these reactions, provide part of the key to understanding precipitate formation vs adsorption as a function of pH and concentration in a iron or aluminum flocculation system. AN example of the type of information that is seen is the literature is given in the Table below.

Reaction type vs Time Scale (Amitharajah, 1987)

Reaction	Time Scale (Seconds)
Al (III) monomer adsorption	<0.1
Al (III) polymer formation and adsorption	0.1 to 1
Formation of sweep floc	1 to 7
aluminum hydroxide precipitate	

I am not sure what understanding can be drawn from these tools when considering the LLOCA. However, I suspect that this information along with the Si chemistry information to match may be very useful in thinking about the probability of metal dissolusion and precipitation causing a serious impact in a LLOCA, as opposed to it simply being an aggravating factor to be considered in working through accident scenarios.

Page 8 of the draft Paragraphs 1&2
There is a list of interesting parameters that were measured during their experimental work, and then there is a list of conclusions. Unfortunately there is no apparent connection between the two. It would be very interesting to know what ZP or EM where measured for the particle systems studied. Likewise it would be interesting to know how those particle systems did or did not compare to the particle systems used in the current work.

Page 9 of the draft Paragraph 5
The last sentence of the paragraph states that it is known that aluminum and iron oxides and hydroxides could easily appear as a gelatinous coating on walls and floors. Is there a reference for this? Under what conditions? It would take a lot of material precipitated to accomplish this, I would like to see some justification for this statement.

Page 10 of the draft Paragraph 2 (3.2.1 Chemical Sources)
This would be a good place to discuss for your reader why phosphate, lithium and boron might or might not be added to the cooling water in a reactor. You may cover this somewhere else, but I came into this section a bit puzzled regarding Li and Bo. This would be a good place to clarify. Consolidate some of the comments from section 3.2.2 on TSP into this section. It would also be nice to show which chemicals would be in the liquid stream at time zero in a LLOCA and which would be added in response to an event.

Table 3.2 might want to give some industry ranges so that the reader can get a feel for where the volunteer plant falls on the continuum.

Page 12 of the draft
Nice concept explaining chemical addition to solution in terms of accident progression. Would be useful to have a figure to discuss this with. Also where do you mention the potential initial flush of oxidized material off the wall during the application of spray and what percent of the total that might represent. Might be appropriate to put such comments in Section 3.3 on page 13. Even if these estimates must be identified as speculation, they give the reader a sense of the author's expectation and intuition.

Page 14 Paragraph 4
I like what you have done with MINTEQA2. I think there should be a couple of disclaimers to go with this section. Make sure the reader understands that this is an equilibrium model being used to evaluate a dynamic process. It is also important that the reader understand that there is not universal agreement with regard to values used as solubility constants. The values used have a good pedigree, but the model is very sensitive to these constants and it is important that the reader understand this source of potential error. These models also have a hard time with meta-stable species that may be very important in a dynamic setting like this one. These issues can be overcome, but they need to be addressed so the reader is clear with regard to assumptions the author has made. Again, this activity represents very valuable contribution, but it needs to be clarified.

It should be noted that there are a large number of metal polymers that are present in solution and highly charged. Aluminum in particular has a rich metal polymer chemistry. However, since most of the interest in this case is at a pH of 9, we can really ignore those species as the authors have.

The species associated with Silica gels need to be added. Also the carbonate chemistry issue needs to be addressed. The discussion indicated that 40,000 gal of 30% by mass NaOH sits open to the atmosphere until needed and is then added to 300,000 to 1,000,000 gal of cooling water as a pH adjuster. There is certainly a large carbonate contribution here. It is just unclear how large. There seemed to be a agreement that information is available regarding the MAX carbonate concentration in the NaOH tanks. This information should be added to the modeling activity.

Page 20

There are two dominant filtration mechanisms, surface filtration and depth filtration. In depth filtration particles being removed from suspension are taken out through out the depth of the bed. This tends to distribute dirt load through the bed and results in a linear increase in headloss as shown in the left hand diagram below (Baumann, 1978, Cleasby, 1990). Surface filtration is a screening mechanism, and if it results in a compressible mat on the surface of the filter, may exhibit an exponential increase in headloss over time (volume treated). As a result of fundamental differences in these two mechanisms, the particle removal efficiency of a depth filter gets better for a while, and then drops off. For surface filtration the particle removal efficiency just keeps getting better. This is shown in the right hand diagram.

Filter headloss vs filter run time for both surface and depth filtration

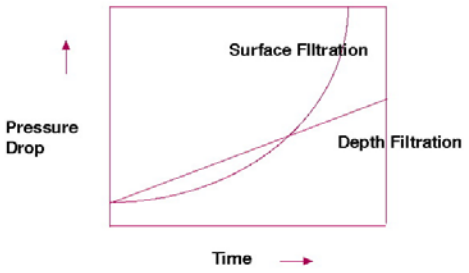

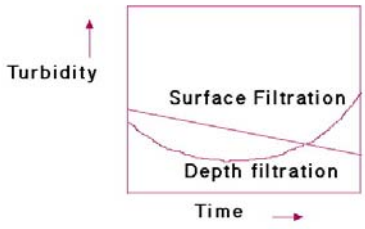

Turbidity in treated water vs time of filter run for surface and depth filtration

In depth filtration the particles being removed are collected on the surface of the media and are held there be Van der Waal's attraction. This is shown in the photograph below on the left (Cleasby, 1990). Cake filtration is a process where a cake is formed on a support media and particles are removed on the cake. The cake is actually a surface filter, but can be caused to act as if it is a depth filter by adding a "body feed" that maintains the porosity of the cake to water flow. This is shown conceptually in the figure below on right.

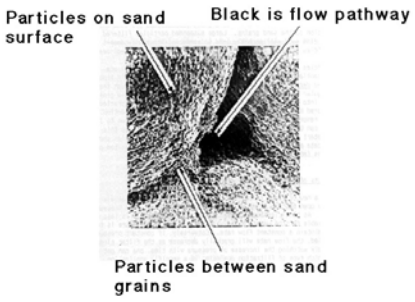

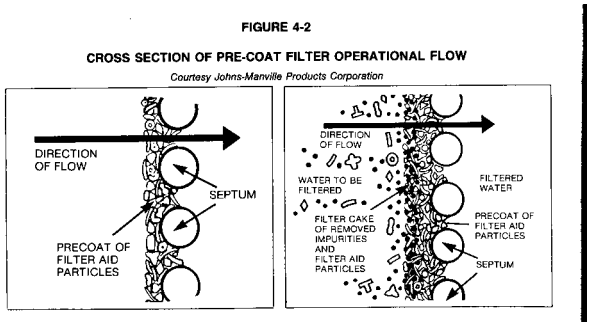

(E.R. Baumann, 1978) If the screen in the LLOCA is in a surface filtration mode it may be possible to continually add some low headloss fibers to the system and prevent the abrupt rise in headloss observed in the experiments reported here. The added fiber would perform a function similar to body feed in the DE filter systems. If on the other hand the

system is in depth filtration mode, there may be little that can be done to reduce headloss without removing solids from the screen.

Page 20 Paragraph 4 (Debris Addition)
It is not clear from this paragraph, that the Nukon fibers were always added at a low flow rate and then an initial flow of 20 gpm (426 gpm/ft^2) is used to compressed the fiber bed prior to addition of the material to be precipitated. It is also not clear from the information provided that the researchers initial goal was to always perform the precipitation tests at 20 gpm as a worst case condition. The test that were performed at less then 20 gpm represent conditions forced on the researchers by the inadequacy of the system pump. None of this invalidates the authors conclusions, but it makes it much easier to understand the results. It also makes it clear that although the headloss potential is real, it is likely that the flows attempted in the study will be higher then the flows during the high precipitation portion of a LLOCA.

Page 25 Paragraph 4 (Section 4.4.3.3)
Head loss was found to be extremely high… It would be more illustrative to state that the headloss of 15.28 feet was much higher then the calculated headloss of 0.25 feet which would be expected with fibers alone.

Page 26 Paragraph 3
I believe that some of the statements here are misleading at best. The headloss would indeed be higher in some of the runs if an approach velocity of 0.5 fps (20gpm) could have been maintained in the system. However, the text seems to imply that higher headloss might be observed or expected in an actual LLOCA. From my understanding of the flow variation during an LLOCA, this is untrue. I think I would be very careful with the interpretation of this data. If the intent of the experiment was to demonstrate that the precipitate may be a significant issue, leave it at that. If you start extrapolating the headloss levels to the LLOCA, it is your responsibility to also deal with the impact of flow variation and anticipated screen areas. You clearly do not have enough data to do that, but you do have enough data to anticipate that an approach velocity of 0.5 fps may not be representative of the flow regime during the period of high solids from precipitation. This really brings one back to the importance of the corrosion rates and the first flush of dissolved metals off from the metal surfaces exposed to spray.

Corrosion Section
Disclaimer: Corrosion is not my area of expertise and I am not comfortable with being dogmatic with regard to things that need to be done in this area. I am concerned because, although this is not my area of expertise, corrosion appears to be the sole source term for the soluble materials that will be flocculated. Realistic headloss expectations can only be determined with good corrosion data.

There appear to be critical issues that have not been addressed. Before headloss due to precipitation can be modeled, a major concern must be evidence that the corrosion products will be in solution and available to be precipitated at a point in time when that precipitation is critical. There are a number of corrosion issues that have not been addressed adequately. It appears the majority of the metal to be corroded is in a spray environment, which may be pacified by the formation of an oxide film. This was not

addressed. It appears that significant silica may be in solution. There are important interactions between silica and the other dissolved species. Another issue which is potentially VERY important is the impact of oxidized material on the metal surfaces at the beginning of the LLOCA and it's potential for being flushed off from the walls as soluble metal. If a substantial fraction of the material precipitated during the LLOCA is washed off the walls by the first flush, the corrosion data may be less important. This would also substantially change the headloss build up scenario, since there would be an immediate substantial mass of material to precipitate during the high flow portion of the event.

Page 33
There are clearly some substantial uncertainties with regard to zinc corrosion in this system. The mass and time issues that are representative of corrosion under LLOCA conditions is extremely important. A first estimate of the maximum potential corrosion rates might be optained as discussed in the meeting of 9/15/03. Process a coupon and then buff off the corrosion prior to weighing the coupon, and/or measure the soluble zinc in the jar. The problem with buffing the coupon is that, corrosion that never leaves the surface, or never goes into solution, will not form a precipitate and will not cause additional headloss at the screen, even though the material is corroded. It appears that some of the cited corrosion rates are unrealistically high. However, the data collected in this study appears to be unrealistically low. This needs to be sorted out and included in an analysis of the LLOCA.

Page 36
The corrosion studies as a function of time should, perhaps, attempt to match corrosion conditions to LOCA environmental conditions (pH, temperature, time, competing species)

Long Term Comments
There is little information on the solubility of the Si in the tests. Is this a long term concern or does this need to be looked at prior to making this report a "Final Report".

Clearly, one of the major concerns is corrosion, especially of zinc in a spray environment, at high temperature. Again, is this long term or the difference between this being a final draft and a final report.

Based on corrosion rates estimated for this system, one must calculate anticipated precipitation based on the rate of solubilization due to corrosion, estimate a turn over time for the cooling pool volume based on the pumping rate at the time of interest, and estimate a mass rate of precipitation accumulation. The mass of precipitate, mix of solid species, rate of accumulation, and screen approach velocities will allow the design of an experiment that represents the reality in the power plant LLOCA scenario.

This background information can be used to design an experimental facility with two interconnected loops. One loop (loop 1) will hold the screen section, the other loop (loop 2) will hold the material being corroded. Add the fiberglass material to loop 1 and compress at the high flow rate for 20 minutes to an hour. Then recirculate the water at a low rate for the time it takes to pump the cooling pool through the screen. During this

time, the water chemistry in loop 2 has been adjusted and the metal specimens in loop 2 have been corroding. After the time for pumping the cooling pool around the circuit once, loop 1 and loop 2 are connected and the water is circulated through the filter at a rate appropriate for that period of the LLOCA. The headloss will be noted. This will deposit any solids formed in the corrosion loop on the screen and provide the headloss at this point in the LLOCA. Each time the two loops are interconnected the silica and metlas solution chemistry is averaged over the system. Note that low solids deposition may be more critical then high solids deposition if the flow rate during the low solids deposition period is high enough. The two loops are once again separated and corrosion allowed to continue separate from the filtration/ silica dissolution loop. After a time sufficient for the cooling water to again circulate, the loops will again be interconnected. This pattern will be continued for the anticipated duration of the LLOCA with flow, headloss, and water chemistry being monitored as a function of time. This experiment will provide a better picture of what happens in the LLOCA corrosion scenario. It will also allow a more realistic filtration mechanism to come to the fore front. The experiments reported in the draft appear to all be surface filtration. A loading of smaller particles spread over time may generate depth filtration and a lower total headloss for the same mass of precipitate.

References:

Amitharajah, A. (1984) Research at Montana State University into Coagulation, Flocculation, and Mixing. Presented at CH2-Mhill Cold Water Coagulation Seminar, Denver, Colo, (July 13)

Baes, Charles and Robert Mesmer, (1986) The Hydrolysis of Cations, Robert E. Krieger Publishing Company, Malabar, Florida.

Baumann, E.R., (1978) Granular Media Deep-bed Filtration. In Water Treatment Plant Design, ed. R. L. Sanks, Ann Arbor Science.

Baumann, E.R., (1978) Precoat Filtration. In Water Treatment Plant Design, ed. R. L. Sanks, Ann Arbor Science.

Burgess, John (1988), Ions in Solution, Basic Principles of Chemical Interaction, Ellis Horwood Series in Inorganic Chemistry, Ellis Horwood Limited, Chichester, West Sussex, England.

Clark, M.M., R. Srivastava , and R. David, (1993) "Mixing and Aluminum Precipitation," *Environmental Science and Technology*, *27* :10, pp. 2181-2189.

Cleasby, J. L., (1990) Filtration, In Water Quality and Treatment, A Handbook of Community Water Supplies, 4th Edition, AWWA-McGraw-Hill, Inc.

Dentel, S. K., (1987) Optimizing Coagulation Additions From Laboratory and Field Test Methods, pp. 49-88. In AWWA Seminar Proceedings: Influence of Coagulation on the Selection, Operation, and Performance of Water Treatment Facilities, AWWA, Denver, June.

Hanson, A. T., and J. Cleasby, (1990) The Effects of Temperature on Turbulent Flocculation: Fluid Dynamics and Chemistry, Journal of American Water Works Association, Vol. 82, No. 11, November, pp. 56-74.

Johnson, P. N. and A. Amitharajah , (1983) Ferric Chloride and Alum as Single and Dual Coagulants, JAWWA, 75, No. 5 (May, 1983), 232 – 239.

Massey, A.G., (1990) Main Group Chemistry, Ellis Horwood Series in Inorganic Chemistry, Ellis Horwood Limited, Chichester, West Sussex, England.

O'Melia, C. R., Coagulation in Waste Water Treatment. In K. J. Ives, ed. The Scientific Basis of Flocculation. Nato Advanced Study Institute Series, Series E, Applied Science – No. 27. Sijthoff & Noorhoff, 1978.

APPENDIX B

LLOCA SEQUENCE OF EVENTS DESCRIPTION

The following description of a large loss-of-coolant accident is extracted from NUREG/CR-6808, "Knowledge Base for the Effect of Debris on Pressurized Water Reactor Emergency Core Cooling Sump Performance,"

1.4.2 Large Loss-of-Coolant Accident

The LLOCA simulated was a cold-leg, pump-discharge, double-ended guillotine break (DEGB). The RCS pressure and average temperature before the break were 2250 psia and 570°F. The cold-leg inside diameter was 27.5 in., corresponding to a cross-section area of 4.12 ft^2. The break was assumed to be instantaneous with a discharge coefficient of unity. A cold-leg break was chosen as the LLOCA event because design-basis accidents typically are cold-leg breaks. With respect to debris generation and transport, any differences between a cold-leg and hot-leg break likely would be small. This is not the case for core response, but with respect to emergency sump blockage, differences between large hot-leg and large cold-leg breaks are probably negligible. This assumption is supported by the results (not presented here) of a supplementary RELAP5 large-hot-leg-break calculation that compares closely with the results of the large-cold-leg-break calculation with respect to break-flow characteristics.

The calculated results for the LLOCA events in large dry and ice condenser containments are provided in Tables 1-2 and 1-3, respectively.[1] These simulations were used to develop a generic description of LLOCA accident progression in a PWR, both in terms of the system's response and its implications on debris generation and transport. Table 1-4 provides a general chronology of events for a PWR LLOCA sequence. Figure 1-4 summarizes key findings to supplement the tabulated results, with further explanation as follows.

1.4.2.1 Reactor Coolant System Blowdown Phase

In this report, the RCS blowdown refers to the event (or process) by which elevated energy in the RCS inventory is vented to the containment as the RCS vents through the breach. Blowdown and the subsequent flashing[2] in the containment cause rapid decay in the RCS pressure and rapid buildup of containment pressure. Either of these initiates reactor scram.[3] With delay built-in, it is expected that reactor scram would occur within the first 2 s. It is during RCS blowdown that flow from the break occurs and the highest (and most destructive) energy is released. Therefore, debris generation by jet impingement would be greatest during this time. Also, debris could be displaced from the vicinity of the break as the flashing two-phase break jet expands into the containment. Large atmospheric velocities may develop in the containment, approaching 200 ft/s in the ice condenser containment and 300 ft/s in the large dry containment, as breach effluent quickly expands to all regions of the containment. In the vicinity of the breach, containment structures would be drenched by water flowing from it. Increase in containment pressure also causes immediate automatic actuation of containment sprays, for all plant types, condensing steam and washing structures throughout containment. Spray water drains over and down containment walls and equipment, carrying both insulation and particulate (e.g., dirt and dust) debris to a growing water pool on the containment floor. In most containments, NaOH liquid stored in the spray additive tank (SAT) will be added to the borated water to facilitate absorption of iodine that may be released to the containment. Therefore, a secondary CS effect is a potential increase in pool pH, which in

[1] Large dry containment LLOCA results are representative of those expected for sub-atmospheric containments as well, with the exception that inside recirculation pump flow for the sub-atmospheric containment would have to be added.

[2] Flashing refers to the phenomenon by which the mainly liquid inventory of the RCS turns into a steam and liquid mixture as it is expelled into the containment atmosphere, which is at a significantly lower pressure.

[3] The accident progression in sequences in which scram does not occur is significantly different and will not be discussed in this document.

turn, could play a role in particulate debris precipitation caused by the interaction of hot, borated, high-pH water with zinc and aluminum surfaces. The rates of these reactions are used in many Final Safety Analysis Reports (FSARs) to estimate the hydrogen source term and evaluate the potential for hydrogen accumulation in the containment.

Accurate characterizations of conditions that exist during the blowdown phase are important for estimating debris generation and, to some degree, debris transport. For LLOCA events, RCS blowdown occurs over a period of approximately 30 s, during which vessel pressure goes from 2250 psia to near containment pressure. During this time, the reactor pressure vessel thermodynamic conditions undergo a rapid change. Initially, the break flow is subcooled at the break plane and flashes as it expands into the containment. Within 2 s, the vessel pressure drops below 2000 psi and the flow in the pipes and the vessel becomes saturated. Thereafter, the break flow quality is equal to or higher than 10%. On the other hand, the void fraction increases to approximately 1.0, clearly indicating that the water content would be dispersed in the vapor continuum in the form of small droplets. The corresponding flow velocity at the break plane reaches a maximum of about 930 ft/s. This clearly indicates that jets would reach supersonic conditions during their expansion upon exiting the break. Based on these simulations, the energetic blowdown terminates within 25–30 s as the vessel pressure decreases to near 150 psig. Although steam at high velocities continues to exit, the stagnation pressure is not sufficient to induce very high pressures at distances far from the break. Thus, it is reasonable to assume that debris generation following an LLOCA occurs within the first minute. (Note: Debris generation by non-jet-related phenomena may occur over a prolonged period of time as a result of high temperature, humidity, and sprays.) The RCS blowdown continues until the vessel pressure falls below the shut-off head for the accumulator tank,[4] the HPSI, and the low-pressure safety injection (LPSI). This causes increasingly large quantities of cooler, borated RWST water to quench the core and terminate blowdown.

1.4.2.2 Emergency Core Cooling System Injection Phase

The injection phase refers to the period during which the RCS relies on safety injection, drawing on the RWST for decay heat removal. In the case of an LLOCA, the injection phase immediately succeeds the initial RCS blowdown. During this phase, core reflood is accomplished and quasi-steady conditions are arrived at in the reactor, where decay heat is removed continually by injection flow. In ice condenser containments, the ice condenser compartment doors open and the recirculation fans move the containment atmosphere through the ice condensers. Opportunities would exist for debris to settle in the pool during this relatively quiescent time before ECCS recirculation. Containment pressure would decrease from its maximum value (reached in the blowdown phase). The injection phase is considered to be over when the RWST inventory is expended and switchover to sump recirculation is initiated.

Accurate characterization of conditions that exist during injection phase may be important for estimating the quantity of debris transported from the upper containment to the pool and for estimating the quantity of debris that may remain in suspension. Following the initial break, safety injection (SI) begins immediately with the combined operation of the accumulators, the charging pumps, the HPSI pumps, and the LPSI (RHR) pumps. The SI flow approaches the design value (which is 11,500 gpm in the plant simulated) in about a minute and continues at that rate until switchover. Current simulations did not take credit for potential reduction in the injection flow (e.g., system-failure scenarios). Containment sprays continue to operate; spray water and water exiting the break will cause washdown of debris from the upper portions of the containment to the pool on the containment floor.

It has been determined that large quantities of water would be introduced into the containment within a few minutes following an LLOCA. As a result, the water-pool depth on the containment floor increases steadily. In the case of a large dry containment, the peak pool height is reached at the end of the injection phase; in an ice-condenser containment, the peak value is reached several hours into the accident after all the ice has melted.

1.4.2.3 Recirculation Phase

[4]The accumulators are also known as safety injection tanks in some designs.

After the RWST inventory is expended, the ECCS pumps would be realigned to take suction from the emergency sump in the containment floor. This would begin the ECCS recirculation phase, in which water would be pulled from the containment pool, passed through heat exchangers, and delivered to the RCS, where it would pick up decay heat from the reactor core, flow out the breach, and return to the containment pool. Pool depth would reach a steady state during the recirculation phase, and containment pressure and temperature would be decreasing gradually. It would be during this accident phase that the potential would exist for debris resulting from an RCS breach (or residing in containment beforehand) to continue to be transported to the containment emergency sump. Because of the suction from the sump, this pool debris may accumulate on the sump screens, restrict flow, and either reduce available NPSH or starve the ECCS recirculation pumps.

The primary observation regarding the RCS and containment conditions during the recirculation phase is that the sump flow rate reaches the design capacity of all the pumps, which in the plants analyzed is 17,500 gpm for the large dry and sub-atmospheric containments and 18,000 gpm for the ice condenser containment.

Table 1-2 Debris Generation and Transport Parameters: LLOCA—Large Dry Containment									
Parameter	**Blowdown Phase**			**Injection Phase**			**Recirculation Phase**		
	0+	**20 s**	**45 s**	**45 s**	**15 min**	**27 min**	**27 min**	**2 h**	**24 h**
RCS pressure at break (psia)	2250	393	55						
RCS temperature at break (°F)	531	291	250	250	173	144	144		
Break flow (lb/s)	7.97e4	1.28e4	4.89e3						
Break flow velocity (ft/s)	296	930	100						
Break flow quality	0	0.25	0.3	0.3	0				
Safety injection (gpm)				11500	11500	11500			
Recirculation flow (gpm)							17500	11800	11800
Spray flow (gpm)				0	5700	5700	5700	0	
Spray temperature (°F)					105	190	190		
Containment pressure (psig)	0	36	33	33	11.5	7	7	1.5	0
Containment temperature (°F)	110	305	250	250	190	163	163	115	95
Pool depth (ft)					2	3.5	3.5	3.5	3.5
Pool temperature (°F)					212	187	187	125	100
Pool pH									
Containment atmosphere velocity (ft/s)	282		7						
Containment relative humidity (%)	50	100	100	100	100	90	90	100	100
Paint temperature (°F)	100			215	240	220	220	145	112
Peak break flow:7.97e4 lb/s at 0+ s						Peak break flow velocity: 930 ft/s at 21 s			
Quality at peak break flow: 0						Quality at peak break flow velocity: 0.25			
Peak containment pressure: 36 psig at 20 s						Peak containment atmosphere velocity: 282 ft/s at 0+ s			

Table 1-3 Debris Generation and Transport Parameters: LLOCA—Ice Condenser Containment									
Parameter	**Blowdown Phase**			**Injection Phase**			**Recirculation Phase**		
	0+	**20 s**	**45 s**	**45 s**	**10 min**	**17 min**	**17 min**	**2 h**	**24 h**
RCS pressure at break (psia)	2250	393	55						
RCS temperature at break (°F)	531	291	250	250	200	160	160		
Break flow (lb/s)	7.97e4	1.28e4	4.89e3						
Break flow velocity (ft/s)	296	930	100						
Break flow quality	0	0.25	0.3	0.3	0				
Safety injection (gpm)				11500	11500	11500			
Recirculation flow (gpm)							18000	18000	18000
Spray flow (gpm)				6400	6400	6400	6400	6400	6400
Spray temperature (°F)				105	105	97	97	95	89
Containment pressure (psig)	0+	14	10.1	10.1	4.5	4.5	4.5	3	2
Containment temperature (°F)	100	168	160	160	103	105	105	98	100
Pool depth (ft)				4	8.5	10.75	10.75	10.8	10.1
Pool temperature (°F)				180	157	159	159	148	126
Pool pH									
Containment atmosphere velocity (ft/s)	184	18	1						
Containment relative humidity (%)	0	50	100	100	80	96	96	97	98
Paint temperature (°F)	100	106	112	112	113	112	112	90	90
Peak break flow:7.97e4 lb/s at 0+ s							Peak break flow velocity: 930 ft/s at 21 s		
Quality at peak break flow: 0							Quality at peak break flow velocity: 0.25		
Peak containment pressure: 14.4 psig at 15 s							Peak containment atmosphere velocity: 184 ft/s at 0+ s		

Table 1-4 PWR LLOCA Sequences					
Time after LOCA (s)	**Accum. (SI Tanks)**	**HPSI**	**LPSI**	**CS**	**Comments**
0-1	Reactor scram. Initially high containment pressure. Followed by low pressure in the pressurizer. Debris generation commences caused by the initial pressure wave, followed by jet impingement. The blowdown flow rate is large. But mostly saturated water. Quality $\leq$0.05. Saturated jet-models are appropriate. SNL/ANSI Models suggest wider jets, but pressures decay rapidly with distance				
2		Initiation signal	Initiation signal	Initiation signal	Initiation signal from low pressurizer pressure or high containment pressure/temp
5	Accumulator injection begins	Pumps start to inject into vessel (bypass flow out)	Pumps start (RCS P > pump dead head)	Pump start and sprays on	In cold-leg break, ECCS bypass is caused by counter-current injection in the downcomer. Hot-leg does not have this problem.
10	The blowdown flow rate decreases steadily from $\approx$20,000 lb/s to 5000 lb/s. Cold-leg pressure falls considerably to about 1000 psia. At the same time, effluent quality increases from 0.1 to 0.5 (especially that from steam generator side of the break). Flow is vapor continuum with water droplets suspended in it. Saturated water or steam jet-models are appropriate. At these conditions, SNL/ANSI models show that jet expansion induces high pressures far from the break location.				
25		End of bypass; HPSI injection			
25-30	Break velocity reaches a maximum > 1000 ft/s. Quality in excess of 0.6. Steam flow at less than 500 lb/s. Highly energetic blowdown is probably complete. However, blowdown continues as residual steam continues to be vented.				
35	Accumulators empty		Vessel LPSI ramps to design flow.		
40	Blowdown is terminated, and therefore, debris generation is complete. Blowdown pressure at the nozzle less than 150 psi. Debris would be distributed throughout the containment. Pool is somewhat turbulent. Height < 1 ft.				
55-200	Reflood and quenching of the fuel rods (T_{max} $\tilde{}$ 1036 ^{o}F). In cold-leg break, quenching occurs between 125 and 150 s. In the case of hot-leg break, quenching occurs between 45 and 60 s (T_{max} $\tilde{}$ 950 ^{o}F).				
200-1200	Debris added to lower containment pool by spray washdown drainage and break washdown. The containment floor keeps filling. No directionality to the flow. Heavy debris may settle down.				
1200	RWST low level indication received by the operator. Operator prepares to turn on ECCS in sump recirculation mode. Actual switchover when the RWST low-low level signal is received.				
1500		Switch suction to sump	Switch suction to sump	Terminate or to sump	Many plants have containment fan coolers for long-term cooling.
1500-18000	Debris may be brought to the sump screen. Buildup of debris on the sump screen may cause excessive head loss. Containment sprays may be terminated in large dry containments at the 2-h mark.				
>36000		Switch to hot-leg recirculation.	Switch to hot-leg recirculation		

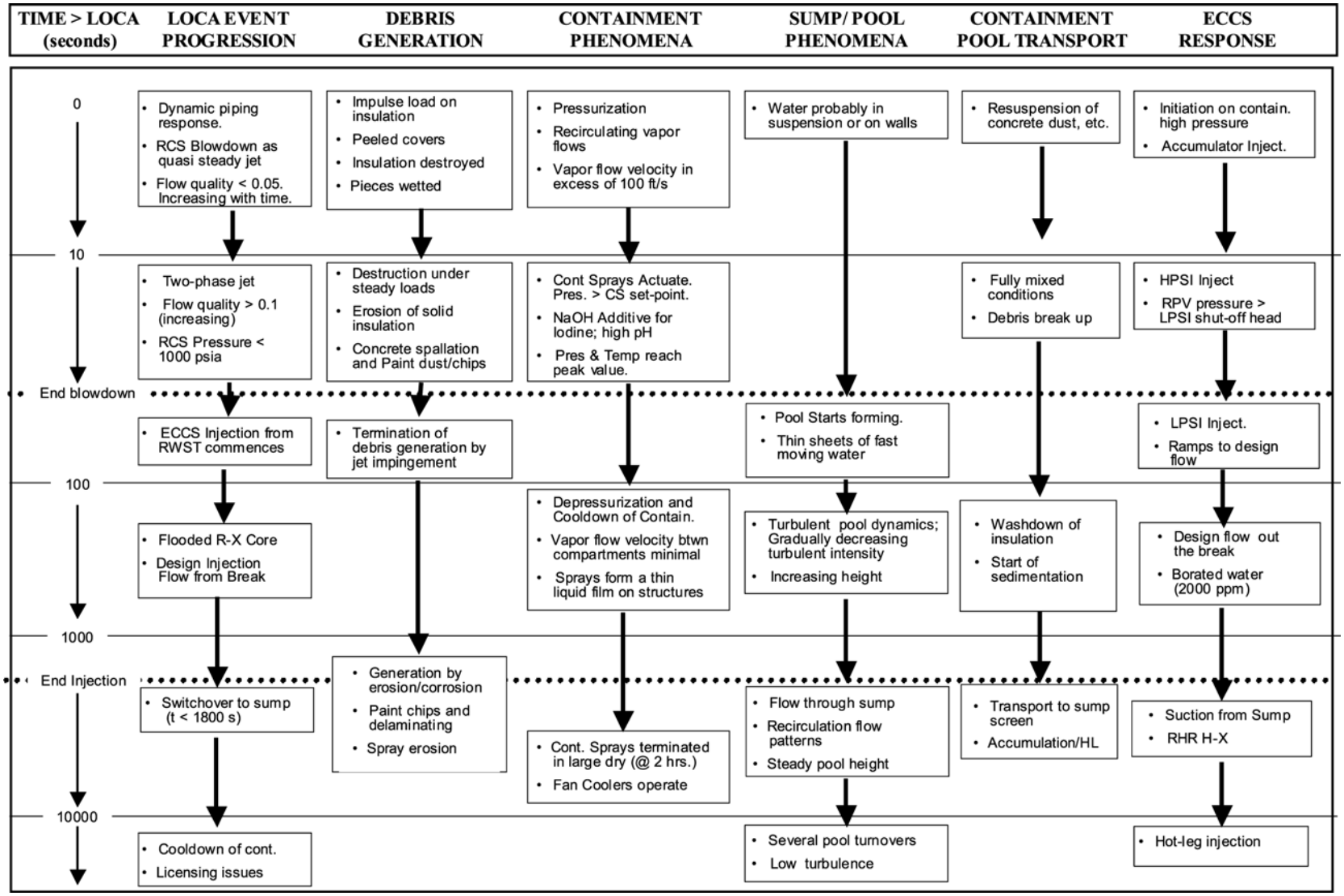

Figure 1-4 PWR LLOCA Accident Progression in a Large Dry Containment

APPENDIX C

CHEMICAL EFFECTS LITERATURE SEARCH

A literature search was performed for information on chemical effects on debris generated by LOCA and other similar accident events that could affect sump screen strainer performance under recirculation conditions.

Six databases were searched for relevant material in this area between 1997–2002. The results of this search are yielded 14 articles. Of these, six were determined to be relevant to our problem. These relevant articles are given as follows:

1. "Nitrogen in a Steam Generator of a PWR Under SBLOCA Conditions: Experimental Investigations in the 'PKL' Test Facility and Comparison with Analytical Studies," Schoen, B. Investigated thermal-hydraulic behavior of a pressurized water reactor. This 'PKL' experiment shows that a sudden stagnation of natural circulation in all loops caused by nitrogen does not impede heat removal from the core.
2. "The PKL Test Facility of Framatome ANP-25 Years Experimental Accident Investigation for Pressurized Water Reactor," Umminger, K., 2002.
3. "Transport Characteristics of Selected Pressurized Water Reactor LOCA-Generated Debris," Maji, A., 2002.
4. "Analysis Method for the Fuel Cladding Integrity During Partial Loss of Reactor Coolant," Sheng, T., 1993.
5. "Uncertainty Evaluation of Reactor Safety Parameters During SBLOCA," Prosek, A., 2001.
6. "Modeling of Hydrogen Stratification in a PWR Containment with the Contain Computer Code," Kljenak et al., 1999.

"Proceedings of the 10^{th}, 9^{th}, and 8^{th} International Conference on Nuclear Engineering (ICONE)" were also searched for any relevant material. The relevant works are given as follows:

10^{th} ICONE – Arlington VA April 14–18, 2002

1. "Evaluation and Repair of Primary Water Stress Corrosion Cracking in Alloy 600/182 Control Rod Drive Mechanism Nozzles," Frye, Charles et al., February 2001, a routine visual inspection of the reactor vessel head of Oconee Nuclear Station Unit 3 identified boric acid crystals at 9 of 69 locations where control rod drive mechanism housings (CRDM nozzles) penetrate the head.
2. Containment Sump Neutralization Using Trisodium Phosphate," Tarek G. Zaki. For post-LOCA conditions, the pH of the aqueous solution collected in the containment sump after completion of injection of containment spray, ECC water, all additives for reactivity control, fission product removal, and other purposes, should be maintained at a level such that the long-term iodine re-evolution does not occur. For this the sump pH should be more than 7. A trisodium phosphate (TSP) based, passive system can be used to achieve this pH. Other than the initial boron concentration, the production of nitric acid from nitrogen in the air due to irradiation would lower the pH in the sump. The author has given curves on dosage of TSP to keep the pH of borated water at different temperatures.

3. “Large Break LOCA Safety Injection Sensitivity for a CE/ABB System 80+ PWR,” Pottor, J. et al.

9th ICONE – No relevant paper

8th ICONE – Baltimore, MD April. 2–6, 2000

1. “Assessment of the Hydrodynamic Loads to a LOCA in a 3-Loop PWR. CASTEM-Plexus Computations,” Robbe, Marie-France et al. The authors studied the depressurization phase and presents results of the pressures and volume flow rates as a consequence of a hypothetical LOCA in the primary circuit.
2. “Application of Large Scale Containment Database to AP600 LOCA Internal Circulation and Stratifications,” Woodcock et al.
3. “Study of the Performance of the Passive Core Cooling System on List SBLOCA Experiments,” Chang, Chin et al.
4. “EPR, the Strategy for Hydrogen Mitigation,” Wagner, Kurt et al.